

Chiral Dynamics of Baryons in a Lorentz Covariant Quark Model

Amand Faessler, Th. Gutsche, V. E. Lyubovitskij, K. Pumsa-ard

*Institut für Theoretische Physik, Universität Tübingen,
Auf der Morgenstelle 14, D-72076 Tübingen, Germany*

(Dated: February 8, 2020)

We develop a manifestly Lorentz covariant chiral quark model for the study of baryons as bound states of constituent quarks dressed by a cloud of pseudoscalar mesons. The approach is based on a non-linear chirally symmetric Lagrangian, which involves effective degrees of freedom - constituent quarks and the chiral (pseudoscalar meson) fields. In a first step, this Lagrangian can be used to perform a dressing of the constituent quarks by a cloud of light pseudoscalar mesons and other heavy states using the calculational technique of infrared dimensional regularization of loop diagrams. We calculate the dressed transition operators with a proper chiral expansion which are relevant for the interaction of quarks with external fields in the presence of a virtual meson cloud. In a second step, these dressed operators are used to calculate baryon matrix elements. Applications are worked out for the masses of the baryon octet, the meson-nucleon sigma terms, the magnetic moments of the baryon octet, the nucleon charge radii, the strong vector meson-nucleon couplings and the full momentum dependence of the electromagnetic form factors of the nucleon.

PACS numbers: 12.39.Fe, 12.39.Ki, 13.40.Gp, 14.20.Dh, 14.20.Jn

Keywords: chiral symmetry, effective Lagrangian, relativistic quark model, nucleon electromagnetic form factors, meson-nucleon sigma-terms, strong vector meson-nucleon couplings

I. INTRODUCTION

Chiral symmetry plays an important role in the low-energy (below 1 GeV) domain of Quantum Chromodynamics (QCD): it governs the strong interaction between hadrons. All known low-energy approaches (effective field theories, Lattice QCD, QCD sum rules, different types of quark models, etc.) in the study of the properties of light hadrons have to incorporate the concept of at least an approximate chiral symmetry to get reasonable agreement with data.

The most convenient language for the treatment of light hadrons at small energies was elaborated in the context of Chiral Perturbation Theory (ChPT) [1, 2], the effective low-energy theory of the strong interaction. ChPT is based on a chiral expansion of the QCD Green functions, i.e. an expansion in powers of the external hadron momenta and quark masses. It was proved [2] that ChPT works perfectly in the meson sector (especially in the description of pion-pion interactions). A manifestly Lorentz invariant form of baryon ChPT was suggested in Ref. [3]. In the baryon sector a new scale parameter associated with the nucleon mass shows up and this leads to certain difficulties in the formulation of a consistent chiral expansion of matrix elements. In particular, the chiral expansion of the loop diagrams starts at the same order as the tree-level graphs. This leads to an inconsistency in the perturbation theory: the higher order graphs contribute to the low-order ones and the physical quantities (e.g., nucleon mass) require renormalization at every order of the expansion. Later, a method, referred to as Heavy Baryon Chiral Perturbation Theory (HBChPT) [4], was suggested, which is able to avoid the problems with chiral power counting. HBChPT keeps track of power counting at every step of the calculation. A disadvantage of HBChPT is the lack of manifest Lorentz covariance due to the nonrelativistic expansion of the nucleon propagator. As was pointed out in Ref. [5] this method also suffers from a further deficiency. Namely, the nonrelativistic expansion of the pion-nucleon scattering amplitude generates a convergence problem of the perturbative series in part of the low-energy region. In Refs. [3, 5, 6] a new method for the study of baryons in ChPT was suggested. It is based on the infrared dimensional regularization of loop diagrams [5], which exploits the advantages of the two frameworks formulated in Ref. [3] and Refs. [4], while avoiding their disadvantages. A successful application of the improved version of Baryon ChPT to nucleon properties has been performed in Refs. [5, 7, 8, 9]. In Ref. [10] the method has been extended to the multi-nucleon sector. An equivalent formulation of Baryon ChPT based on the extended on-mass-shell renormalization was suggested in Refs. [11].

Unfortunately, in the context of Baryon ChPT one is able to calculate the momentum dependence of hadronic matrix elements only in a sufficiently narrow region (e.g., an accurate description of nucleon electromagnetic form factors has been achieved up to about $Q^2 = 0.4 \text{ GeV}^2$ [8]). Also, chiral symmetry is not the only important feature of strong interactions in the low-energy domain. There are the problems of hadronization and confinement which are completely avoided in the effective field theories dealing with hadronic degrees of freedom. These additional effects certainly have a strong impact on the hadronic interactions at intermediate energies. As an illustration of the importance of hadronization and confinement phenomena related to hadronic properties we recommend the review [12]. In Ref. [12] the general principles of QCD-motivated relativistic quark models have been formulated with the explicit incorporation of the three low-energy key phenomena: hadronization, confinement and approximate chiral symmetry. Many properties of light and heavy flavored baryons (including such sophisticated characteristics as slope parameters and form factors) have been successfully described in this approach [12] and in a later developed similar model [13, 14].

The main objective of the present work is to develop a Lorentz covariant chiral quark model [15] which is consistent with the latest developments in the baryon sector of ChPT and leaves space for the additional features of low-energy QCD - hadronization and confinement. The full approach [15] is an extension of the original chiral quark model suggested and developed in Refs. [16, 17, 18, 19]. We treat the constituent quarks as the intermediate degrees of freedom between the current quarks (building blocks of the QCD Lagrangian) and the hadrons (building blocks of ChPT). This concept dates back to the pioneering works of Refs. [20, 21]. Furthermore, our strategy in dressing the constituent quarks by a cloud of pseudoscalar mesons is motivated by the procedure pursued in Ref. [21]. Recent analyses of experiments at Jefferson Lab (TJLAB) [22], Fermilab [23], BNL [24] and IHEP (Protvino) [25] renewed the interest in the concept of constituent quarks. The obtained data can be interpreted in a picture, where the hadronic quasiparticle substructure is assumed to consist of constituent quarks with nontrivial form factors. These experiments also initiated new progress in the manifestation of constituent degrees of freedom in hadron phenomenology (see, e.g. Refs. [26]).

The broader concept of chiral quark models dates back to the work of the early eighties [27, 28, 29], where the nucleon is described as a bound system of valence quarks with a surrounding pion cloud simulating the sea-quark contributions. These models aim to include the two main features of low-energy hadron structure, confinement and chiral symmetry. With respect to the treatment of the pion cloud these approaches fall essentially into two categories. The first type of chiral quark models assumes that the valence quark content dominates the nucleon, thereby treating pion contributions perturbatively [16, 27, 28]. Originally, this idea was formulated in the context of the cloudy bag model [27]. By imposing chiral symmetry the MIT bag model [30] was extended to include the interaction of the confined quarks with the pion fields on the bag surface. With the pion cloud treated as a perturbation on the basic features of the MIT bag, pionic effects generally improve the description of nucleon observables. Later, similar perturbative chiral

models [16, 28] were developed where the rather unphysical sharp bag boundary is replaced by a finite surface thickness of the quark core. By introducing a static quark potential of general form, these quark models contain a set of free parameters characterizing the confinement (coupling strength) and/or the quark masses. The perturbative technique allows a fully quantized treatment of the pion field up to a given order in accuracy, usually evaluated in leading order. Although formulated on the quark level, where confinement is put in phenomenologically, perturbative chiral quark models are conceptually close to chiral perturbation theory on the hadron level. Alternatively, when the pion cloud is assumed to dominate the nucleon structure this effect has to be treated non-perturbatively. The non-perturbative approaches are based for example on Refs. [29], where the chiral quark soliton model was derived. This model is based on the concept that the QCD instanton vacuum is responsible for the spontaneous breaking of chiral symmetry, which in turn leads to an effective chiral Lagrangian at low energy as "derived" from QCD. On the phenomenological level the chiral quark soliton model tends to be advantageous in the description of the nucleon spin structure, that is for large momentum transfers, but is comparable to the original perturbative chiral quark models in the description of low-energy nucleon properties.

As a further development of chiral quark models with a perturbative treatment of the pion cloud [16, 27, 28], we extended the relativistic quark model suggested in [16] for the study of the low-energy properties of the nucleon [17, 18, 19]. In the current manuscript we perform an extension of our previous approach in two directions: we formulate a chiral quark Lagrangian, which dynamically generates the dressing of the bare constituent quarks by meson degrees of freedom up to fourth order. We also formulate a manifestly Lorentz-covariant version concerning the structure of the bare constituent quarks, exemplified mainly for the case of the electromagnetic form factors of the nucleon. The resulting expectation values of dressed constituent quark operators evaluated for nucleon states are matched and checked in their low-energy behaviour with results of Baryon ChPT.

In the manuscript we proceed as follows. First, in Section II, we derive an effective Lagrangian, which is taken from Baryon ChPT [3, 5, 31, 32], and formulate it in terms of quark and mesonic degrees of freedom by also including external fields. Second, we use this Lagrangian to perform a dressing of the constituent quarks by a cloud of light pseudoscalar mesons and by other heavy states. In this vein we use the calculational technique developed by Becher and Leutwyler [5]. We derive dressed transition operators with a proper chiral expansion, which in turn are relevant for the interaction of quarks with external fields in the presence of a virtual meson cloud. In Section III, we work out the implications for the chiral expansion of the nucleon mass and the meson-nucleon sigma terms, which, in consistency with Baryon ChPT, gives constraints on the parameters entering in the chiral quark Lagrangian. Applications to various quantities are worked out and presented in Section IV. We discuss the masses of the baryon octet and mainly the pion-nucleon sigma term. Using model-independent constraints on the bare constituent quark distributions in the octet baryons, we work out model predictions for the magnetic moments. Using finally a full parameterization of the bare constituent quark distributions in the nucleon, we give results for the full momentum dependence of the electromagnetic form factors of the nucleon and indicate the role of the meson cloud contributions.

II. APPROACH

A. Chiral Lagrangian

The chiral quark Lagrangian \mathcal{L}_{qU} (up to order p^4), which dynamically generates the dressing of the constituent quarks by mesonic degrees of freedom, consists of the two main pieces \mathcal{L}_q and \mathcal{L}_U :

$$\mathcal{L}_{qU} = \mathcal{L}_q + \mathcal{L}_U, \quad \mathcal{L}_q = \mathcal{L}_q^{(1)} + \mathcal{L}_q^{(2)} + \mathcal{L}_q^{(3)} + \mathcal{L}_q^{(4)} + \dots, \quad \mathcal{L}_U = \mathcal{L}_U^{(2)} + \dots. \quad (1)$$

The superscript (i) attached to $\mathcal{L}_{q(U)}^{(i)}$ denotes the low energy dimension of the Lagrangian:

$$\begin{aligned} \mathcal{L}_U^{(2)} &= \frac{F^2}{4} \langle u_\mu u^\mu + \chi_+ \rangle, \quad \mathcal{L}_q^{(1)} = \bar{q} \left[i \not{D} - m + \frac{1}{2} g \not{\mu} \gamma^5 \right] q, \\ \mathcal{L}_q^{(2)} &= c_1 \langle \chi_+ \rangle \bar{q} q - \frac{c_2}{4m^2} \langle u_\mu u_\nu \rangle (\bar{q} D^\mu D^\nu q + \text{h.c.}) + \frac{c_3}{2} \langle u_\mu u^\mu \rangle \bar{q} q \\ &+ \frac{c_4}{4} \bar{q} i \sigma^{\mu\nu} [u_\mu, u_\nu] q + \frac{1}{8m} \bar{q} \sigma^{\mu\nu} c_{\mu\nu} q + \dots, \\ \mathcal{L}_q^{(3)} &= \frac{i}{2m} \bar{q} [D^\mu, d_{\mu\nu}] D^\nu q + \text{h.c.} + \dots, \\ \mathcal{L}_q^{(4)} &= -\frac{e_1}{16} \langle \chi_+ \rangle^2 \bar{q} q + \frac{e_2}{4} \langle \chi_+ \rangle \square (\bar{q} q) - \frac{1}{2} \bar{q} [D^\alpha, [D_\alpha, e_{\mu\nu}^{(1)}]] \sigma^{\mu\nu} q + \frac{\langle \chi_+ \rangle}{2} \bar{q} e_{\mu\nu}^{(2)} \sigma^{\mu\nu} q + \dots, \end{aligned} \quad (2)$$

where

$$\begin{aligned} c_{\mu\nu} &= c_6 F_{\mu\nu}^{+Q} + c_7 F_{\mu\nu}^{+I} + c_8 F_{\mu\nu}^{+\lambda_3}, & d_{\mu\nu} &= d_6 F_{\mu\nu}^{+Q} + d_7 F_{\mu\nu}^{+I} + d_8 F_{\mu\nu}^{+\lambda_3}, \\ e_{\mu\nu}^{(1)} &= e_{54} F_{\mu\nu}^{+Q} + e_{74} F_{\mu\nu}^{+I} + e_{94} F_{\mu\nu}^{+\lambda_3}, & e_{\mu\nu}^{(2)} &= e_{105} F_{\mu\nu}^{+Q} + e_{106} F_{\mu\nu}^{+I} + e_{107} F_{\mu\nu}^{+\lambda_3}. \end{aligned} \quad (3)$$

The couplings m and g denote the quark mass and axial charge in the chiral limit, c_i , d_i and e_i are the second-, third- and fourth-order low-energy coupling constants, respectively, which encode the contributions of heavy states. Note, that the inclusion of higher-dimensional terms in the chiral quark Lagrangian was originally suggested in Ref. [21]. In particular, as a dimensional parameter in the higher-dimensional terms one can use the scale parameter of spontaneously broken chiral symmetry $\Lambda_\chi \simeq 4\pi F \sim 1$ GeV (F is the octet decay constant [9, 32]) instead of the constituent quark mass. This replacement is equivalent to a redefinition of the values of the low-energy constants, e.g. $c_2 \rightarrow c_2(m/\Lambda_\chi)^2$, $d_6 \rightarrow d_6(m/\Lambda_\chi)$, etc. Both scale parameters m and Λ_χ are counted as the same order quantities in the chiral expansion, i.e as quantities of order $O(1)$.

Additional terms in the Lagrangian denoted generically by dots do not contribute to the electromagnetic nucleon form factors and meson-nucleon sigma-terms, which are explicitly worked out later on in the applications. Here q is the quark field, the octet of pseudoscalar fields

$$\phi = \sum_{i=1}^8 \phi_i \lambda_i = \sqrt{2} \begin{pmatrix} \pi^0/\sqrt{2} + \eta/\sqrt{6} & \pi^+ & K^+ \\ \pi^- & -\pi^0/\sqrt{2} + \eta/\sqrt{6} & K^0 \\ K^- & \bar{K}^0 & -2\eta/\sqrt{6} \end{pmatrix}. \quad (4)$$

is contained in the $SU(3)$ matrix $U = u^2 = \exp(i\phi/F)$ where F the octet decay constant [9, 32]. We introduce the standard notations [3, 5, 31]

$$\begin{aligned} D_\mu &= \partial_\mu + \Gamma_\mu, & \Gamma_\mu &= \frac{1}{2}[u^\dagger, \partial_\mu u] - \frac{i}{2}u^\dagger R_\mu u - \frac{i}{2}u L_\mu u^\dagger, \\ u_\mu &= iu^\dagger \nabla_\mu U u^\dagger, & \chi_\pm &= u^\dagger \chi u^\dagger \pm u \chi^\dagger u, & \chi &= 2B(s + ip), & s &= \mathcal{M} + \dots \end{aligned} \quad (5)$$

The fields R_μ and L_μ include sources

$$\begin{aligned} R_\mu &= v_\mu + a_\mu = e Q A_\mu^{em} - Q \tan\theta_W Z_\mu^0 + \dots, \\ L_\mu &= v_\mu - a_\mu = e Q A_\mu^{em} + \left(\frac{e}{\sin^2\theta_W} \lambda_3 - Q \right) \tan\theta_W Z_\mu^0 + \frac{e}{\sin\theta_W\sqrt{2}} (W_\mu^+ T_+ + \text{h.c.}) + \dots \end{aligned} \quad (6)$$

where s, p, v_μ and a_μ denote the external scalar, pseudoscalar, vector and axial fields; A_μ^{em} , W_μ^\pm and Z_μ^0 are the electromagnetic field, the weak charged and neutral boson fields. The quark charge matrix is denoted by $Q = \text{diag}\{2/3, -1/3, -1/3\}$ and

$$T_+ = \begin{pmatrix} 0 & V_{ud} & V_{us} \\ 0 & 0 & 0 \\ 0 & 0 & 0 \end{pmatrix} \quad (7)$$

is the weak matrix containing the Cabibbo-Kobayashi-Maskawa quark-mixing matrix elements V_{ij} . The electromagnetic field strength tensors $F_{\mu\nu}^{+T}$ ($T = Q, I, \lambda_3$) are defined as

$$F_{\mu\nu}^{+T} = c_T (u^\dagger F_{\mu\nu} T u + u F_{\mu\nu} T u^\dagger), \quad c_Q = 1, \quad c_I = 1/3, \quad c_{\lambda_3} = 1/2, \quad (8)$$

where I is the 3×3 flavor unit matrix. The symbol $\langle \rangle$ occurring in Eq.(2) denotes the trace over flavor matrices. Here $\mathcal{M} = \text{diag}\{\hat{m}_u, \hat{m}_d, \hat{m}_s\}$ is the mass matrix of current quarks (we restrict to the isospin symmetry limit with $\hat{m}_u = \hat{m}_d = \hat{m} = 7$ MeV and the mass of the strange quark \hat{m}_s is related to the nonstrange one as $\hat{m}_s = 25 \hat{m}$). The quark vacuum condensate parameter is denoted by

$$B = -\frac{1}{F^2} \langle 0 | \bar{u} u | 0 \rangle = -\frac{1}{F^2} \langle 0 | \bar{d} d | 0 \rangle.$$

To distinguish between constituent and current quark masses we attach the symbol $\hat{}$ ("hat") when referring to the current quark masses. We rely on the standard picture of chiral symmetry breaking ($B \gg F$). In the leading order of the chiral expansion the masses of pseudoscalar mesons are given by

$$M_\pi^2 = 2\hat{m}B, \quad M_K^2 = (\hat{m} + \hat{m}_s)B, \quad M_\eta^2 = \frac{2}{3}(\hat{m} + 2\hat{m}_s)B. \quad (9)$$

In the numerical analysis we will use: $M_\pi = 139.57$ MeV, $M_K = 493.677$ MeV (the charged pion and kaon masses), $M_\eta = 574.75$ MeV and the canonical set of differentiated decay constants: $F_\pi = 92.4$ MeV, $F_K/F_\pi = 1.22$ and $F_\eta/F_\pi = 1.3$ [33]. The use of the physical masses and decay constants of pseudoscalar mesons incorporates only part of the corrections due to the breaking of unitary flavor symmetry. To generate another part of $SU(3)$ symmetry-breaking corrections we add a string of terms to the Lagrangian (1):

$$\begin{aligned}\mathcal{L}_{qU,SB} &= \mathcal{L}_{q,SB}^{(2)} + \mathcal{L}_{q,SB}^{(4)} + \dots \\ \mathcal{L}_{q,SB}^{(2)} &= -\bar{q}\mathcal{M}q + c_5\bar{q}\hat{\chi}_+q + \dots, \quad \mathcal{L}_{q,SB}^{(4)} = -\frac{e_5}{16}\bar{q}\hat{\chi}_+^2q + \dots\end{aligned}\tag{10}$$

where $\hat{\chi}_+ = \chi_+ - \frac{1}{3}\langle\chi_+\rangle$.

B. Inclusion of vector mesons

Following Refs. [2, 8, 34] we also include vector mesons in the chiral quark Lagrangian. In particular, we employ the tensor field representation of the spin-1 fields: vector mesons are written in terms of the antisymmetric tensor fields $W_{\mu\nu} = -W_{\nu\mu}$ where the three degrees of freedom W_{ij} ($i, j = 1, 2, 3$) are frozen out. The latter representation is most convenient to construct the chirally invariant couplings of vector mesons to pions, photons and fermions (baryons, quarks):

$$\mathcal{L}_V = \mathcal{L}_V^0 + \mathcal{L}_V^{\text{int}}\tag{11}$$

where \mathcal{L}_V^0 is the free vector meson Lagrangian

$$\mathcal{L}_V^0 = -\frac{1}{2}\partial^\mu W_{\mu\nu}^a \partial_\rho W^{\rho\nu,a} + \frac{M_V^2}{4}W_{\mu\nu}^a W^{\mu\nu,a}\tag{12}$$

and $\mathcal{L}_V^{\text{int}} = \mathcal{L}_V^{\text{int},1} + \mathcal{L}_V^{\text{int},2}$ is the interaction Lagrangian of vector mesons with external vector and axial-vector sources ($\mathcal{L}_V^{\text{int},1}$) and with baryons ($\mathcal{L}_V^{\text{int},2}$):

$$\begin{aligned}\mathcal{L}_V^{\text{int},1} &= \frac{F_V}{2\sqrt{2}}\langle W^{\mu\nu} F_{\mu\nu}^+ \rangle + \frac{iG_V}{2\sqrt{2}}\langle W^{\mu\nu} [u_\mu, u_\nu] \rangle, \\ \mathcal{L}_V^{\text{int},2} &= \bar{q}\sigma^{\mu\nu} R_{\mu\nu} q + \bar{q}\gamma^\mu S_\mu q + \bar{q}\sigma^{\alpha\beta} U_{\mu\beta} [D_\alpha, [D^\mu, q]].\end{aligned}\tag{13}$$

Here we define

$$W_{\mu\nu} = \begin{pmatrix} (\rho^0 + \omega)/\sqrt{2} & \rho^+ & K^{*+} \\ \rho^- & (-\rho^0 + \omega)/\sqrt{2} & K^{*0} \\ K^{*-} & \bar{K}^{*0} & -\phi \end{pmatrix}_{\mu\nu},\tag{14}$$

$$R_{\mu\nu} = R_T W_{\mu\nu} + R_S \langle W_{\mu\nu} \rangle, \quad S_\mu = S_T [D^\nu, W_{\mu\nu}] + S_S \langle [D^\nu, W_{\mu\nu}] \rangle, \quad U_{\mu\beta} = U_T W_{\mu\beta} + U_S \langle W_{\mu\beta} \rangle,$$

where R_i , S_i and U_i are the effective couplings related to the ones (g_{Vqq} and k_V) used in the canonical interaction Lagrangian of vector mesons with quarks (for details on the nucleon-level Lagrangian see Ref. [8]):

$$\mathcal{L}_{Vqq} = \frac{g_{Vqq}}{\sqrt{2}}\bar{q}\left(\gamma^\mu V_\mu - \frac{k_V}{2m}\sigma^{\mu\nu}\partial_\nu V_\mu\right)q.\tag{15}$$

The standard nonet matrix of vector mesons is denoted by V_μ (its flavor content coincides with the one of the antisymmetric tensor $W_{\mu\nu}$). The matching conditions relating the couplings are:

$$R_S = 0, \quad R_T = -k_V g_{Vqq} \frac{M_V}{4m\sqrt{2}}, \quad U_S = \frac{2}{m} S_S, \quad U_T = \frac{2}{m} \left(\frac{g_{Vqq}}{M_V \sqrt{2}} + S_T \right).\tag{16}$$

The couplings F_V and G_V are determined by the decays widths of $\rho \rightarrow e^+e^-$ and $\rho \rightarrow \pi\pi$. Using low-energy theorems, e.g. ρ -meson universality and the Kawarabayashi-Suzuki-Fayyazuddin-Riazuddin (KSFR) relation, one can express F_V and G_V by g_{Vqq} and the vector meson mass M_V [8, 35]: $F_V = M_V/g_{Vqq}$ and $G_V = F_V/2$. Hence, in the vector-meson sector we only deal with a single free parameter k_V .

C. Power counting

The Lagrangian set up for constituent quarks, pseudoscalar and vector mesons is assumed to be valid in the region between the chiral symmetry breaking Λ_χ and confinement Λ_{QCD} scales. Such a Lagrangian is non-renormalizable due to the existence of an infinite tower of higher dimensional terms. A solution to this problem can be achieved if there is a dimensional parameter in the theory which suppresses corresponding non-renormalizable terms in the matrix elements. The problem of power counting in non-renormalizable effective chiral quark theories was discussed in detail in Ref. [21]. It was shown in the framework of the so-called "naive dimensional analysis" that higher-order corrections in the matrix elements can be suppressed by a dimensional parameter $\Lambda_\chi = 4\pi F \sim 1 \text{ GeV}$.

D. Dressing of quark operators

The total effective Lagrangian \mathcal{L}_{eff} includes the two terms \mathcal{L}_{qU} and \mathcal{L}_V . The first term (\mathcal{L}_{qU}) is responsible for the dressing of quarks by a cloud of pseudoscalar mesons and heavy states, while the second one (\mathcal{L}_V) generates the coupling to vector mesons. Any bare quark operator (both one- and two-body) can be dressed in a straightforward manner by use of the effective chirally-invariant Lagrangian \mathcal{L}_{eff} . To illustrate the idea of such a dressing we consider the Fourier-transform of the electromagnetic quark operator:

$$J_{\mu, \text{em}}^{\text{bare}}(q) = \int d^4x e^{-iqx} j_{\mu, \text{em}}^{\text{bare}}(x), \quad j_{\mu, \text{em}}^{\text{bare}}(x) = \bar{q}(x) \gamma_\mu Q q(x). \quad (17)$$

In Figs.1 and 2 we display the tree and loop diagrams which contribute to the dressed electromagnetic operator J_μ^{dress} up to fourth order.

The Fourier transform of the dressed quark operator has the following form

$$J_{\mu, \text{em}}^{\text{dress}}(q) = \int d^4x e^{-iqx} \bar{q}(x) \left[\gamma_\mu f_D(q^2) + \frac{i}{2m} \sigma^{\mu\nu} q_\nu f_P(q^2) \right] q(x), \quad (18)$$

where $f_D = \text{diag}\{f_D^u, f_D^d, f_D^s\}$ and $f_P = \text{diag}\{f_P^u, f_P^d, f_P^s\}$ are the diagonal matrices of Dirac and Pauli form factors of u , d and s quarks. Here we use the appropriate sub- and superscripts with a definite normalization of the set of $f_D(0) \equiv Q$ due to charge conservation.

Evaluation of the diagrams in Figs.1 and 2 is based on the *infrared dimensional regularization* suggested in Ref. [5] to guarantee a straightforward connection between loop and chiral expansion in terms of quark masses and small external momenta. We relegate the discussion of the calculational technique [8] to the Appendices A (infrared regularization) and B (explicit form of the loop integrals).

To calculate the electromagnetic form factors of the nucleon (or any baryon) we project the dressed quark operator between the nucleon (baryon) states. In the following we restrict to the case of the nucleon (the extension to any baryon is straightforward). The master formula is:

$$\begin{aligned} \langle N(p') | J_{\mu, \text{em}}^{\text{dress}}(q) | N(p) \rangle &= (2\pi)^4 \delta^4(p' - p - q) \bar{u}_N(p') \left\{ \gamma_\mu F_1^N(q^2) + \frac{i}{2 \overset{\circ}{m}_N} \sigma_{\mu\nu} q^\nu F_2^N(q^2) \right\} u_N(p) \\ &= (2\pi)^4 \delta^4(p' - p - q) \left\{ f_D^{ij}(q^2) \langle N(p') | j_{\mu,ij}^{\text{bare}}(0) | N(p) \rangle + i \frac{q^\nu}{2m} f_P^{ij}(q^2) \langle N(p') | j_{\mu\nu,ij}^{\text{bare}}(0) | N(p) \rangle \right\}, \end{aligned} \quad (19)$$

where i, j are the flavor indices, $\overset{\circ}{m}_N$ is the bare nucleon mass (or the nucleon mass in the chiral limit), $u_N(p)$ is the nucleon spinor normalized as $\bar{u}(p)u(p) = 2 \overset{\circ}{m}_N$, $F_1^N(q^2)$ and $F_2^N(q^2)$ are the Dirac and Pauli nucleon form factors. In Eq. (19) we express the matrix elements of the dressed quark operator by the matrix elements of the bare operators. In our case we deal with the bare quark operators of the vector $j_{\mu,ij}^{\text{bare}}(0)$ and tensor $j_{\mu\nu,ij}^{\text{bare}}(0)$ structures defined as

$$j_{\mu,ij}^{\text{bare}}(0) = \bar{q}_i(0) \gamma_\mu q_j(0), \quad j_{\mu\nu,ij}^{\text{bare}}(0) = \bar{q}_i(0) \sigma_{\mu\nu} q_j(0). \quad (20)$$

Eq. (19) contains our main result: we perform a model-independent factorization of the effects of hadronization and confinement contained in the matrix elements of the bare quark operators $j_{\mu,ij}^{\text{bare}}(0)$ and $j_{\mu\nu,ij}^{\text{bare}}(0)$ and the effects dictated by chiral symmetry (or chiral dynamics) which are encoded in the relativistic form factors $f_D^{ij}(q^2)$ and $f_P^{ij}(q^2)$. Due to this factorization the calculation of $f_D^{ij}(q^2)$ and $f_P^{ij}(q^2)$, on one side, and the matrix elements of $j_{\mu,ij}^{\text{bare}}(0)$ and $j_{\mu\nu,ij}^{\text{bare}}(0)$, on the other side, can be done independently. In particular, in a first step we derived a model-independent

formalism based on the ChPT Lagrangian, which is formulated in terms of constituent quark degrees of freedom, for the calculation of $f_D^{ij}(q^2)$ and $f_P^{ij}(q^2)$. The calculation of the matrix elements of the bare quark operators can then be relegated to quark models based on specific assumptions about hadronization and confinement. The explicit forms of $f_D^{ij}(q^2)$ and $f_P^{ij}(q^2)$ are given in Appendix C. Note that we also show in Fig.3 the diagrams contributing to the strong vector meson-nucleon interactions ρNN and ωNN at one loop which will be discussed in Sec. IV(D).

E. Matching to ChPT

The matrix elements of the bare quark operators should be calculated using specific model assumptions about hadronization and confinement. However, the use of certain symmetry constraints, discussed in the following, leads to a set of relationships between the nucleon and the corresponding quark form factors at their normalization point at zero momentum. In general, due to Lorentz and gauge invariance, the matrix elements in Eq. (19) can be written as

$$\begin{aligned} \langle N(p') | j_{\mu,ij}^{\text{bare}}(0) | N(p) \rangle &= \delta_{ij} \bar{u}_N(p') \left\{ \gamma_\mu F_1^{Ni}(q^2) + \frac{i}{2 \overset{\circ}{m}_N} \sigma_{\mu\nu} q^\nu F_2^{Ni}(q^2) \right\} u_N(p), \\ i \frac{q^\nu}{2m} \langle N(p') | j_{\mu\nu,ij}^{\text{bare}}(0) | N(p) \rangle &= \delta_{ij} \bar{u}_N(p') \left\{ \gamma_\mu G_1^{Ni}(q^2) + \frac{i}{2 \overset{\circ}{m}_N} \sigma_{\mu\nu} q^\nu G_2^{Ni}(q^2) \right\} u_N(p), \end{aligned} \quad (21)$$

where $F_{1(2)}^{Ni}(q^2)$ and $G_{1(2)}^{Ni}(q^2)$ are the Pauli and Dirac form factors describing the distribution of quarks of flavor $i = u, d$ in the nucleon.

The first set of relations arise from charge conservation and isospin invariance:

$$\begin{aligned} F_1^{pu}(0) &= F_1^{nd}(0) = 2, & F_1^{pd}(0) &= F_1^{nu}(0) = 1, & G_1^{Ni}(0) &= 0, \\ F_2^{pu}(0) &= F_2^{nd}(0), & F_2^{pd}(0) &= F_2^{nu}(0), & G_2^{pu}(0) &= G_2^{nd}(0), & G_2^{pd}(0) &= G_2^{nu}(0). \end{aligned} \quad (22)$$

Note, that the quantities $G_2^{Ni}(0)$ are related to the bare nucleon tensor charges $\delta_{Ni}^{\text{bare}}$:

$$\begin{aligned} G_2^{pu}(0) &= G_2^{nd}(0) = \frac{\overset{\circ}{m}_N}{m} \delta_{pu}^{\text{bare}} = \frac{\overset{\circ}{m}_N}{m} \delta_{nd}^{\text{bare}}, \\ G_2^{pd}(0) &= G_2^{nu}(0) = \frac{\overset{\circ}{m}_N}{m} \delta_{pd}^{\text{bare}} = \frac{\overset{\circ}{m}_N}{m} \delta_{nu}^{\text{bare}}, \end{aligned} \quad (23)$$

where $\delta_{Ni}^{\text{bare}}$ are defined by [36]:

$$\langle N(p) | j_{\mu\nu,ii}^{\text{bare}}(0) | N(p) \rangle = \delta_{Ni}^{\text{bare}} \bar{u}_N(p) \sigma_{\mu\nu} u_N(p). \quad (24)$$

The second set of constraints are the so-called *chiral symmetry constraints*. They are dictated by the infrared-singular structure of QCD in order to reproduce the leading nonanalytic (LNA) contributions to the magnetic moments and the charge and magnetic radii of nucleons [8, 37]:

$$\begin{aligned} \mu_p &= -\frac{g_A^2}{8\pi} \frac{M_\pi}{F_\pi^2} \overset{\circ}{m}_N + \dots, \\ \langle r^2 \rangle_p^E &= -\frac{1+5g_A^2}{16\pi^2 F_\pi^2} \ln \frac{M_\pi}{\overset{\circ}{m}_N} + \dots, \\ \langle r^2 \rangle_p^M &= \frac{g_A^2}{16\pi F_\pi^2 \mu_p} \frac{\overset{\circ}{m}_N}{M_\pi} + \dots, \end{aligned} \quad (25)$$

where g_A is the nucleon axial charge in the chiral limit. In particular, the LNA contribution to the magnetic moments is proportional to M_π . The nucleon radii are divergent in the chiral limit. The LNA contribution to the charge radii is proportional to the chiral logarithm $\ln(M_\pi / \overset{\circ}{m}_N)$. The LNA contributions to the magnetic radii are represented by the same logarithm as in the case of the charge radii and by the singular term proportional to $1/M_\pi$. In order to fulfill the chiral symmetry constraints (25) we derive the following identities involving the $F_2^{Ni}(0)$ and $G_2^{Ni}(0)$ form factors and the low-energy constant (LEC) d_6 :

$$\begin{aligned} 1 + F_2^{pu}(0) - F_2^{pd}(0) &= G_2^{pu}(0) - G_2^{pd}(0) = \left(\frac{g_A}{g} \right)^2 \frac{\overset{\circ}{m}_N}{m}, \\ 1 + F_2^{nd}(0) - F_2^{nu}(0) &= G_2^{nd}(0) - G_2^{nu}(0) = \left(\frac{g_A}{g} \right)^2 \frac{\overset{\circ}{m}_N}{m} \end{aligned} \quad (26)$$

and

$$\bar{d}_6^{\text{ChPT}} + \frac{1+5g_A^2}{96\pi^2 F_\pi^2} \ln \frac{M_\pi}{\overset{\circ}{m}_N} \equiv \bar{d}_6 + \frac{1+5g^2}{96\pi^2 F_\pi^2} \ln \frac{M_\pi}{\overset{\circ}{m}_N}. \quad (27)$$

Here \bar{d}_6^{ChPT} and \bar{d}_6 denote the renormalized LECs d_6^{ChPT} and d_6 , respectively, at $\mu = \overset{\circ}{m}_N$:

$$\bar{d}_6^{\text{ChPT}} = d_6^{\text{ChPT}} + \frac{1+5g_A^2}{6F_\pi^2} \bar{\lambda} \quad (28)$$

where

$$\lambda(\mu) = \frac{\mu^{d-4}}{(4\pi)^2} \left[\frac{1}{d-4} - \frac{1}{2}(\ln 4\pi + \Gamma'(1) + 1) \right], \quad \bar{\lambda} = \lambda(\overset{\circ}{m}_N). \quad (29)$$

Identity (27) represents the matching condition between the LEC of the ChPT Lagrangian and our quark-level Lagrangian. Analogous conditions involving other LECs can be derived when matching other physical amplitudes/quantities (see, e.g. Sec. III).

Applying simple SU(6)-algebra of the naive nonrelativistic quark model for the ratios of the magnetic moments and the tensor charges of the nucleon we can derive additional and well-known relations between $F_2^{Ni}(0)$ and $G_2^{Ni}(0)$, respectively:

$$\frac{2+F_2^{pu}(0)}{1+F_2^{pd}(0)} = \frac{2+F_2^{nd}(0)}{1+F_2^{nu}(0)} = \frac{G_2^{pu}(0)}{G_2^{pd}(0)} = \frac{G_2^{nd}(0)}{G_2^{nu}(0)} = -4. \quad (30)$$

Substituting Eq. (30) into Eq. (26), we arrive at

$$\begin{aligned} F_2^{pu}(0) = F_2^{nd}(0) &= \frac{4}{5} \left(\frac{g_A}{g} \right)^2 \frac{\overset{\circ}{m}_N}{m} - 2, \\ F_2^{pd}(0) = F_2^{nu}(0) &= -\frac{1}{5} \left(\frac{g_A}{g} \right)^2 \frac{\overset{\circ}{m}_N}{m} - 1, \\ G_2^{pu}(0) = G_2^{nd}(0) &= \frac{4}{5} \left(\frac{g_A}{g} \right)^2 \frac{\overset{\circ}{m}_N}{m}, \\ G_2^{pd}(0) = G_2^{nu}(0) &= -\frac{1}{5} \left(\frac{g_A}{g} \right)^2 \frac{\overset{\circ}{m}_N}{m}. \end{aligned} \quad (31)$$

Other interesting results are the predictions for the nucleon magnetic moments and tensor charges in the chiral limit (without inclusion of meson-cloud effects):

$$\mu_p^{\text{bare}} \equiv -\frac{3}{2} \mu_n^{\text{bare}} = \sum_{i=u,d} Q_i [F_1^{pi}(0) + F_2^{pi}(0)] = \frac{3}{5} \left(\frac{g_A}{g} \right)^2 \frac{\overset{\circ}{m}_N}{m} \quad (32)$$

and

$$\delta_{pu}^{\text{bare}} \equiv -4 \delta_{pd}^{\text{bare}} = \frac{m}{\overset{\circ}{m}_N} G_2^{pu}(0) = \frac{4}{5} \left(\frac{g_A}{g} \right)^2, \quad (33)$$

where $Q_u = 2/3$ and $Q_d = -1/3$ are the electric charges of u and d quarks. Below, in Sec. III, we also derive the constraint relating the axial charge of the nucleon g_A and of the constituent quark g .

III. NUCLEON MASS AND MESON-NUCLEON σ -TERMS

In this chapter we consider two other important quantities of low-energy nucleon physics: the nucleon mass and meson-nucleon σ -terms which are constrained by the Feynman-Hellmann theorem (FHT) [38]. In particular, the FHT relates the derivative of the nucleon mass with respect to the current quark masses to the pion-nucleon sigma-term $\sigma_{\pi N}$ and to the strange quark condensate in the nucleon:

$$\begin{aligned}\sigma_{\pi N} \bar{u}_N(p) u_N(p) &\doteq \hat{m} \langle N(p) | \bar{u}(0) u(0) + \bar{d}(0) d(0) | N(p) \rangle = \hat{m} \frac{\partial m_N}{\partial \hat{m}} \bar{u}_N(p) u_N(p), \\ y_s \bar{u}_N(p) u_N(p) &\doteq \langle N(p) | \bar{s}(0) s(0) | N(p) \rangle = \frac{\partial m_N}{\partial \hat{m}_s} \bar{u}_N(p) u_N(p).\end{aligned}\quad (34)$$

In quantum field theory the nucleon mass m_N is defined as the matrix element of the trace of the energy-momentum tensor $\Theta^{\mu\nu}(x)$:

$$m_N \bar{u}_N(p) u_N(p) \doteq \langle N(p) | \Theta_\mu^\mu(0) | N(p) \rangle. \quad (35)$$

In the constituent quark (CQ) approach the master formula (35) spells as

$$m_N \bar{u}_N(p) u_N(p) \doteq \langle N(p) | \mathcal{H}_{\text{mass}}(0) | N(p) \rangle, \quad (36)$$

where $\mathcal{H}_{\text{mass}}(x) = \bar{q}(x) m_q q(x)$ is the part of the Hamiltonian referred to as the quark mass term where $m_q = \text{diag}\{m_u, m_d, m_s\}$ is the matrix of constituent quark masses. In some CQ models the nontrivial dependence of m_q (or m_N) on the current quark masses is missing. This leads to a contradiction with the low-energy behavior of the nucleon mass as a function of $\hat{m}(\hat{m}_s)$ and with the Feynman-Hellmann theorem. The use of the effective Lagrangian (1) constrained by Baryon ChPT enables one to perform an accurate and consistent calculation of the nucleon mass and the corresponding sigma-terms. Again, as in the case of the electromagnetic form factors, the extension to other baryons is straightforward.

In analogy with the electromagnetic form factors we define the nucleon mass and later on the sigma-terms as expectation values of the dressed operators. First, we write down the bare quark mass term:

$$\mathcal{H}_{\text{mass}}^{\text{bare}}(x) = m \bar{q}(x) q(x) \quad (37)$$

i.e. the quark mass term at leading order of the chiral expansion (in the chiral limit). Here m is the value of the constituent quark mass in the chiral limit introduced before in the Lagrangian (1). The nucleon mass in the chiral limit $\overset{\circ}{m}_N$ is defined by

$$\overset{\circ}{m}_N \bar{u}_N(p) u_N(p) = \langle N(p) | \mathcal{H}_{\text{mass}}^{\text{bare}}(0) | N(p) \rangle = m \langle N(p) | \bar{q}(0) q(0) | N(p) \rangle. \quad (38)$$

The dressed quark mass term and the physical nucleon mass are given by

$$\begin{aligned}\mathcal{H}_{\text{mass}}^{\text{dress}}(x) &= \bar{q}(x) m_q q(x), \\ m_N \bar{u}_N(p) u_N(p) &= \langle N(p) | \mathcal{H}_{\text{mass}}^{\text{dress}}(0) | N(p) \rangle = \langle N(p) | \bar{q}(0) m_q q(0) | N(p) \rangle\end{aligned}\quad (39)$$

where $m_q = \text{diag}\{m_u, m_d, m_s\}$ is the matrix of the dressed (physical) constituent quark masses (in our case the constituent quark mass at one loop with inclusion of chiral corrections) with $m_u = m_d$ due to isospin invariance. The constituent quark masses $m_q \doteq m_q(\hat{m}, \hat{m}_s)$ have a nontrivial dependence on the current quark masses \hat{m} and \hat{m}_s which can be accurately calculated with the use of the chiral Lagrangian (1). For illustration we discuss the explicit expressions for the nonstrange and strange constituent quark masses at one loop and at $O(p^4)$ with

$$m_q = m + \Sigma_q(m). \quad (40)$$

The quark mass operator $\Sigma_q = \text{diag}\{\Sigma_u, \Sigma_d, \Sigma_s\}$, with $\Sigma_u = \Sigma_d = \Sigma$ due to isospin invariance, is evaluated on the mass-shell $\not{p} = m$, which is ultraviolet-finite by construction. All ultraviolet divergencies are removed via the renormalization of the fourth-order LECs e_1 and e_5 contributing to the Σ_q operator. Here and in the following we identify the quark mass occurring in the loop integrals with its leading order value $m_q \rightarrow m$. The operator Σ_q is described by the diagrams in Fig.4 and after expansion in powers of meson masses is given by:

$$\begin{aligned}\Sigma &= \hat{m} - \frac{3g^2}{32\pi} \left\{ \frac{M_\pi^3}{F_\pi^2} + \frac{2}{3} \frac{M_K^3}{F_K^2} + \frac{M_\eta^3}{9F_\eta^2} \right\} - \frac{3g^2}{64\pi^2 m} \left\{ \frac{M_\pi^4}{F_\pi^2} + \frac{2}{3} \frac{M_K^4}{F_K^2} + \frac{M_\eta^4}{9F_\eta^2} \right\} \\ &- 4c_1 M^2 + \frac{3c_2}{128\pi^2} M^2 \left\{ \frac{M_\pi^2}{F_\pi^2} + \frac{4}{3} \frac{M_K^2}{F_K^2} + \frac{M_\eta^2}{3F_\eta^2} \right\} + \frac{2}{3} c_5 (M_K^2 - M_\pi^2) \\ &+ \hat{e}_1 M^4 + \frac{\hat{e}_5}{36} (M_K^2 - M_\pi^2)^2\end{aligned}\quad (41)$$

and

$$\begin{aligned}\Sigma_s &= \hat{m}_s - \frac{3g^2}{32\pi} \left\{ \frac{4}{3} \frac{M_K^3}{F_K^2} + \frac{4}{9} \frac{M_\eta^3}{F_\eta^2} \right\} - \frac{3g^2}{64\pi^2 m} \left\{ \frac{4}{3} \frac{M_K^4}{F_K^2} + \frac{4}{9} \frac{M_\eta^4}{F_\eta^2} \right\} \\ &\quad - 4c_1 M^2 + \frac{3c_2}{128\pi^2} M^2 \left\{ \frac{M_\pi^2}{F_\pi^2} + \frac{4}{3} \frac{M_K^2}{F_K^2} + \frac{M_\eta^2}{3F_\eta^2} \right\} - \frac{4}{3} c_5 (M_K^2 - M_\pi^2) \\ &\quad + \hat{e}_1 M^4 + \frac{\hat{e}_5}{9} (M_K^2 - M_\pi^2)^2\end{aligned}\quad (42)$$

where

$$M^2 = M_\pi^2 - M_K^2 + \frac{3}{2} M_\eta^2. \quad (43)$$

Note, Σ and Σ_s are degenerate for $\hat{m} = \hat{m}_s$ and M^2 coincides with M_π^2 at $\hat{m}_s = 0$. For simplicity the chiral logarithms are hidden in the renormalized LECs \hat{e}_1 and \hat{e}_5 :

$$\begin{aligned}\hat{e}_1 &= e_1^r(\mu) + \frac{3}{32\pi^2} (8c_1 - c_2 - 4c_3) \left\{ \frac{Q_\pi}{F_\pi^2} \ln \frac{M_\pi}{\mu} + \frac{4Q_K}{3F_K^2} \ln \frac{M_K}{\mu} + \frac{Q_\eta}{3F_\eta^2} \ln \frac{M_\eta}{\mu} \right\} \\ &\quad - \frac{g^2}{8\pi^2 m} \left\{ \frac{Q_\pi^2}{F_\pi^2} \ln \frac{M_\pi}{\mu} + \frac{Q_K^2}{3F_K^2} \ln \frac{M_K}{\mu} \right\} \\ \hat{e}_5 &= e_5^r(\mu) + \frac{9g^2}{8\pi^2 m} \left\{ \frac{R_\pi}{F_\pi^2} \ln \frac{M_\pi}{\mu} - \frac{2R_K}{3F_K^2} \ln \frac{M_K}{\mu} - \frac{R_\eta}{3F_\eta^2} \ln \frac{M_\eta}{\mu} \right\}\end{aligned}\quad (44)$$

where

$$Q_P = \frac{M_P^2}{M^2}, \quad R_P = \frac{M_P^4}{(M_K^2 - M_\pi^2)^2} \quad (45)$$

and

$$\begin{aligned}e_1^r(\mu) &= e_1 + \frac{3}{2} (8c_1 - c_2 - 4c_3) \lambda(\mu) \left\{ \frac{Q_\pi}{F_\pi^2} + \frac{4Q_K}{3F_K^2} + \frac{Q_\eta}{3F_\eta^2} \right\} - \frac{2g^2}{m} \lambda(\mu) \left\{ \frac{Q_\pi^2}{F_\pi^2} + \frac{Q_K^2}{3F_K^2} \right\}, \\ e_5^r(\mu) &= e_5 + \frac{18g^2}{m} \lambda(\mu) \left\{ \frac{R_\pi}{F_\pi^2} - \frac{2R_K}{3F_K^2} - \frac{R_\eta}{3F_\eta^2} \right\}.\end{aligned}\quad (46)$$

The LECs e_1 and e_5 contain the poles at $d = 4$ which are cancelled by the divergencies proportional to $\lambda(\mu)$ in the r.h.s. of Eq. (46). Therefore, the renormalized couplings $e_1^r(\mu)$ and $e_5^r(\mu)$ (or \hat{e}_1 and \hat{e}_5) are finite. Note, that the $m_s - m_u(m_d)$ splitting is mainly generated by the difference in the values of the strange and the nonstrange current quark masses. The chiral symmetry constraints and the matching of the nucleon mass calculated within our approach to the model-independent derivation of [5] allow to deduce certain relations between the set of our parameters and the ones in Baryon ChPT. In particular, the coefficient connected with M_π^3/F_π^2 , referred to in the literature as the *leading nonanalytic coefficient* (LNAC) [2, 5], is model-independent and constant due to dimensional arguments. Precisely, this coefficient is equal to $-3g_A^2/(32\pi F_\pi^2)$. The cubic term in powers of the meson mass shows up due to the infrared singularity of the diagram in Fig.4(3). Using this requirement, we can relate the value of axial charge of the constituent quark in the chiral limit to the corresponding nucleon quantity:

$$g_A^2 \bar{u}_N(p) u_N(p) = g^2 \langle N(p) | \bar{q}(0) q(0) | N(p) \rangle. \quad (47)$$

The matching condition gives a constraint for the matrix element of the bare scalar-density operator in the nucleon. A rough estimate with $g_A = 1.25$ [3], $g \sim 1$ and by taking into account the normalization of the nucleon spinors gives a quite reasonable value for the scalar condensate: $\langle N(p) | \bar{q}(0) q(0) | N(p) \rangle \sim (25/8) m_N$. Using the matching condition (47) we derive a final expression for the nucleon mass at one loop:

$$m_N = \overset{\circ}{m}_N + \Sigma_N \quad (48)$$

where

$$m_N = \left(\frac{g_A}{g} \right)^2 m_{u(d)}, \quad \overset{\circ}{m}_N = \left(\frac{g_A}{g} \right)^2 m \quad (49)$$

and

$$\begin{aligned}\Sigma_N &= -\frac{3g_A^2}{32\pi} \left\{ \frac{M_\pi^3}{F_\pi^2} + \frac{2}{3} \frac{M_K^3}{F_K^2} + \frac{M_\eta^3}{9F_\eta^2} \right\} - \frac{3g_A^2}{64\pi^2 m} \left\{ \frac{M_\pi^4}{F_\pi^2} + \frac{2}{3} \frac{M_K^4}{F_K^2} + \frac{M_\eta^4}{9F_\eta^2} \right\} \\ &+ \left(\frac{g_A}{g} \right)^2 \left[\hat{m} - 4c_1 M^2 + \frac{c_2}{24\pi^2} M^2 \left\{ \frac{M_\pi^2}{F_\pi^2} - \frac{M_K^2}{F_K^2} + \frac{3}{2} \frac{M_\eta^2}{F_\eta^2} \right\} \right. \\ &\left. + \frac{2}{3} c_5 (M_K^2 - M_\pi^2) + \hat{e}_1 M^4 + \frac{\hat{e}_5}{36} (M_K^2 - M_\pi^2)^2 \right].\end{aligned}\quad (50)$$

The constituent quark mass can be removed from the expressions for nucleon observables using the matching conditions (49). In the SU(2) picture (when neglecting the kaon and η -meson loops and putting c_5 and e_5 to be equal to zero) we reproduce the result of ChPT for the nucleon mass at one loop and at order $O(p^4)$ [5]

$$\begin{aligned}m_N &= \overset{\circ}{m}_N - 4c_1^{\text{ChPT}} - \frac{3g_A^2}{32\pi} \frac{M_\pi^3}{F_\pi^2} + k_1 M_\pi^4 \ln \frac{M_\pi}{\overset{\circ}{m}_N} + k_2 M_\pi^4 + O(M_\pi^5), \\ k_1 &= -\frac{3}{32\pi^2 F_\pi^2} \left(\frac{g_A^2}{\overset{\circ}{m}_N} - 8c_1^{\text{ChPT}} + c_2^{\text{ChPT}} + 4c_3^{\text{ChPT}} \right), \\ k_2 &= \bar{e}_1^{\text{ChPT}} - \frac{3}{128\pi^2 F_\pi^2} \left(\frac{2g_A^2}{\overset{\circ}{m}_N} - c_2^{\text{ChPT}} \right), \\ \bar{e}_1^{\text{ChPT}} &= e_1^{\text{ChPT}} - \frac{3\bar{\lambda}^{\text{ChPT}}}{2F_\pi^2} \left(\frac{g_A^2}{\overset{\circ}{m}_N} - 8c_1^{\text{ChPT}} + c_2^{\text{ChPT}} + 4c_3^{\text{ChPT}} \right),\end{aligned}\quad (51)$$

if we fulfill the following matching conditions between the LECs of the ChPT Lagrangian and our quark-level Lagrangian:

$$\begin{aligned}-4c_1^{\text{ChPT}} M_\pi^2 &= \left[\hat{m} - 4c_1 M_\pi^2 \right] \left(\frac{g_A}{g} \right)^2, \\ 8c_1^{\text{ChPT}} - c_2^{\text{ChPT}} - 4c_3^{\text{ChPT}} - \frac{g_A^2}{\overset{\circ}{m}_N} &\equiv \left[8c_1 - c_2 - 4c_3 - \frac{g_A^2}{\overset{\circ}{m}_N} \right] \left(\frac{g_A}{g} \right)^2, \\ \bar{e}_1^{\text{ChPT}} - \frac{3}{64\pi^2 F_\pi^2} \left(\frac{2g_A^2}{\overset{\circ}{m}_N} - c_2^{\text{ChPT}} \right) &\equiv \left[\bar{e}_1 - \frac{3}{64\pi^2 F_\pi^2} \left(\frac{2g_A^2}{\overset{\circ}{m}_N} - c_2 \right) \right] \left(\frac{g_A}{g} \right)^2,\end{aligned}\quad (52)$$

where \bar{e}_1 is a $SU(2)$ analogue of \hat{e}_1 .

Note, that there is an additional condition on g and g_A which shows up in the calculation of the axial nucleon charge:

$$g_A \bar{u}_N(p) \gamma^\mu \gamma^5 \tau_3 u_N(p) = g \langle N(p) | \bar{q}(0) \gamma^\mu \gamma^5 \tau_3 q(0) | N(p) \rangle. \quad (53)$$

Eq. (53) gives a constraint on the matrix element of the isovector axial current.

As an example for the sigma-terms we consider the pion-nucleon sigma-term $\sigma_{\pi N}$. In QCD (see Eq. (34)) this quantity is related to the expectation value of the scalar density operator. It is connected to the derivative of the part of the QCD Hamiltonian, explicitly breaking chiral symmetry, with respect to the current quark mass. This definition is consistent with the FH theorem [38]. In the context of CQ models, we should proceed with the dressed Hamiltonian $\mathcal{H}_{\text{mass}}^{\text{dress}}(x)$ which already showed up in the calculation of the physical nucleon mass. In particular, the dressed scalar density operators $j_i^{\text{dress}}(x)$ (where $i = u, d, s$ is the flavor index), relevant for the calculation of the meson-baryon sigma-terms within our approach, are defined as the partial derivatives of $\mathcal{H}_{\text{mass}}^{\text{dress}}(x)$ with respect to the current quark mass \hat{m}_i of i -th flavor:

$$j_i^{\text{dress}}(x) \doteq \frac{\partial \mathcal{H}_{\text{mass}}^{\text{dress}}(x)}{\partial \hat{m}_i} = \bar{q}(x) \frac{\partial m_q}{\partial \hat{m}_i} q(x) = \bar{q}(x) \frac{\partial \Sigma_q}{\partial \hat{m}_i} q(x). \quad (54)$$

In the case of $\sigma_{\pi N}$ we have:

$$\sigma_{\pi N} \bar{u}_N(p) u_N(p) \doteq \hat{m} \langle N(p) | j_u^{\text{dress}}(0) + j_d^{\text{dress}}(0) | N(p) \rangle. \quad (55)$$

It should be clear that Eq. (55) is consistent with the FH theorem:

$$\sigma_{\pi N} \bar{u}_N(p) u_N(p) = \hat{m} \frac{\partial}{\partial \hat{m}} \underbrace{\langle N(p) | \mathcal{H}_{\text{mass}}^{\text{dress}}(0) | N(p) \rangle}_{= m_N \bar{u}_N(p) u_N(p)} = \hat{m} \frac{\partial m_N}{\partial \hat{m}} \bar{u}_N(p) u_N(p). \quad (56)$$

Below we give the definitions of the strangeness content of the nucleon y_N , the kaon-nucleon σ_{KN} and the eta-nucleon $\sigma_{\eta N}$ sigma-terms:

$$\begin{aligned} y_N &= 2 \frac{\partial m_N / \partial \hat{m}_s}{\partial m_N / \partial \hat{m}}, \\ \bar{u}_N(p) u_N(p) \sigma_{KN}^{u(d)} &= \frac{\hat{m} + \hat{m}_s}{2} \langle N(p) | j_{u(d)s;+}^{\text{dress}}(0) | N(p) \rangle, \\ \bar{u}_N(p) u_N(p) \sigma_{KN}^{I=0} &= \frac{\hat{m} + \hat{m}_s}{4} \langle N(p) | j_{us;+}^{\text{dress}}(0) + j_{ds;+}^{\text{dress}}(0) | N(p) \rangle, \\ \bar{u}_N(p) u_N(p) \sigma_{KN}^{I=1} &= \frac{\hat{m} + \hat{m}_s}{2} \langle N(p) | j_{ud;+}^{\text{dress}}(0) | N(p) \rangle, \\ \bar{u}_N(p) u_N(p) \sigma_{\eta N} &= \frac{1}{3} \langle N(p) | \hat{m} j_{ud;+}^{\text{dress}}(0) + 4 \hat{m}_s j_s^{\text{dress}}(0) | N(p) \rangle, \end{aligned} \quad (57)$$

where $j_{q\bar{q};\pm}^{\text{dress}} = j_q^{\text{dress}} \pm j_{q'}^{\text{dress}}$ and $|N(p)\rangle$ denotes a proton state. All further details can be found in our previous papers [18] and in Appendix D.

IV. PHYSICAL APPLICATIONS

In this chapter we consider the application of our approach to specific nucleon properties: magnetic moments, electromagnetic radii and form factors, nucleon mass, meson-nucleon sigma-terms and strong vector meson-nucleon form factors. We also calculate some canonical properties of hyperons: masses and magnetic moments. Note, that these properties have been studied within different approaches: QCD sum rules [39], ChPT and HBChPT [3, 4, 5, 8, 9, 11, 40, 41, 42, 43], lattice QCD [44], approaches based on vector dominance [45] and on solutions of Schwinger-Dyson and Bethe-Salpeter equations [46], different types of chiral and quark models [12, 13, 17, 27, 28, 29, 30, 47], etc. Our main interest will be restricted to the region of small external momenta where the contribution of the meson cloud is supposed to be largest.

A. Masses of the baryon octet and the meson-nucleon sigma-terms

The nucleon mass and the meson-nucleon sigma-terms at one loop depend on the set of parameters: g , m , c_1 , c_2 , c_5 , \hat{e}_1 and \hat{e}_5 . First, we discuss a choice for g and m . Note, that these parameters are constrained in our approach by the matching condition (49): $\hat{m}_N = (g_A/g)^2 m$. In literature the value of the axial charge of the constituent quark varies approximately from 0.9 to 1 (see detailed discussion in Refs. [48]). The nucleon mass in the chiral limit was estimated in HBChPT: $\hat{m}_N = 770 \pm 110$ MeV [41] and $\hat{m}_N = 890 \pm 180$ MeV [43]. Inserting this range of values for g and \hat{m}_N and also the experimental value for $g_A = 1.267$ [49] into Eq. (49) gives the following limits for the constituent quark mass in the chiral limit:

$$m \simeq 500 \pm 167 \text{ MeV}. \quad (58)$$

Finally, we choose:

$$m = 420 \text{ MeV} \quad \text{and} \quad g = 0.9. \quad (59)$$

Using the experimental value for the nucleon axial charge $g_A = 1.267$ [49] and Eq. (49) we get $\hat{m}_N = 832.4$ MeV which is rather close to our previous estimate done in the framework of the perturbative chiral quark model (PCQM): $\hat{m}_N = 828.5$ MeV [18]. Here we do not pretend on a more accurate determination of m and g . This will be done in a possible forthcoming paper where we intend to involve more constraints from data. However, we stress that we

need a rather small value for g in the interval $0.9 - 1$ to justify perturbation theory. In particular, the use of $g = 0.9$ gives the shift of the nonstrange constituent quark mass equal to $\Delta m = 53$ MeV. For $g = 0.95$ and $g = 1$ we get $\Delta m = 107$ MeV and $\Delta m = 164$ MeV, respectively. On the other hand, the choice of g is constrained by the bare magnetic moments of the nucleon (see Eq. (71)). The use of $g = 0.9$ gives a reasonable contribution of the valence quark to the nucleon magnetic moments (see discussion in the next section). Finally, the couplings c_1, c_2, c_5 and \hat{e}_5 are fixed by four conditions:

$$m_N = 938.27 \text{ MeV}, \quad \sigma_{\pi N} = 45 \text{ MeV}, \quad y_N = 0.2, \quad m_s - m_{u(d)} \simeq 170 \text{ MeV}. \quad (60)$$

The result of the fit is:

$$\begin{aligned} c_1 &= (-0.357 + 0.007 \tilde{e}_1) \text{ GeV}^{-1}, & c_2 &= (2.502 - 2.385 \tilde{e}_1) \text{ GeV}^{-1}, \\ c_5 &= (-0.640 - 0.0004 \tilde{e}_1) \text{ GeV}^{-1}, & \hat{e}_5 &= (-0.807 - 0.043 \tilde{e}_1) \text{ GeV}^{-3}, \end{aligned} \quad (61)$$

where for convenience we introduce the dimensionless parameter $\tilde{e}_1 = \hat{e}_1 \times 1 \text{ GeV}^3$. Note, the mass difference $m_s - m_{u(d)}$ is a crucial quantity to roughly describe the splittings between the octet baryon masses. Latter quantities are proportional to $m_s - m_{u(d)}$. Neglecting isospin-breaking and hyperfine-splitting effects we have in our approach:

$$\begin{aligned} m_\Lambda - m_N &= m_s - m_{u(d)} \simeq 170 \text{ MeV} & (\text{data : } 177 \text{ MeV}), \\ m_\Sigma - m_N &= m_s - m_{u(d)} \simeq 170 \text{ MeV} & (\text{data : } 251 \text{ MeV}), \\ m_\Xi - m_N &= 2[m_s - m_{u(d)}] \simeq 340 \text{ MeV} & (\text{data : } 383 \text{ MeV}). \end{aligned} \quad (62)$$

The meson cloud corrections are important to reproduce the full empirical value of $\sigma_{\pi N}$, contributing about 2/3 to the total value (for a detailed discussion see Ref. [18]). In particular, our result for $\sigma_{\pi N}$ is compiled as: the total value is $\sigma_{\pi N} = 45$ MeV, the contribution of the valence quarks is $\sigma_{\pi N}^{val} = 13.87$ MeV (30% of the total value), the contribution of the pion cloud is dominant $\sigma_{\pi N}^\pi = 31.74$ MeV - 0.35 MeV \tilde{e}_1 , the kaon and η -meson cloud generates $\sigma_{\pi N}^{K+\eta} = -0.61$ MeV + 0.35 MeV \tilde{e}_1 . The separate contributions $\sigma_{\pi N}^\pi$ and $\sigma_{\pi N}^{K+\eta}$ depend on the parameter \tilde{e}_1 , while the total contribution is independent on \tilde{e}_1 . Our predictions for the kaon-nucleon σ_{KN} and eta-nucleon $\sigma_{\eta N}$ sigma-terms are: $\sigma_{KN}^u = 411.1$ MeV, $\sigma_{KN}^d = 381.1$ MeV, $\sigma_{KN}^{I=0} = 396.1$ MeV, $\sigma_{KN}^{I=1} = 15.0$ MeV, and $\sigma_{\eta N} = 165.0$ MeV.

B. Magnetic moments of baryon octet

The magnetic moments of the nucleon can be written in terms of the Dirac and Pauli form factors as

$$\mu_N = F_1^N(0) + F_2^N(0), \quad (63)$$

where in our formalism $F_1^N(0)$ and $F_2^N(0)$ are of the form

$$\begin{aligned} F_1^N(0) &= \sum_{i=u,d} f_D^i(0) F_1^{Ni}(0), \\ F_2^N(0) &= \sum_{i=u,d} [f_D^i(0) F_2^{Ni}(0) + f_P^i(0) G_2^{Ni}(0)]. \end{aligned} \quad (64)$$

It is convenient to separate the expressions for $F_1^N(0)$ and $F_2^N(0)$ into two contributions: the bare (valence-quark) and the meson cloud (sea-quark) contributions.

The bare contribution is

$$\begin{aligned} F_1^{N \text{ bare}}(0) &= \sum_{i=u,d} Q_i F_1^{Ni}(0), \\ F_2^{N \text{ bare}}(0) &= \sum_{i=u,d} Q_i F_2^{Ni}(0), \end{aligned} \quad (65)$$

where $Q_i \equiv f_D^i(0)$ are the elements of the charge quark matrix which coincide with the diagonal matrix $f_D(0)$ derived in Eq. (18) due to charge conservation.

The meson cloud gives rise to

$$\begin{aligned} F_1^{N \text{ cloud}}(0) &\equiv 0, \\ F_2^{N \text{ cloud}}(0) &= \sum_{i=u,d} f_P^i(0) G_2^{Ni}(0). \end{aligned} \quad (66)$$

Note, that the contribution of the meson cloud to the Dirac form factor $F_1^N(0)$ is zero due to the charge conservation of the nucleon. Therefore, the nucleon magnetic moments are given in additive form with

$$\mu_N = \mu_N^{\text{bare}} + \mu_N^{\text{cloud}}. \quad (67)$$

where

$$\mu_N^{\text{bare}} = F_1^N \text{bare}(0) + F_2^N \text{bare}(0) \quad (68)$$

and

$$\mu_N^{\text{cloud}} = F_1^N \text{cloud}(0) + F_2^N \text{cloud}(0). \quad (69)$$

With the constraints laid out in Sec.II, we derived a relation for the bare contributions to the nucleon magnetic moments [see Eq. (32)]:

$$\mu_p^{\text{bare}} \equiv -\frac{3}{2} \mu_n^{\text{bare}} = \frac{3}{5} \left(\frac{g_A}{g} \right)^2 \frac{\overset{\circ}{m}_N}{m}. \quad (70)$$

Note that Eq. (70) can be further simplified using the constraints of (49):

$$\mu_p^{\text{bare}} \equiv -\frac{3}{2} \mu_n^{\text{bare}} = \frac{3}{5} \left(\frac{g_A}{g} \right)^4. \quad (71)$$

As already mentioned in the previous section, the choice of g is constrained by the bare magnetic moments of the nucleon (see Eq. (71)). The value of $g = 0.9$ results in a reasonable contribution of the valence quarks to the nucleon magnetic moments with:

$$\mu_p^{\text{bare}} \equiv -\frac{3}{2} \mu_n^{\text{bare}} = \frac{3}{5} \left(\frac{g_A}{g} \right)^4 \simeq 2.357 \quad (72)$$

which is about 84% (for the proton) and about 82% (for the neutron) of the experimental (total) values, where the remainder comes from the meson cloud.

The main parameters contained in the meson cloud piece that play an important role in fitting the magnetic moments are c_6 , c_7 , and c_8 . To constrain these values we need besides the experimental values for the nucleon (p and n) an additional value from the baryon octet. Therefore, we will proceed with an extension of our formalism to calculate the magnetic moments of the whole baryon octet.

In the following, for convenience, we introduce the bare Dirac (F_1^{qi}, G_1^{qi}) and Pauli (F_2^{qi}, G_2^{qi}) form factors of the quark of flavor i :

$$\begin{aligned} \langle q(p') | j_{\mu,ij}^{\text{bare}}(0) | q(p) \rangle &= \delta_{ij} \bar{u}_q(p') \left\{ \gamma_\mu F_1^{qi}(q^2) + \frac{i}{2m} \sigma_{\mu\nu} q^\nu F_2^{qi}(q^2) \right\} u_q(p), \\ i \frac{q^\nu}{2m} \langle q(p') | j_{\mu\nu,ij}^{\text{bare}}(0) | q(p) \rangle &= \delta_{ij} \bar{u}_q(p') \left\{ \gamma_\mu G_1^{qi}(q^2) + \frac{i}{2m} \sigma_{\mu\nu} q^\nu G_2^{qi}(q^2) \right\} u_q(p). \end{aligned} \quad (73)$$

The Sachs form factors of the quark of flavor i are:

$$\mathcal{F}_i^E(t) = F_i^E(t) + G_i^E(t), \quad \mathcal{F}_i^M(t) = F_i^M(t) + G_i^M(t), \quad (74)$$

where

$$F\{G\}_i^E(t) = F\{G\}_1^{qi}(t) - \frac{t}{4m^2} F\{G\}_2^{qi}(t), \quad F\{G\}_i^M(t) = F\{G\}_1^{qi}(t) + F\{G\}_2^{qi}(t), \quad t = -q^2, \quad (75)$$

are the contributions to the Sachs form factors associated with the expectation values of the vector and tensor currents, respectively.

By using SU(6)-algebra one can relate the Dirac and Pauli form factors describing the distribution of quarks of flavor $i = u, d, s$ in the baryon "B", that is $F_{1(2)}^{Bi}(t)$ and $G_{1(2)}^{Bi}(t)$, to $F_i^{E(M)}(t)$ and $G_i^{E(M)}(t)$ by

$$F_1^{Bi}(t) = \frac{1}{1 + \tau_N} \left\{ \alpha_E^{Bi} F_i^E(t) + \alpha_M^{Bi} \chi^{Bi} F_i^M(t) \tau_N \right\},$$

$$\begin{aligned}
F_2^{Bi}(t) &= \frac{1}{1 + \tau_N} \left\{ -\alpha_E^{Bi} F_i^E(t) + \alpha_M^{Bi} \chi^{Bi} F_i^M(t) \right\}, \\
G_1^{Bi}(t) &= \frac{1}{1 + \tau_N} \left\{ \alpha_E^{Bi} G_i^E(t) + \alpha_M^{Bi} \chi^{Bi} G_i^M(t) \tau_N \right\}, \\
G_2^{Bi}(t) &= \frac{1}{1 + \tau_N} \left\{ -\alpha_E^{Bi} G_i^E(t) + \alpha_M^{Bi} \chi^{Bi} G_i^M(t) \right\},
\end{aligned} \tag{76}$$

where $\tau_N = t/(4m_N^2)$. In addition to the strict evaluation of SU(6) we have introduced the additional parameter χ^{Bi} for each quark of flavor i . The interpretation for adding these factors is such that to allow the quark distributions for hyperons to be different from that for the nucleons. In the case of the nucleons we set $\chi^{Bi} = 1$. The values for α_E^{Bi} and α_M^{Bi} for the baryon octet as derived from SU(6)-algebra are given in Table 1.

The quark Sachs form factors are modeled by the dipole characteristics with damping functions of an exponential form. This phenomenological form is required to reproduce in particular the deviation of the electromagnetic form factors of the nucleon from the dipole fit as evident from recent experimental measurements. We use the parameterization

$$\begin{aligned}
F_i^E(t) &= \frac{\rho_i^E(t)}{[1 + t/\Lambda_{iE}^2]^2}, & F_i^M(t) &= \mu_i^F \frac{\rho_i^M(t)}{[1 + t/\Lambda_{iM}^2]^2}, \\
G_i^E(t) &= \gamma_i \rho_i^E(t) \frac{t/\Lambda_{iE}^2}{[1 + t/\Lambda_{iE}^2]^3}, & G_i^M(t) &= \mu_i^G \frac{\rho_i^M(t)}{[1 + t/\Lambda_{iM}^2]^2},
\end{aligned} \tag{77}$$

where $\rho_i^E(t) = \exp(-t/\lambda_{iE}^2)$ and $\rho_i^M(t) = \exp(-t/\lambda_{iM}^2)$. The parameters μ_i^F and μ_i^G are fixed by the symmetry constraints [see Eqs. (31) and (70)]:

$$\mu_i^F = \mu_i^G = \mu_p^{\text{bare}}. \tag{78}$$

The remaining parameters γ_i , $\Lambda_{iE(M)}$ and $\lambda_{iE(M)}$ are to be fixed later when we consider the full momentum dependence of the nucleon electromagnetic form factors. Note, that in Ref. [50] a similar parametrization of the nucleon form factors has been considered. In Ref. [51] the damping functions $\rho(t)$ have been parametrized with constant values.

The magnetic moment of the octet baryon "B" can be written in complete analogy to the nucleon case as

$$\mu_B = \mu_B^{\text{bare}} + \mu_B^{\text{cloud}} \tag{79}$$

where

$$\begin{aligned}
\mu_B^{\text{bare}} &= \sum_{i=u,d,s} Q_i (F_1^{Bi}(0) + F_2^{Bi}(0)), \\
\mu_B^{\text{cloud}} &= \sum_{i=u,d,s} f_P^i(0) G_2^{Bi}(0).
\end{aligned} \tag{80}$$

At $t = 0$, only the parameters c_6 , c_7 , c_8 , \tilde{e}_1 , and k_V contained in $f_P^i(0)$ will contribute. Three of them can now be fixed using the experimental values for the magnetic moments of the nucleons and of a hyperon in the baryon octet. We choose the Λ^0 -hyperon with $\mu_{\Lambda^0} = -0.613 \pm 0.004$ (in units of the nuclear magneton).

In our analysis of the magnetic moments of the octet baryons we present two cases. First, we restrict to the SU(6) case by setting all values $\chi^{Bi} = 1$. Secondly, we allow the χ^{Bi} to be additional parameters. From now on we will name these two cases shortly as "Set I" and "Set II", respectively.

A variation in the value of the axial charge g of the constituent quark will also give rise to different contributions of the bare and the meson cloud parts to the total values of the magnetic moments. However, the total magnetic moments are the same in any case. As was discussed in the previous section, for the axial charge we choose $g = 0.9$. In case of Set I we then obtain for c_6 , c_7 , and c_8 :

$$\begin{aligned}
c_6 &= (-0.698 + 0.104 \tilde{e}_1^V - 1.109 k_V) \text{ GeV}^{-1} \\
c_7 &= (0.180 + 0.018 \tilde{e}_1^V - 0.019 k_V) \text{ GeV}^{-1} \\
c_8 &= (0.417 + 0.013 \tilde{e}_1^V - 0.014 k_V) \text{ GeV}^{-1},
\end{aligned} \tag{81}$$

where $\tilde{e}_1^V = \tilde{e}_1(1 + k_V)$. The resulting values for the magnetic moments of the baryon octet for this case (Set I) are shown in Table 2, where reasonable agreement with data is obtained. Meson cloud contributions to the total values of the magnetic moments are about 5–30% depending on the baryon. Note, although that c_6 , c_7 , and c_8 also depend

on \tilde{e}_1^V and k_V , in the numerical analysis for the total magnetic moments the terms proportional to \tilde{e}_1^V and k_V are strongly suppressed and for convenience \tilde{e}_1^V and k_V can be set to zero. Therefore, the main parameters controlling the magnetic moments are c_6 , c_7 , and c_8 .

For the case of Set II we start from the SU(6) result with the additional breaking parameter $\chi^{\Lambda s}$ for $\mu_{\Lambda^0}^{\text{bare}}$ which can be written in terms of μ_p^{bare} as $\mu_{\Lambda^0}^{\text{bare}} = -\mu_p^{\text{bare}} \chi^{\Lambda s} / 3$. Then we have

$$\chi^{\Lambda s} = -3 \frac{\mu_{\Lambda^0}^{\text{bare}}}{\mu_p^{\text{bare}}} \approx -3 \frac{\mu_{\Lambda^0}}{\mu_p}, \quad (82)$$

where we further assume that the contributions from the meson cloud part to the total magnetic moments both of Λ^0 and of p are of the same order. With the experimental values for μ_{Λ^0} and μ_p we get $\chi^{\Lambda s} = 0.66$. By fitting μ_p , μ_n , and μ_{Λ^0} , with $\chi^{\Lambda s} = 0.66$ as an additional input, we obtain

$$\begin{aligned} c_6 &= (-0.583 + 0.104 \tilde{e}_1^V - 1.109 k_V) \text{ GeV}^{-1} \\ c_7 &= (0.145 + 0.018 \tilde{e}_1^V - 0.019 k_V) \text{ GeV}^{-1} \\ c_8 &= (0.302 + 0.013 \tilde{e}_1^V - 0.014 k_V) \text{ GeV}^{-1}, \end{aligned} \quad (83)$$

where the constants contained in these parameters are slightly different from Set I. With appropriate values for the remaining χ^{Bi} , the central values of the experimental results of the other magnetic moments in the baryon octet can be fully reproduced. For the set of χ^{Bi} we get

$$\begin{aligned} \chi^{\Sigma u} &= \chi^{\Sigma d} = 0.963, & \chi^{\Sigma s} &= 0.259, \\ \chi^{\Xi u} &= \chi^{\Xi d} = 0.633, & \chi^{\Xi s} &= 0.694, \\ \chi^{\Sigma \Lambda u} &= \chi^{\Sigma \Lambda d} = 0.988. \end{aligned} \quad (84)$$

relying on isospin symmetry. The isotriplet Σ^+ , Σ^0 , and Σ^- shares the same set of $\chi^{\Sigma i}$ for the quark of flavor i , while Ξ^0 and Ξ^- contains the same set of $\chi^{\Xi i}$. The parameters $\chi^{\Sigma \Lambda u}$ and $\chi^{\Sigma \Lambda d}$ are directly related to the $\Sigma - \Lambda$ magnetic transition moment. For completeness, our corresponding results for the magnetic moments are also listed in Table 2. In the following we will use the last set of values for c_6 , c_7 , and c_8 , when considering the electromagnetic nucleon form factors.

C. Nucleon electromagnetic form factors

Using the parameters from the analysis of the magnetic moments and the masses of the baryon octet, further supplied by the ones from the meson-nucleon sigma-terms, we now can consider the full nucleon electromagnetic form factors. We recall that the Dirac and Pauli form factors for the nucleons are

$$\begin{aligned} F_1^N(t) &= \sum_{i=u,d} [f_D^i(t) F_1^{Ni}(t) + f_P^i(t) G_1^{Ni}(t)], \\ F_2^N(t) &= \sum_{i=u,d} [f_D^i(t) F_2^{Ni}(t) + f_P^i(t) G_2^{Ni}(t)], \end{aligned} \quad (85)$$

where $F_{1(2)}^{Ni}(t)$ and $G_{1(2)}^{Ni}(t)$ refer to the bare constituent quark structure, while $f_D^i(t)$ and $f_P^i(t)$ contain the chiral dynamics due to dressing of the quark operators. For clarity we recall the forms of $F_{1(2)}^{Ni}(t)$ and $G_{1(2)}^{Ni}(t)$ of Eq. (76) with:

$$\begin{aligned} F_1^{Ni}(t) &= \frac{1}{1 + \tau_N} \left\{ \alpha_E^{Ni} F_i^E + \alpha_M^{Ni} F_i^M \tau_N \right\}, & F_2^{Ni}(t) &= \frac{1}{1 + \tau_N} \left\{ -\alpha_E^{Ni} F_i^E + \alpha_M^{Ni} F_i^M \right\}, \\ G_1^{Ni}(t) &= \frac{1}{1 + \tau_N} \left\{ \alpha_E^{Ni} G_i^E + \alpha_M^{Ni} G_i^M \tau_N \right\}, & G_2^{Ni}(t) &= \frac{1}{1 + \tau_N} \left\{ -\alpha_E^{Ni} G_i^E + \alpha_M^{Ni} G_i^M \right\}, \end{aligned} \quad (86)$$

where α_E^{Ni} and α_M^{Ni} are the SU(6) spin-flavor couplings ($\alpha_E^{pu} = \alpha_E^{nd} = 2$, $\alpha_E^{pd} = \alpha_E^{nu} = 1$, $\alpha_M^{pu} = \alpha_M^{nd} = 4/3$, $\alpha_M^{pd} = \alpha_M^{nu} = -1/3$); $t = -q^2$ is the Euclidean momentum squared and $\tau_N = t/(4m_N^2)$. The Dirac and Pauli form factors $f_{D(P)}^i(t)$ of the quark of flavor i are shown explicitly in Appendix C. Again, Eq. (86) can be separated into a

bare part and a meson cloud part as

$$\begin{aligned} F_1^{N \text{ bare}}(t) &= \sum_{i=u,d} Q_i F_1^{Ni}(t), \\ F_2^{N \text{ bare}}(t) &= \sum_{i=u,d} Q_i F_2^{Ni}(t), \end{aligned} \quad (87)$$

and the meson cloud contribution is

$$\begin{aligned} F_1^{N \text{ cloud}}(t) &= \sum_{i=u,d} [(f_D^i(t) - Q_i) F_1^{Ni}(t) + f_P^i(t) G_1^{Ni}(t)], \\ F_2^{N \text{ cloud}}(t) &= \sum_{i=u,d} [(f_D^i(t) - Q_i) F_2^{Ni}(t) + f_P^i(t) G_2^{Ni}(t)]. \end{aligned} \quad (88)$$

where Q_i are the electric quark charges.

In the following we try to achieve a reasonable description of the electromagnetic form factors of the nucleon by an appropriate set of parameters contained in $F_1^N(t)$ and $F_2^N(t)$. In general both the bare and the meson cloud parts will contribute to the form factors. The bare part should well describe the form factors up to high Q^2 whereas the meson cloud part should play a role only for small Q^2 . Our strategy is that we first fit the bare part of all the form factors to the experimental data from $Q^2 \sim 0.5 \text{ GeV}^2$ to high Q^2 . After that we reconsider the low Q^2 region by taking into account the meson cloud effect. At this point we do not pretend on an accurate analysis (or prediction) of the nucleon form factors at large Q^2 . This is a task more appropriate for perturbative QCD (pQCD) which is the most convenient theoretical tool in this momentum region (for recent progress see e.g. Refs. [52, 53]). In particular, in Ref. [53] the following large Q^2 -behavior for the ratio of the nucleon Pauli F_2 and Dirac F_1 form factors has been derived using pQCD:

$$\frac{F_2}{F_1} \propto \frac{\ln^2(Q^2/\Lambda^2)}{Q^2}, \quad (89)$$

where Λ is a soft scale related to the size of the nucleon. Our main idea is to use a physically reasonable parametrization of the nucleon form factors (valence quark contribution) which fits the data at intermediate and high Q^2 scale, while the derived constraints at zero recoil [see Sec. II] are also satisfied. Then on top of the valence (or bare) form factors we place the meson cloud contribution which is relevant only at small Q^2 . Finally we might conclude on the role of the meson cloud in the infrared domain.

Due to the finite size of the source of the meson fields, meson loops are expected to be strongly suppressed for large Q^2 . To mimic the effect of additional regularisation of the integral, which leads to a restriction of the meson cloud contribution in the low Q^2 region, we introduce the cutoff function $f_{cut}(t)$. The modification is such that

$$F_{1(2)}^{N \text{ cloud}}(t) \rightarrow f_{cut}(t) F_{1(2)}^{N \text{ cloud}}(t). \quad (90)$$

The specific form of $f_{cut}(t)$ should not modify $F_{1(2)}^{N \text{ cloud}}(t)$ in the low Q^2 region, but should diminish its contribution beyond a certain Q^2 . This function $f_{cut}(t)$ should have zero (or almost zero) slope at the point $Q^2 = 0 \text{ GeV}^2$ to ensure that it will not artificially contribute to the slope of the form factors. First the step function seems to be an appropriate choice for $f_{cut}(t)$ but its sharp boundary affects the continuity of the form factors, and hence one must be careful. To avoid the problems associated with a sharp boundary we choose a smeared-out version for $f_{cut}(t)$ with

$$f_{cut}(t) = \frac{1 + \exp(-A/B)}{1 + \exp[(t - A)/B]}, \quad (91)$$

where the parameter A characterizes the cut-off and B the smearing of the function.

In our fitting procedure we use the experimental data (compilation of Ref. [51] and Ref. [54, 55]) on the ratios of the electromagnetic Sachs form factors of nucleons to the corresponding dipole form factors and on the neutron charge form factors. For the axial charge of the constituent quark $g = 0.9$ we first fit the contribution of the bare part, where the parameters are contained in the ansatz of Eq. (77). Our parameter results for the fit of the bare part are (in units of GeV)

$$\begin{aligned} \lambda_{uE} &= 2.0042, \quad \lambda_{dE} = 0.9996, \quad \lambda_{uM} = 7.3367, \quad \lambda_{dM} = 2.2954, \\ \Lambda_{uE} &= 0.8616, \quad \Lambda_{dE} = 0.9234, \quad \Lambda_{uM} = 0.9278, \quad \Lambda_{dM} = 1.0722. \end{aligned} \quad (92)$$

Note that the parameters γ_u and γ_d entering in Eq. (77) cannot be fixed by considering only the bare part since they also occur in $F_1^{N\text{cloud}}(t)$ and $F_2^{N\text{cloud}}(t)$.

We simplify the further fitting of the meson cloud contribution by the following conditions. First, we set $\tilde{e}_1 = 0$ which results in $c_2 = 2.502 \text{ GeV}^{-1}$, $c_6 = -0.583 \text{ GeV}^{-1}$, $c_7 = 0.145 \text{ GeV}^{-1}$, and $c_8 = 0.302 \text{ GeV}^{-1}$. Second, for the parameter k_V as will be discussed in the next section, for the sake of simplicity we set $k_V = 0$. Therefore, the remaining parameters needed to be fitted are c_4 , d_6 , d_7 , d_8 , e_{54} , e_{74} , e_{94} , γ_u , and γ_d .

The complete fit to the full data on the electromagnetic form factors of the nucleon fixes the remaining low-energy constants in the effective Lagrangian as

$$\begin{aligned} \gamma_u &= 1.525, \quad \gamma_d = 2.373, \quad c_4 = 1.667 \text{ GeV}^{-1}, \\ \hat{d}_6 &= -0.043 \text{ GeV}^{-2}, \quad d_7 = 0.249 \text{ GeV}^{-2}, \quad \bar{d}_8 = 0.337 \text{ GeV}^{-2}, \\ e_{54} &= 0.157 \text{ GeV}^{-3}, \quad \hat{e}_{74} = -0.743 \text{ GeV}^{-3}, \quad \bar{e}_{94} = -0.301 \text{ GeV}^{-3}, \end{aligned} \quad (93)$$

where the couplings \hat{d}_6 , \bar{d}_8 , \hat{e}_{74} and \bar{e}_{94} are defined in Appendix C. With the choice $A = 0.55 \text{ GeV}^2$ and $B = 0.05 \text{ GeV}^2$ in $f_{cut}(t)$ the meson cloud contributions are suitably suppressed for values larger than $t \sim 0.5 \text{ GeV}^2$.

Results for the measured ratio of the electromagnetic form factors of the nucleon to the dipole form factor $G_D(t) = (1 + t/0.71 \text{ GeV}^2)^{-2}$ are presented in Figs. 5-7. In Fig. 8 we indicate the result for the neutron charge form factor. For completeness, the electromagnetic form factors of the nucleon are also shown in Figs. 8-11, where the meson cloud contributions are shown explicitly in comparison to the dipole form factor. The role of $f_{cut}(t)$, which restricts the meson cloud contribution to the low Q^2 region, is indicated in Figs. 12-15. In Fig. 16 we also present our result for the ratio of charge to magnetic form factor of the proton. Although the bare constituent quark contribution is fully parameterized, a consistent explanation of the form factors can only be achieved, when meson cloud corrections are included. We stress that the bare constituent quark Sachs form factors and hence the magnetic form factors at zero recoil ($t = 0$) are determined by the general constraints discussed in Sect. III.B. At this point the specific form of the quark form factors of Eq. (77), leading to a satisfactory description in particular beyond $t \sim 0.5 \text{ GeV}^2$, is not required. The results concerning the charge and magnetic radii of nucleons are

$$\begin{aligned} r_E^p &= 0.871 \text{ fm}, \quad \langle r^2 \rangle_E^n = -0.1154 \text{ fm}^2, \\ r_M^p &= 0.870 \text{ fm}, \quad r_M^n = 0.847 \text{ fm}. \end{aligned} \quad (94)$$

The experimental values reported in Ref. [49] for the charge radii of nucleons are $r_E^p = 0.875 \pm 0.007 \text{ fm}$ and $\langle r^2 \rangle_E^n = -0.1161 \pm 0.0022 \text{ fm}^2$. For the magnetic radii, the analysis of Refs. [59, 60] gives $r_M^p = 0.855 \pm 0.035 \text{ fm}$ and $r_M^n = 0.873 \pm 0.011 \text{ fm}$, respectively.

For further illustration we follow Ref. [50] to deduce the radial dependence of the charge and magnetization densities of nucleons. The charge and magnetization densities of nucleons in the rest frame are

$$\rho_E^N(r) = \frac{2}{\pi} \int_0^\infty dk k^2 j_0(kr) \tilde{\rho}_E^N(k), \quad \rho_M^N(r) = \frac{2}{\pi} \int_0^\infty dk k^2 j_0(kr) \tilde{\rho}_M^N(k), \quad (95)$$

where $k^2 = t/(1 + \tau_N)$ and $j_0(kr)$ is the Bessel function. The intrinsic form factors $\tilde{\rho}_E^N(k)$ and $\tilde{\rho}_M^N(k)$ are

$$\tilde{\rho}_E^N(k) = G_E^N(Q^2)(1 + \tau_N)^{\lambda^E}, \quad \tilde{\rho}_M^N(k) = \frac{G_M^N(Q^2)}{\mu_N}(1 + \tau_N)^{\lambda^M}. \quad (96)$$

Restricting to the discrete values $\lambda^E = 0, 1, 2$, where the full range is discussed in Ref. [50], the results for the charge and magnetization densities of the nucleon are shown in Figs. 17-20.

In Ref. [51] the electromagnetic form factors of the nucleons are represented by the phenomenological ansatz

$$G_N(Q^2) = G_s(Q^2) + a_b \cdot Q^2 G_b(Q^2), \quad (97)$$

where the "smooth" part $G_s(Q^2)$ and the structured or "bump" part $G_b(Q^2)$ are parameterized as

$$\begin{aligned} G_s(Q^2) &= \frac{a_{10}}{(1 + Q^2/a_{11})^2} + \frac{a_{20}}{(1 + Q^2/a_{21})^2}, \\ G_b(Q^2) &= e^{-\frac{1}{2} \left(\frac{Q - Q_b}{\sigma_b} \right)^2} + e^{-\frac{1}{2} \left(\frac{Q + Q_b}{\sigma_b} \right)^2}. \end{aligned} \quad (98)$$

The parameters a_{10} , a_{11} , a_{20} , a_{21} , a_b , Q_b , and σ_b are obtained by a fit to experimental data and the values are reported in Table 2 of Ref. [51]. The meson cloud part of our evaluation cannot be directly compared or matched to $G_b(Q^2)$,

since meson corrections contribute to the magnetic form factors even at $Q^2 = 0$, which is not the case in the treatment of Ref. [51]. However, charge conservation restricts the meson cloud not to contribute to the charge form factors at zero recoil. Therefore, we can compare our results for the charge form factors to the phenomenological ones of Ref. [51]. Fig. 21 shows such a comparison for the case of the charge form factor of the proton. Based on the phenomenological ansatz of Ref. [51] our result can be reproduced by readjusting the parameters of Eq. (98) as compiled in Table 3, which are not so much different from the original analysis of Ref. [51].

D. Coupling of vector mesons to the nucleon

Finally, we calculate the strong vector meson-nucleon form factors ρNN and ωNN at one loop. We follow the strategy already developed for the electromagnetic nucleon form factors. The corresponding bare operator is derived from the tree-level Lagrangian (15):

$$J_{\mu,V}^{\text{bare}}(q) = \int d^4x e^{-iqx} j_{\mu,V}^{\text{bare}}(x), \quad j_{\mu,V}^{\text{bare}}(x) = g_{Vqq} \bar{q} \left(\gamma_\mu + \frac{k_V}{2m} \sigma_{\mu\nu} \overset{\leftrightarrow}{\partial}^\nu \right) \frac{\lambda_V}{2} q, \quad (99)$$

where $\bar{q} \overset{\leftrightarrow}{\partial}^\nu q = \bar{q} (\overset{\leftarrow}{\partial}^\nu + \overset{\rightarrow}{\partial}^\nu) q$ and λ_V is the corresponding flavor matrix: $\lambda_\rho = \text{diag}\{1, -1, 0\}$ for the ρ^0 and $\lambda_\omega = \text{diag}\{1, 1, 0\}$ for the ω meson.

The diagrams contributing to these quantities are displayed in Fig.3: tree-level diagrams (Figs.3(1) and 3(2)) and one-loop diagrams due to the dressing by a cloud of pseudoscalar mesons (Figs.3(3) and 3(4)).

The Fourier transform of the dressed vector-meson-quark transition operator has the following form

$$J_{\mu,V}^{\text{dress}}(q) = \frac{1}{2} \int d^4x e^{-iqx} \bar{q}(x) \left[\gamma_\mu f_{V_D}(q^2) + \frac{i}{2m} \sigma_{\mu\nu} q^\nu f_{V_P}(q^2) \right] q(x) \quad (100)$$

where f_{V_D} and f_{V_P} are the matrices of the Dirac and Pauli form factors describing the coupling of u , d and s quarks to the ρ and ω vector mesons. These form factors are given in terms of the Euclidean values of momentum squared $t = -q^2$ with:

$$f_{V_D}(t) = \sum_{i=u,d,s} f_{V_D}^i(t), \quad f_{V_P}(t) = \sum_{i=u,d,s} f_{V_P}^i(t). \quad (101)$$

and

$$\begin{aligned} f_{\rho_D}^u(t) &= -f_{\rho_D}^d(t) = g_{Vqq} \left\{ 1 - \epsilon_5^\pi(t) + \frac{1}{3} \epsilon_5^\eta(t) \right\}, \\ f_{\omega_D}^u(t) &= f_{\omega_D}^d(t) = g_{Vqq} \left\{ 1 + 3\epsilon_5^\pi(t) + \frac{1}{3} \epsilon_5^\eta(t) \right\}, \\ f_{\rho_D}^s(t) &= 0, \quad f_{\omega_D}^s(t) = g_{Vqq} \left\{ -4 \epsilon_5^K(t) \right\}, \\ f_{\rho_P}^u(t) &= -f_{\rho_P}^d(t) = k_V g_{Vqq} \left\{ 1 - m_{10}^\pi(t) + \frac{1}{3} m_{10}^\eta(t) \right\}, \\ f_{\omega_P}^u(t) &= f_{\omega_P}^d(t) = k_V g_{Vqq} \left\{ 1 + 3m_{10}^\pi(t) + \frac{1}{3} m_{10}^\eta(t) \right\}, \\ f_{\rho_P}^s(t) &= 0, \quad f_{\omega_P}^s(t) = k_V g_{Vqq} \left\{ -4 m_{10}^K(t) \right\}, \end{aligned} \quad (102)$$

where $\lambda_\phi = \text{diag}\{0, 0, 1\}$. Here $\epsilon_5^P(t)$ and $m_5^P(t)$ are the meson-cloud contributions. Their expressions are given in Appendix C (see Eq. (C11)).

To project the dressed quark operator (100) onto the nucleon we proceed in analogy to the electromagnetic operator (see Eq. 19) as:

$$\begin{aligned} \langle N(p') | J_{\mu,V}^{\text{dress}}(q) | N(p) \rangle &= (2\pi)^4 \delta^4(p' - p - q) \bar{u}_N(p') \frac{1}{2} \left\{ \gamma_\mu G_{VNN}(q^2) + \frac{i}{2m_N} \sigma_{\mu\nu} q^\nu F_{VNN}(q^2) \right\} u_N(p) \\ &= (2\pi)^4 \delta^4(p' - p - q) \frac{1}{2} \left\{ f_{V_D}^{ij}(q^2) \langle N(p') | j_{\mu,ij}^{\text{bare}}(0) | N(p) \rangle + i \frac{q^\nu}{2m} f_{V_P}^{ij}(q^2) \langle N(p') | j_{\mu\nu,ij}^{\text{bare}}(0) | N(p) \rangle \right\}, \end{aligned} \quad (103)$$

where the bare matrix elements $\langle N(p') | j_{\mu\nu,ij}^{\text{bare}}(0) | N(p) \rangle$ are defined in Eq. (20). Here $G_{VNN}(q^2)$ and $F_{VNN}(q^2)$ are the vectorial and tensorial couplings of vector mesons to nucleons. We can express the strong ρNN and ωNN form factors through the bare electromagnetic nucleon form factors. After a simple algebra we arrive at:

$$\begin{aligned} G_{\rho NN}(t) &= g_{Vqq} [F_1^{p-}(t) f_{\rho_D}^u(t) + G_1^{p-}(t) f_{\rho_P}^u(t)], \\ G_{\omega NN}(t) &= g_{Vqq} [F_1^{p+}(t) f_{\omega_D}^u(t) + G_1^{p+}(t) f_{\omega_P}^u(t)], \\ F_{\rho NN}(t) &= g_{Vqq} [F_2^{p-}(t) f_{\rho_D}^u(t) + G_2^{p-}(t) f_{\rho_P}^u(t)], \\ F_{\omega NN}(t) &= g_{Vqq} [F_2^{p+}(t) f_{\omega_D}^u(t) + G_2^{p+}(t) f_{\omega_P}^u(t)], \end{aligned} \quad (104)$$

where $t = -q^2$ and $H_I^{p\pm} = H_I^{pu} \pm H_I^{pd}$ with $H = F$ or G and $I = 1$ or 2 .

Finally, we present the expressions for the values of the vector-meson nucleon form factors at zero recoil or the coupling constants G_{VNN} and F_{VNN} which originate from the nucleon-level Lagrangian (for details on the nucleon-level Lagrangian see Ref. [8]):

$$\mathcal{L}_{VNN} = \frac{1}{2} \bar{N} \left\{ \left(\gamma^\mu G_{\rho NN} - \frac{F_{\rho NN}}{2 \overset{\circ}{m}_N} \sigma^{\mu\nu} \partial_\nu \right) \vec{\rho}_\mu \vec{\tau} + \left(\gamma^\mu G_{\omega NN} - \frac{F_{\omega NN}}{2 \overset{\circ}{m}_N} \sigma^{\mu\nu} \partial_\nu \right) \omega_\mu \right\} N. \quad (105)$$

After a simple algebra we arrive at:

$$\begin{aligned} G_{\rho NN} &= g_{Vqq}, \quad \frac{F_{\rho NN}}{G_{\rho NN}} = \mu_p^{\text{bare}} - \mu_n^{\text{bare}} - 1 + k_V \frac{\overset{\circ}{m}_N}{m} (\delta_{pu}^{\text{bare}} - \delta_{pd}^{\text{bare}}) [1 + \delta_\rho], \\ G_{\omega NN} &= 3 g_{Vqq}, \quad \frac{F_{\omega NN}}{G_{\omega NN}} = \mu_p^{\text{bare}} + \mu_n^{\text{bare}} - 1 + k_V \frac{\overset{\circ}{m}_N}{m} (\delta_{pu}^{\text{bare}} + \delta_{pd}^{\text{bare}}) [1 + \delta_\omega], \end{aligned} \quad (106)$$

where

$$\delta_\rho = -m_{10}^\pi(0) + \frac{1}{3} m_{10}^\eta(0), \quad \delta_\omega = 3m_{10}^\pi(0) + \frac{1}{3} m_{10}^\eta(0) \quad (107)$$

are the corresponding one-loop corrections. For $k_V \equiv 0$ these equations reduce to the well-known SU(3) relations, relating the matrix elements of the vector current with different flavor content [61]. Using the actual expressions for the bare magnetic moments and the tensor charges of the nucleons we finally obtain for the ratios of the tensor and vector couplings:

$$\frac{F_{\rho NN}}{G_{\rho NN}} = \left(\frac{g_A}{g} \right)^4 \left(1 + k_V [1 + \delta_\rho] \right) - 1, \quad \frac{F_{\omega NN}}{G_{\omega NN}} = \frac{1}{5} \left(\frac{g_A}{g} \right)^4 \left(1 + 3 k_V [1 + \delta_\omega] \right) - 1. \quad (108)$$

Note, that numerically the one-loop corrections to the tree-level results for the strong vector-meson nucleon form factors $F_{\rho NN}$ and $F_{\omega NN}$ are rather small: $\delta_\rho = 0.005$ and $\delta_\omega = 0.011$.

V. SUMMARY

We developed a manifestly Lorentz covariant chiral quark model for the study of baryons as bound states of constituent quarks. The approach is based on the effective chiral Lagrangian involving constituent quarks and the chiral fields as effective degrees of freedom. This Lagrangian is used in the calculation of the dressed transition operators which are relevant for the interaction of quarks with external fields in the presence of a virtual meson cloud. Then the dressed operators are used in the calculation of baryon matrix elements.

Our main result is as follows: we perform a model-independent factorization of the effects of hadronization and confinement contained in the matrix elements of the bare quark operators and the effects dictated by chiral symmetry which are encoded in the corresponding relativistic form factors [see e.g. Eq. (19)]. Due to this factorization the calculation of chiral effects and the effects of hadronization and confinement can be done independently. All low-energy theorems are reproduced in our approach due to the chiral invariance of the effective Lagrangian. The evaluated meson-cloud corrections are in agreement with the infrared-singular structure of the corresponding nucleon matrix elements [8, 37]. In particular, we reproduce the leading nonanalytic (LNA) contributions to the nucleon mass, to the pion-nucleon sigma-term, to the magnetic moments and to the charge radii of the nucleons. The LNA contributions to the nucleon mass and magnetic moment are proportional to the M_P^3 and M_P , respectively, where M_P is the pseudoscalar meson mass. The nucleon radii are divergent in the chiral limit. Using model-independent constraints on the bare constituent quark distributions in the octet baryons, we work out model predictions for the magnetic moments. Based on a full parameterization of the bare constituent quark distributions in the nucleon, we give results for the full momentum dependence of the electromagnetic form factors of the nucleon and indicate the role of the meson cloud contributions. Presently, the calculation of the matrix elements of the bare quark operators is, besides the model independent constraints, based on parameterizations. The direct calculation of these matrix elements should be performed in quark models based on specific assumptions about hadronization and confinement.

Acknowledgments

This work was supported by the DFG under contracts FA67/25-3 and GRK683. This research is also part of the EU Integrated Infrastructure Initiative Hadronphysics project under contract number RI3-CT-2004-506078 and President grant of Russia "Scientific Schools" No. 1743.2003. K.P. thanks the Development and Promotion of Science and Technology Talent Project (DPST), Thailand for financial support.

APPENDIX A: CALCULATIONAL TECHNIQUE OF LOOP DIAGRAMS

The calculational technique of the loop diagrams in Figs.1, 2, 3 and 4 is referred to as *the infrared dimensional regularization* (IDR) and has been discussed in detail in Refs. [5, 8]. Our case here differs by the use of the constituent quark degrees of freedom instead of the nucleon. We briefly recall the basic ideas of this technique. As we discussed before, in Baryon ChPT loop integrals are non-homogeneous functions of the mesonic momenta and the quark masses due to the presence of a new scale parameter, the nucleon mass. As a result, the loop integral contains an infrared singular part containing the fractional powers of the meson masses and an infrared regular part involving the fractional powers of the nucleon mass. Due to the presence of the regular parts in the loop integrals, their chiral expansion starts at the same order as the tree graphs, it therefore spoils the power counting rules. The idea of the IDR method is to remove the infrared regular parts of the loop integrals from the consideration and to absorb them in the low-energy couplings of the underlying chiral Lagrangian. The IDR method is consistent with Lorentz and gauge invariance. Also, the chiral power countings are preserved and the Ward identities of chiral symmetry are fulfilled.

The method can be explained by using the simple example of the self-energy graph shown in Fig.4(3) contributing to the quark mass operator [5, 8]. We consider the scalar loop integral in d dimensions:

$$H(p^2) = \int \frac{d^d k}{(2\pi)^d} \frac{1}{[M^2 - k^2 - i\epsilon][m^2 - (p - k)^2 - i\epsilon]} \quad (A1)$$

where M and m are the meson and constituent quark masses, respectively. Using the master formula in d -dimensions

$$\int \frac{d^d k}{(2\pi)^d} \frac{k^{2n}}{[M^2 - k^2]^m} = \frac{i^{2n+1}}{(4\pi)^{d/2}} \frac{\Gamma(n + d/2) \Gamma(m - n - d/2)}{\Gamma(d/2) \Gamma(m)} M^{2(n-m)+d} \quad (A2)$$

we get at threshold $p^2 = (m + M)^2$:

$$H(p^2) = \underbrace{c_d \frac{M^{d-3}}{m+M}}_{=I(p^2)} + \underbrace{c_d \frac{m^{d-3}}{m+M}}_{=R(p^2)}, \quad c_d = \frac{\Gamma(2 - d/2)}{(4\pi)^{d/2} (d - 3)}, \quad (A3)$$

Here $I(p^2)$ is the infrared singular piece which is characterized by fractional powers of M and generated by the loop momenta of order of the meson mass. For $I(p^2)$ the usual power counting applies. Another piece in the decomposition of $H(p^2)$ defined by $R(p^2)$ is the infrared regular part which is generated by the loop momenta of the order of the constituent quark mass m (in our counting m is of the order of $\Lambda_{\chi SB} \sim 1$ GeV). As discussed before, we remove the regular part $R(p^2)$ by redefining the low-energy coupling constants in the chiral Lagrangian. In Ref. [5] a recipe was suggested how to split the integral $H(p^2)$ into the singular and regular parts. We use the Feynman parametrization to combine two multipliers $a = M^2 - k^2 - i\epsilon$ and $b = m^2 - (p - k)^2 - i\epsilon$ in the denominator of $H(p^2)$:

$$\int \frac{d^d k}{(2\pi)^d} \frac{1}{a b} = \int \frac{d^d k}{(2\pi)^d} \int_0^1 \frac{dx}{[a(1-x) + bx]^2} \quad (A4)$$

and then to write down the integral from 0 to 1 as the difference of two integrals:

$$\int_0^1 dx \dots = \left[\int_0^\infty - \int_1^\infty \right] dx \dots \quad (A5)$$

Then the integral from 0 to ∞ is exactly the infrared singular part and the integral from 1 to ∞ is the infrared regular one. This method can be applied to any general one-loop integral with adjustable number of meson and quark propagators. The calculational technique suggests that: one should separate numerator and denominator; simplify the numerator using the standard (invariant integration) methods. Finally, the result can be reduced to the master integral $I(p^2)$ and its derivatives (like in the conventional dimensional regularization). The integrals containing only the quark propagators do not contribute to the infrared singular parts, and therefore, vanish in the *infrared dimensional regularization*.

The ultraviolet divergencies contained in the one-loop integrals are removed via the renormalization of the low-energy constants in the chiral Lagrangian. To perform the renormalization of the constituent quark at one loop and to guarantee charge conservation we need the Z -factor (the wave-function renormalization constant), which is

determined by the derivative of the quark mass operator (generated by the diagrams in Fig.4) with respect to its momentum:

$$Z_q^{-1} = 1 - \frac{\partial \Sigma_q(\not{p})}{\partial \not{p}} \Big|_{\not{p}=m_q}, \quad q = u, d, s. \quad (\text{A6})$$

The matrix $Z_q = \text{diag}\{Z_u, Z_d, Z_s\}$ with $Z_u = Z_d = Z$ is given up to fourth order by

$$Z_q = I + \sum_{P=\pi, K, \eta} \frac{1}{F_P^2} \left[-g^2 \alpha_P \Delta_P + Q_P \right] \quad (\text{A7})$$

where

$$\begin{aligned} \Delta_P &= 2 M_P^2 \left[\lambda(\mu) + \frac{1}{16\pi^2} \ln \left(\frac{M_P}{\mu} \right) \right], \quad \lambda(\mu) = \frac{\mu^{d-4}}{(4\pi)^2} \left[\frac{1}{d-4} - \frac{1}{2} (\ln 4\pi + \Gamma'(1) + 1) \right], \\ Q_P &= \frac{g^2 M_P^2}{24\pi^2} \alpha_P \left[-1 + \frac{3\pi}{2} \frac{M_P}{m} + \frac{3}{2} \frac{M_P^2}{m^2} \right] + \frac{3c_2 M_P^4}{64\pi^2 m} \beta_P I, \\ \alpha_\pi &= \frac{9}{2} Q + \frac{3}{2} I - \frac{9}{4} \lambda_3, \quad \alpha_K = -3Q + 2I + \frac{3}{2} \lambda_3, \quad \alpha_\eta = -\frac{3}{2} Q + \frac{I}{2} + \frac{3}{4} \lambda_3, \\ \beta_\pi &= 1, \quad \beta_K = \frac{4}{3}, \quad \beta_\eta = \frac{1}{3}. \end{aligned} \quad (\text{A8})$$

For the evaluation of the form factor $f_D^{ij}(q^2)$, the quark charge Q [diagram in Fig.1(1)] has to be multiplied by Z_q . For $f_D^{ij}(q^2)$, a second-order contribution to the quark anomalous magnetic moment proportional to the c_i with $i = 6, 7, 8$ [diagrams in Figs.1(2) and 2(2*)] has to be renormalized by the Z_q -factor. The term proportional to c_2 must be dropped, because the product $c_i c_2$ is of higher-order when compared to the accuracy we are working in.

APPENDIX B: LOOP INTEGRALS

In this appendix, we present the loop integrals contributing to the electromagnetic transition operator between constituent quarks and evaluate them in the infrared regularization scheme [5]. Originally, these integrals have been introduced in chiral perturbation theory (ChPT) [5, 8].

For the momenta of initial, final quark and photon field we introduce the notations: p, p' and $q = p' - p$, respectively. We also introduce the notation $P = p' + p$. Since the external quarks are on the mass shell $p^2 = p'^2 = m^2$, the structure integrals can be expanded through a set of scalar functions which exclusively depend on the transverse momentum squared $t = Q^2 = -q^2$ and the masses of meson M and constituent quark m . As usual [5, 8], we identify the masses of particles occurring in the loop integrals with their leading order values, $M_P \rightarrow \overset{\circ}{M}_P$ and $m_q \rightarrow m$. For universality, we calculate the integrals for adjustable values of the constituent quark mass inside the loop (m^*) and for the external line (m). Finally, in numerical calculations we will neglect the difference between the masses m^* and m , setting $m^* \equiv m$.

1. Infrared parts of loop integrals

We deal with the following loop integrals:

$$\int_I \frac{d^d k}{(2\pi)^d i} \frac{1}{M^2 - k^2} = \Delta_M, \quad (\text{B1})$$

$$\int_I \frac{d^d k}{(2\pi)^d i} \frac{1}{[M^2 - k^2][M^2 - (k + q)^2]} = J^{(0)}(t, M^2), \quad (\text{B2})$$

$$\int_I \frac{d^d k}{(2\pi)^d i} \frac{k_\mu}{[M^2 - k^2][M^2 - (k + q)^2]} = -\frac{1}{2} q_\mu J^{(0)}(t, M^2), \quad (\text{B3})$$

$$\int_I \frac{d^d k}{(2\pi)^d i} \frac{k_\mu k_\nu}{[M^2 - k^2][M^2 - (k+q)^2]} = (q_\mu q_\nu - g_{\mu\nu} t) J^{(1)}(t, M^2) + q_\mu q_\mu J^{(2)}(t, M^2), \quad (\text{B4})$$

$$\int_I \frac{d^d k}{(2\pi)^d i} \frac{1}{[M^2 - k^2][m^{*2} - (p-k)^2]} = I^{(0)}(M^2, m^2, m^{*2}), \quad (\text{B5})$$

$$\int_I \frac{d^d k}{(2\pi)^d i} \frac{k_\mu}{[M^2 - k^2][m^{*2} - (p-k)^2]} = p_\mu I^{(1)}(M^2, m^2, m^{*2}), \quad (\text{B6})$$

$$\int_I \frac{d^d k}{(2\pi)^d i} \frac{1}{[M^2 - k^2][m^{*2} - (p-k)^2][m^{*2} - (p'-k)^2]} = I_{12}^{(0)}(t, M^2, m^2, m^{*2}), \quad (\text{B7})$$

$$\int_I \frac{d^d k}{(2\pi)^d i} \frac{k_\mu}{[M^2 - k^2][m^{*2} - (p-k)^2][m^{*2} - (p'-k)^2]} = P_\mu I_{12}^{(1)}(t, M^2, m^2, m^{*2}), \quad (\text{B8})$$

$$\begin{aligned} \int_I \frac{d^d k}{(2\pi)^d i} \frac{k_\mu k_\nu}{[M^2 - k^2][m^{*2} - (p-k)^2][m^{*2} - (p'-k)^2]} &= g_{\mu\nu} I_{12}^{(2)}(t, M^2, m^2, m^{*2}) \\ &+ P_\mu P_\nu I_{12}^{(3)}(t, M^2, m^2, m^{*2}) + q_\mu q_\nu I_{12}^{(4)}(t, M^2, m^2, m^{*2}), \end{aligned} \quad (\text{B9})$$

$$\int_I \frac{d^d k}{(2\pi)^d i} \frac{1}{[M^2 - k^2][M^2 - (k+q)^2][m^{*2} - (p-k)^2]} = I_{21}^{(0)}(t, M^2, m^2, m^{*2}), \quad (\text{B10})$$

$$\begin{aligned} \int_I \frac{d^d k}{(2\pi)^d i} \frac{k_\mu}{[M^2 - k^2][M^2 - (k+q)^2][m^{*2} - (p-k)^2]} &= P_\mu I_{21}^{(1)}(t, M^2, m^2, m^{*2}) \\ &- \frac{1}{2} q_\mu I_{21}^{(0)}(t, M^2, m^2, m^{*2}), \end{aligned} \quad (\text{B11})$$

$$\begin{aligned} \int_I \frac{d^d k}{(2\pi)^d i} \frac{k_\mu k_\nu}{[M^2 - k^2][M^2 - (k+q)^2][m^{*2} - (p-k)^2]} &= g_{\mu\nu} I_{21}^{(2)}(t, M^2, m^2, m^{*2}) \\ &+ P_\mu P_\nu I_{21}^{(3)}(t, M^2, m^2, m^{*2}) + q_\mu q_\nu I_{21}^{(4)}(t, M^2, m^2, m^{*2}) \\ &- \frac{1}{2} (P_\mu q_\nu + P_\nu q_\mu) I_{21}^{(1)}(t, M^2, m^2, m^{*2}), \end{aligned} \quad (\text{B12})$$

where the symbol \int_I represents the loop integration according to the infrared dimensional regularization scheme [5, 8].

2. Reduction formulas for loop integrals

Higher-order tensorial integrals can be reduced to the basic scalar integrals using the invariant integration [5, 8]:

$$J^{(1)}(t, M^2) = \frac{1}{4(d-1)t} \left[(t+4M^2) J^{(0)}(t, M^2) - 2\Delta_M \right], \quad (\text{B13})$$

$$J^{(2)}(t, M^2) = \frac{1}{4} J^{(0)}(t, M^2) + \frac{1}{2t} \Delta_M, \quad (\text{B14})$$

$$I^{(1)}(M^2, m^2, m^{*2}) = \frac{1}{2m^2} \left[M^{*2} I^{(0)}(M^2, m^2, m^{*2}) + \Delta_M \right], \quad (\text{B15})$$

$$I_{12}^{(1)}(t, M^2, m^2, m^{*2}) = \frac{1}{4m^2 + t} \left[I^{(0)}(M^2, m^2, m^{*2}) + M^{*2} I_{12}^{(0)}(t, M^2, m^2, m^{*2}) \right], \quad (\text{B16})$$

$$I_{12}^{(2)}(t, M^2, m^2, m^{*2}) = \frac{1}{d-2} \left[M^2 I_{12}^{(0)}(t, M^2, m^2, m^{*2}) - M^{*2} I_{12}^{(1)}(t, M^2, m^2, m^{*2}) \right], \quad (B17)$$

$$\begin{aligned} I_{12}^{(3)}(t, M^2, m^2, m^{*2}) &= \frac{1}{(d-2)(4m^2+t)} \left[M^{*2} (d-1) I_{12}^{(1)}(t, M^2, m^2, m^{*2}) \right. \\ &\quad \left. - M^2 I_{12}^{(0)}(t, M^2, m^2, m^{*2}) + \frac{d-2}{2} I^{(1)}(M^2, m^2, m^{*2}) \right], \end{aligned} \quad (B18)$$

$$\begin{aligned} I_{12}^{(4)}(t, M^2, m^2, m^{*2}) &= \frac{1}{(d-2)t} \left[-M^{*2} I_{12}^{(1)}(t, M^2, m^2, m^{*2}) \right. \\ &\quad \left. + M^2 I_{12}^{(0)}(t, M^2, m^2, m^{*2}) + \frac{d-2}{2} I^{(1)}(M^2, m^2, m^{*2}) \right], \end{aligned} \quad (B19)$$

$$\begin{aligned} I_{21}^{(1)}(t, M^2, m^2, m^{*2}) &= \frac{1}{2(4m^2+t)} \left[(2M^{*2} + t) I_{21}^{(0)}(t, M^2, m^2, m^{*2}) \right. \\ &\quad \left. - 2I^{(0)}(M^2, m^2, m^{*2}) + 2J^{(0)}(t, M^2) \right], \end{aligned} \quad (B20)$$

$$\begin{aligned} I_{21}^{(2)}(t, M^2, m^2, m^{*2}) &= \frac{1}{4(d-2)} \left[(4M^2 + t) I_{21}^{(0)}(t, M^2, m^2, m^{*2}) \right. \\ &\quad \left. - 2(2M^{*2} + t) I_{21}^{(1)}(t, M^2, m^2, m^{*2}) - 2I^{(0)}(M^2, m^2, m^{*2}) \right], \end{aligned} \quad (B21)$$

$$\begin{aligned} I_{21}^{(3)}(t, M^2, m^2, m^{*2}) &= \frac{1}{4(d-2)(4m^2+t)} \left[-(4M^2 + t) I_{21}^{(0)}(t, M^2, m^2, m^{*2}) \right. \\ &\quad + 2(d-1)(2M^{*2} + t) I_{21}^{(1)}(t, M^2, m^2, m^{*2}) \\ &\quad \left. + 2I^{(0)}(M^2, m^2, m^{*2}) - 2(d-2)I^{(1)}(M^2, m^2, m^{*2}) \right], \end{aligned} \quad (B22)$$

$$\begin{aligned} I_{21}^{(4)}(t, M^2, m^2, m^{*2}) &= \frac{1}{4(d-2)} \left[-(4M^2 + (d-1)t) I_{21}^{(0)}(t, M^2, m^2, m^{*2}) \right. \\ &\quad + 2(2M^{*2} + t) I_{21}^{(1)}(t, M^2, m^2, m^{*2}) \\ &\quad \left. - 2(d-3)I^{(0)}(M^2, m^2, m^{*2}) + 2(d-2)I^{(1)}(M^2, m^2, m^{*2}) \right]. \end{aligned} \quad (B23)$$

where $M^{*2} = M^2 + m^2 - m^{*2}$.

3. Scalar loop integrals

The scalar loop integrals are given as [5, 8]

$$\Delta_M = 2M^2\lambda_M, \quad \lambda_M = \frac{M^{d-4}}{(4\pi)^2} \left\{ \frac{1}{d-4} - \frac{1}{2}(\ln 4\pi + \Gamma'(1) + 1) \right\}, \quad (B24)$$

$$J^{(0)}(t, M^2) = -2\lambda_M - \frac{1}{16\pi^2} \left[1 + k\left(\frac{t}{M^2}\right) \right], \quad (B25)$$

$$I^{(0)}(M^2, m^2, m^{*2}) = -\frac{M^{*2}}{m^2} \left[\lambda_M - \frac{1}{32\pi^2} \right] - \frac{\mu^*}{8\pi^2} g(0, M, m, m^*) [1 - \Omega^2] r^{*3}, \quad (B26)$$

$$I_{12}^{(1)}(t, M^2, m^2, m^{*2}) = -\frac{f\left(\frac{t}{m^2}\right)}{m^2} \left[\lambda_M + \frac{1}{32\pi^2} \right] + \frac{M^{*2}}{32\pi^2 M m^3} g\left(\frac{t}{m^2}, M, m, m^*\right), \quad (B27)$$

$$I_{21}^{(1)}(t, M^2, m^2, m^{*2}) = \frac{f\left(\frac{t}{m^2}\right)}{m^2} \left[\lambda_M + \frac{1}{32\pi^2} \right] + \frac{1}{32\pi^2 m^2} \left[h_1\left(\frac{t}{M^2}, M, m, m^*\right) + 2 \left(\frac{1}{\mu^*} + \Omega \right) h_2\left(\frac{t}{M^2}, M, m, m^*\right) \right], \quad (B28)$$

where

$$\Omega = \frac{m^2 - m^{*2} - M^2}{2m^*M}, \quad \mu = \frac{M}{m}, \quad \mu^* = \frac{M}{m^*}, \quad r^* = \frac{m^*}{m}.$$

The dimensionless functions k , f , g , h_1 and h_2 are given by the expressions

$$k(s) = \int_0^1 dx \ln(1 + x(1-x)s) = \sqrt{\frac{4+s}{s}} \ln \frac{\sqrt{4+s} + \sqrt{s}}{\sqrt{4+s} - \sqrt{s}} - 2, \quad (B29)$$

$$f(s) = \int_0^1 dx \frac{1}{1 + x(1-x)s} = \frac{2}{\sqrt{s(4+s)}} \ln \frac{\sqrt{4+s} + \sqrt{s}}{\sqrt{4+s} - \sqrt{s}}, \quad (B30)$$

$$g(s, M, m, m^*) = \int_0^1 dx \frac{\arccos \left[-r^* (\Omega + \mu^*) \frac{\sqrt{r^{*2} + x(1-x)s}}{1 + x(1-x)s} \right]}{[1 + x(1-x)s] \sqrt{(1 - \Omega^2)r^{*2} + x(1-x)s}}, \quad (B31)$$

$$h_1(s, M, m, m^*) = \int_0^1 dx \frac{\ln[1 + x(1-x)s]}{1 + \mu^2 x(1-x)s}, \quad (B32)$$

$$h_2(s, M, m, m^*) = \int_0^1 dx \arccos \left[-\frac{[\mu^*(1 + x(1-x)s) + \Omega] r^*}{\sqrt{1 + \mu^2 x(1-x)s} \sqrt{1 + sx(1-x)}} \right] \times \frac{1}{[1 + \mu^2 x(1-x)s] \sqrt{1 + \Omega^2 + x(1-x)s}}. \quad (B33)$$

APPENDIX C: ELECTROMAGNETIC MESON-CLOUD FORM FACTORS

We explicitly show the contributions of the diagrams in Figs. 1 and 2 to the Dirac and Pauli quark form factors. We use the following notations $f_D^{(i)}(t)$ and $f_P^{(i)}(t)$ where the superscript i refers to the numbering of the diagrams. We expand the diagonal 3×3 matrices $f_D^{(i)}(t)$ and $f_P^{(i)}(t)$ in the basis of the 3×3 matrices Q , I , and λ_3 :

$$Q = \begin{pmatrix} 2/3 & 0 & 0 \\ 0 & -1/3 & 0 \\ 0 & 0 & -1/3 \end{pmatrix}, \quad I = \begin{pmatrix} 1 & 0 & 0 \\ 0 & 1 & 0 \\ 0 & 0 & 1 \end{pmatrix}, \quad \lambda_3 = \begin{pmatrix} 1 & 0 & 0 \\ 0 & -1 & 0 \\ 0 & 0 & 0 \end{pmatrix}. \quad (C1)$$

The contributions of the diagrams in Fig.1 to the Dirac form factors of the u , d and s quark are

$$\begin{aligned} f_D^{(1)}(t) &= Q \bar{Z}_q, \\ f_D^{(2)}(t) &= f_D^{(4)}(t) = f_D^{(8)}(t) = f_D^{(12)}(t) = 0, \\ f_D^{(3)}(t) &= t \left(\hat{d}_6 \lambda_3 + \frac{2}{3} d_7 I + 2 \bar{d}_8 Q \right), \\ f_D^{(i)}(t) &= \sum_{P=\pi,K,\eta} \lambda_i^P \epsilon_i^P, \quad i = 5, 6, 7, 9, 10, 11, \end{aligned} \quad (C2)$$

where \bar{Z}_q is the finite part of the renormalization matrix Z_q defined in Eq. (A7),

$$\begin{aligned}
\lambda_5^\pi &= Q + \frac{1}{3}I - \lambda_3, \quad \lambda_5^K = Q - \frac{1}{9}I - \frac{1}{3}\lambda_3, \quad \lambda_5^\eta = -\frac{8}{3}Q - \frac{2}{9}I + \frac{4}{3}\lambda_3, \\
\lambda_6^\pi &= \lambda_7^\pi = \lambda_9^\pi = \lambda_3, \quad \lambda_6^K = \lambda_7^K = \lambda_9^K = 3Q - \lambda_3, \quad \lambda_6^\eta = \lambda_7^\eta = \lambda_9^\eta = 0, \\
\lambda_{10}^\pi &= c_6 \left(Q + \frac{1}{3}I - \lambda_3 \right) + c_7 \left(2Q + \frac{2}{3}I - \lambda_3 \right) - c_8 \frac{\lambda_3}{2}, \\
\lambda_{10}^K &= c_6 \left(-\frac{8}{3}Q - \frac{2}{9}I + \frac{4}{3}\lambda_3 \right) + c_7 \left(-\frac{4}{3}Q + \frac{8}{9}I + \frac{2}{3}\lambda_3 \right), \\
\lambda_{10}^\eta &= c_6 \left(Q - \frac{1}{9}I - \frac{1}{3}\lambda_3 \right) + c_7 \left(-\frac{2}{3}Q + \frac{2}{9}I + \frac{1}{3}\lambda_3 \right) + c_8 \frac{\lambda_3}{6}, \\
\lambda_{11}^\pi &= Q, \quad \lambda_{11}^K = \frac{4}{3}Q, \quad \lambda_{11}^\eta = \frac{1}{3}Q. \tag{C3}
\end{aligned}$$

$$\begin{aligned}
\epsilon_5^P &= -\frac{g^2 m^2}{F_P^2} \left\{ \bar{I}^{(1)}(M_P^2, m^2, m^2) + M_P^2 \bar{I}_{12}^{(0)}(t, M_P^2, m^2, m^2) - 2\bar{I}_{12}^{(2)}(t, M_P^2, m^2, m^2) \right. \\
&\quad \left. - 8m^2 \bar{I}_{12}^{(3)}(t, M_P^2, m^2, m^2) \right\}, \\
\epsilon_6^P &= \frac{g^2}{F_P^2} \left\{ t \bar{J}^{(1)}(t, M_P^2) - 4m^2 \bar{I}_{21}^{(2)}(t, M_P^2, m^2, m^2) - 16m^4 \bar{I}_{21}^{(3)}(t, M_P^2, m^2, m^2) \right\}, \\
\epsilon_7^P &= -\frac{2g^2 m^2}{F_P^2} \bar{I}^{(1)}(M_P^2, m^2, m^2), \\
\epsilon_9^P &= -\frac{t}{F_P^2} \bar{J}^{(1)}(t, M_P^2, m^2, m^2), \\
\epsilon_{10}^P &= -\frac{2tg^2 m^2}{F_P^2} \bar{I}_{12}^{(3)}(t, M_P^2, m^2, m^2), \\
\epsilon_{11}^P &= -\frac{3c_2}{64\pi^2 m F_P^2} M_P^4. \tag{C4}
\end{aligned}$$

The contributions of the diagrams in Fig.1 to the Pauli form factors of the u , d and s quark are

$$\begin{aligned}
f_P^{(1)}(t) &= f_P^{(7)}(t) = f_P^{(8)}(t) = f_D^{(9)}(t) = 0, \\
f_P^{(2)}(t) &= \bar{Z}_q \left(c_6 Q + \frac{1}{3}c_7 I + \frac{1}{2}c_8 \lambda_3 \right), \\
f_P^{(3)}(t) &= -t \left(\hat{d}_6 \lambda_3 + \frac{2}{3}d_7 I + 2\bar{d}_8 Q \right), \\
f_P^{(4)}(t) &= -4mt \left(\frac{1}{3}e_{54}I + \frac{1}{2}\hat{e}_{74}\lambda_3 + \bar{e}_{94}Q \right) - 8m\bar{M}^2 \left(\frac{2}{3}\hat{e}_{105}I + \hat{e}_{106}\lambda_3 + 2\hat{e}_{107}Q \right), \\
f_P^{(i)}(t) &= \sum_{P=\pi, K, \eta} \lambda_i^P m_i^P, \quad i = 5, 6, 10, 11, 12, \tag{C5}
\end{aligned}$$

where

$$\lambda_{12}^\pi = \lambda_3, \quad \lambda_{12}^K = 3Q - \lambda_3, \quad \lambda_{12}^\eta = 0, \tag{C6}$$

$$m_5^P = -\frac{8g^2 m^4}{F_P^2} \bar{I}_{12}^{(3)}(t, M_P^2, m^2, m^2),$$

$$\begin{aligned}
m_6^P &= \frac{16g^2m^4}{F_P^2} \bar{I}_{21}^{(3)}(t, M_P^2, m^2, m^2), \\
m_{10}^P &= \frac{g^2m^2}{F_P^2} \left\{ \bar{I}^{(1)}(M_P^2, m^2, m^2) - M_P^2 \bar{I}_{12}(t, M_P^2, m^2, m^2) + 4\bar{I}_{12}^{(2)}(t, M_P^2, m^2, m^2) \right. \\
&\quad \left. + 2t \left(\bar{I}_{12}^{(3)}(t, M_P^2, m^2, m^2) - \bar{I}_{12}^{(4)}(t, M_P^2, m^2, m^2) \right) \right\}, \\
m_{11}^P &= \frac{3c_2}{64\pi^2 m F_P^2} M_P^4, \\
m_{12}^P &= \frac{4mtc_4}{F_P^2} \bar{J}^{(1)}(t, M_P^2, m^2, m^2).
\end{aligned} \tag{C7}$$

The contributions of the diagrams in Fig.2 (vector mesons contributions) to the Dirac and Pauli form factors of the u , d and s quark are

$$\begin{aligned}
f_D^{(2^*)}(t) &= f_D^{(11^*)}(t) = f_D^{(12^*)}(t) = 0, \\
f_D^{(3^*)}(t) &= -\frac{t}{2} \left\{ \lambda_\rho D_\rho(t) + \frac{1}{3} \lambda_\omega D_\omega(t) + \frac{2}{3} \lambda_\phi D_\phi(t) \right\}, \\
f_D^{(10^*)}(t) &= \frac{k_V}{2} \left\{ [\lambda_\omega D_\omega(t) - \lambda_\rho D_\rho(t)] \epsilon_{10}^\pi - \frac{4}{3} [\lambda_\phi D_\omega(t) + \lambda_\omega D_\phi(t)] \epsilon_{10}^K \right. \\
&\quad \left. + \frac{1}{9} [3\lambda_\rho D_\rho(t) + \lambda_\omega D_\omega(t) + 8\lambda_\phi D_\phi(t)] \epsilon_{10}^\eta \right\}, \\
f_P^{(2^*)}(t) &= \frac{k_V}{2} \left\{ \bar{Z} \lambda_\rho D_\rho(t) + \frac{1}{3} \bar{Z} \lambda_\omega D_\omega(t) + \frac{2}{3} \bar{Z}_s \lambda_\phi D_\phi(t) \right\}, \\
f_P^{(3^*)}(t) &= f_P^{(11^*)}(t) = 0, \\
f_P^{(10^*)}(t) &= \frac{k_V}{2} \left\{ [\lambda_\omega D_\omega(t) - \lambda_\rho D_\rho(t)] m_{10}^\pi - \frac{4}{3} [\lambda_\phi D_\omega(t) + \lambda_\omega D_\phi(t)] m_{10}^K \right. \\
&\quad \left. + \frac{1}{9} [3\lambda_\rho D_\rho(t) + \lambda_\omega D_\omega(t) + 8\lambda_\phi D_\phi(t)] m_{10}^\eta \right\}, \\
f_P^{(12^*)}(t) &= -\frac{t}{2} k_V \left\{ \lambda_\rho D_\rho(t) \left[\frac{2}{F_\pi^2} \bar{J}^{(1)}(t, M_\pi^2) + \frac{1}{F_K^2} \bar{J}^{(1)}(t, M_K^2) \right] \right. \\
&\quad \left. + \frac{\lambda_\omega}{F_K^2} D_\omega(t) \bar{J}^{(1)}(t, M_K^2) + \frac{2\lambda_\phi}{F_K^2} D_\phi(t) \bar{J}^{(1)}(t, M_K^2) \right\},
\end{aligned} \tag{C8}$$

where $\lambda_\rho = \lambda_3$, $\lambda_\omega = 2Q + 2I/3 - \lambda_3$, $\lambda_\phi = 2Q - I/3 - \lambda_3$ and $D_V(t) = 1/(M_V^2 + t)$.

In the expressions above, the convergent parts of the structure integrals are

$$\begin{aligned}
\bar{J}^{(1)}(t, M^2) &= -\frac{1}{576\pi^2 t} [t + 3k(t)(t + 4M^2)], \\
\bar{I}^{(1)}(M^2, m^2, m^2) &= \frac{\mu^3}{64\pi^2} [\mu - g(0, M, m, m)(4 - \mu^2)], \\
\bar{I}_{12}(t, M^2, m^2, m^2) &= \frac{1}{32\pi^2 m^2} [g(t, M, m, m)\mu - f(t)], \\
\bar{I}_{12}^{(2)}(t, M^2, m^2, m^2) &= \frac{\mu^3}{256\pi^2} \left[-2\mu D_\tau + g(t, M, m, m)(4 - \mu^2 D_\tau) + g(0, M, m, m)(4 - \mu^2) D_\tau \right], \\
\bar{I}_{12}^{(3)}(t, M^2, m^2, m^2) &= \frac{\mu^3 D_\tau}{1024\pi^2 m^2} \left[2\mu(1 + 2D_\tau) - \mu f(t) - g(t, M, m, m)(4 - 3\mu^2 D_\tau) \right. \\
&\quad \left. + g(0, M, m, m)(4 - \mu^2)(2 + 3D_\tau) \right], \\
\bar{I}_{12}^{(4)}(t, M^2, m^2, m^2) &= \frac{\mu^3}{512\pi^2 m^2 \tau} \left[\mu \tau D_\tau - 2g(t, M, m, m)(1 - \mu^2 D_\tau) \right. \\
&\quad \left. - g(0, M, m, m)(8 - 4\mu^2 + (\mu^2 - 4)D_\tau) \right],
\end{aligned}$$

$$\begin{aligned}
\bar{I}_{21}^{(2)}(t, M^2, m^2, m^2) &= \frac{1}{512\pi^2} \left[2D_\tau \mu (\mu^2 - 2)(2\mu - g(0, M, m, m)(4 - \mu^2)) + k(t)(2 + (\mu^2 - 2)D_\tau) \right. \\
&\quad \left. + 2H_{12}(t, M, m, m)(4 - (2 - \mu^2)^2 D_\tau) \right], \\
\bar{I}_{21}^{(3)}(t, M_P^2, m^2, m^2) &= \frac{D_\tau}{1024\pi^2 m^2} \left[2(4 + 6\mu^2 - \mu^4 + 2(\mu^2 - 2)(\mu^2 + 1)D_\tau) - 6k(t)(2 + (\mu^2 - 2)D_\tau) \right. \\
&\quad + 2f(t)(2 + (\mu^2 - 2)D_\tau)^2 + g(0, M, m, m)\mu(4 - \mu^2)[2(\mu^2 + 2) + 3(\mu^2 - 2)D_\tau] \\
&\quad \left. - H_{12}(t, M, m, m)(12 - 8\mu^2 + 2\tau - 3(\mu^2 - 2)^2 D_\tau) \right]. \tag{C9}
\end{aligned}$$

where

$$\begin{aligned}
H_{12}(t, M, m, m) &= h_1(t, M, m, m) + h_2(t, M, m, m) \left(\frac{2 - \mu^2}{\mu} \right) \\
D_\tau &= \frac{1}{1 + \tau/4}. \tag{C10}
\end{aligned}$$

In the practical calculation, we keep the exact form of the function $f(t)$, while we expand the functions $k(t)$, $g(t, M, m, m)$, $h_1(t, M, m, m)$ and $h_2(t, M, m, m)$ in powers of θ and μ with $\theta = t/M^2$ and $\mu = M/m$.

Finally, we keep our expressions for ϵ_i^P and m_i^P up to $O(\theta_P, \mu_P^4)$ which are explicitly given as

$$\epsilon_5^P = \frac{g^2 m^2 \mu_P^2}{32\pi^2 F_P^2} \left[f(t) \left(1 - \frac{3}{4} \mu_P^2 D_\tau^2 \right) + \pi \mu_P \left(1 - \frac{D_\tau}{2} - 2D_\tau^2 \right) + \frac{\mu_P^2}{2} (1 - D_\tau - \frac{3}{2} D_\tau^2) \right], \tag{C11}$$

$$\epsilon_6^P = \frac{g^2 m^2}{16\pi^2 F_P^2} \left[\mu_P^2 \left(1 - \frac{5\pi}{2} \mu_P - 2\mu_P^2 \right) + \tau \left(\frac{7}{2} - \frac{35\pi}{24} \mu_P - \frac{13}{6} \mu_P^2 + \frac{105\pi}{64} \mu_P^3 + \frac{107}{72} \mu_P^4 \right) \right],$$

$$\epsilon_7^P = \frac{g^2 m^2 \mu_P^3}{16\pi^2 F_P^2} \left(\pi + \frac{\mu_P}{2} \right),$$

$$\epsilon_9^P = \frac{t}{192\pi^2 F_P^2},$$

$$\epsilon_{10}^P = \frac{g^2 m^2 \mu_P^3}{32\pi^2 F_P^2} (1 - D_\tau) \left[\pi(1 + 2D_\tau) + \frac{\mu_P}{2} \left(1 + \frac{3}{2} D_\tau \right) + \frac{3}{4} \mu_P D_\tau f(t) \right],$$

$$\epsilon_{11}^P = -\frac{3c_2 m^3 \mu_P^4}{64\pi^2 F_P^2} Q,$$

$$m_5^P = \frac{g^2 m^2 \mu_P^3}{16\pi^2 F_P^2} \left\{ \frac{3}{8} \mu_P f(t) D_\tau^2 + D_\tau \left[\pi \left(\frac{1}{2} + D_\tau \right) + \frac{3}{8} \left(\frac{2}{3} + D_\tau \right) \right] \right\},$$

$$\begin{aligned}
m_6^P &= -\frac{g^2 m^2}{\pi F_P^2} \left[\frac{\mu_P}{8} \left(\pi + \mu_P - \frac{15}{8} \pi \mu_P^2 - \frac{4}{3} \mu_P^3 \right) \right. \\
&\quad \left. + \frac{\tau}{96\mu_P} \left(\pi + 8\mu_P - \frac{105\pi}{8} \mu_P^2 - \frac{52}{3} \mu_P^3 + \frac{1575\pi}{128} \mu_P^4 + \frac{107}{10} \mu_P^5 \right) \right],
\end{aligned}$$

$$\begin{aligned}
m_{10}^P &= \frac{g^2 m^2 \mu_P^2}{32\pi^2 F_P^2} \left\{ f(t) \left[1 - \frac{3}{4} D_\tau \mu_P^2 (1 - D_\tau) \right] - \pi \mu_P \left(1 + \frac{1}{2} D_\tau - 2D_\tau^2 \right) \right. \\
&\quad \left. - \frac{1}{2} \mu_P^2 \left(1 + \frac{1}{2} D_\tau - \frac{3}{2} D_\tau^2 \right) \right\},
\end{aligned}$$

$$m_{11}^P = \frac{3c_2 m^3 \mu_P^4}{64\pi^2 F_P^2},$$

$$m_{12}^P = \frac{c_4 m t}{48\pi^2 F_P^2}.$$

Finally, the renormalized LECs are

$$\begin{aligned} \hat{d}_6 &= d_6^r(\mu) - \frac{\beta_{d_6}}{16\pi^2} \left[\frac{1}{F_\pi^2} \ln \frac{M_\pi}{\mu} - \frac{1}{F_K^2} \ln \frac{M_K}{\mu} \right], \\ \bar{d}_8 &= d_8^r(\mu) - \frac{\beta_{d_8}}{16\pi^2 F_K^2} \ln \frac{M_K}{\mu}, \\ \hat{e}_{74} &= e_{74}^r(\mu) - \frac{\beta_{e_{74}}}{16\pi^2} \left[\frac{1}{F_\pi^2} \ln \frac{M_\pi}{\mu} - \frac{1}{F_K^2} \ln \frac{M_K}{\mu} \right], \\ \bar{e}_{94} &= e_{94}^r(\mu) - \frac{\beta_{e_{94}}}{16\pi^2 F_K^2} \ln \frac{M_K}{\mu}, \\ \hat{e}_{105} &= e_{105}^r(\mu) - \frac{1}{16\pi^2} \sum_{P=\pi, K, \eta} \frac{\beta_{e_{105}}^P}{F_P^2} \ln \frac{M_P}{\mu}, \\ \hat{e}_{106} &= e_{106}^r(\mu) - \frac{1}{16\pi^2} \sum_{P=\pi, K, \eta} \frac{\beta_{e_{106}}^P}{F_P^2} \ln \frac{M_P}{\mu}, \\ \hat{e}_{107} &= e_{107}^r(\mu) - \frac{1}{16\pi^2} \sum_{P=\pi, K, \eta} \frac{\beta_{e_{107}}^P}{F_P^2} \ln \frac{M_P}{\mu}, \end{aligned} \tag{C12}$$

where

$$\beta_{d_6} = -\frac{2}{3} \beta_{d_8} = \frac{1}{6} (1 + 5g^2), \tag{C13}$$

$$\beta_{e_{74}} = -\frac{2}{3} \beta_{e_{94}} = -\frac{1}{12m} (1 - 7g^2 + k_V + 4mc_4),$$

$$\begin{aligned} \beta_{105}^P &= \begin{cases} -\frac{g^2 M_\pi^2}{8m M^2} (1 + c_6 + 2c_7 + k_V) & \text{for } P = \pi \\ \frac{g^2 M_K^2}{12m M^2} (1 + c_6 - 4c_7 + k_V) & \text{for } P = K \\ \frac{g^2 M_\eta^2}{24m M^2} (1 + c_6 - 2c_7 + k_V) & \text{for } P = \eta, \end{cases} \\ \beta_{106}^P &= \begin{cases} \frac{M_\pi^2}{8m M^2} \{4mc_4 - c_6 - c_8 - 6g^2 (1 + \frac{1}{6}c_6 - \frac{1}{3}c_7 + \frac{1}{3}c_8 + \frac{1}{6}k_V)\} & \text{for } P = \pi \\ \frac{M_K^2}{8m M^2} \{c_6 - 4mc_4 - \frac{1}{2}c_8 + \frac{16}{3}g^2 (1 + \frac{1}{16}c_6 - \frac{1}{4}c_7 - \frac{9}{32}c_8 + \frac{1}{16}k_V)\} & \text{for } P = K \\ \frac{g^2 M_\eta^2}{12m M^2} (1 + c_6 - c_7 - \frac{1}{2}c_8 + k_V) & \text{for } P = \eta, \end{cases} \\ \beta_{107}^P &= \begin{cases} \frac{M_\pi^2}{16m M^2} \{-\frac{3c_2}{m} M_\pi^2 - 2g^2 (1 + c_6 + 2c_7 + k_V)\} & \text{for } P = \pi \\ \frac{M_K^2}{16m M^2} \{12mc_4 - \frac{5c_2}{m} M_K^2 - 3c_6 - \frac{1}{3}g^2 (56 + 11c_6 - 8c_7 + 11k_V)\} & \text{for } P = K \\ \frac{M_\eta^2}{16m M^2} \{-\frac{c_2}{m} M_\eta^2 - 2g^2 (1 + c_6 - \frac{2}{3}c_7 + k_V)\} & \text{for } P = \eta, \end{cases} \end{aligned}$$

and

$$M^2 = M_\pi^2 - M_K^2 + \frac{3}{2} M_\eta^2. \tag{C14}$$

APPENDIX D: MESON-NUCLEON SIGMA-TERMS

Two important identities are involved in the evaluation of the meson-nucleon sigma-terms. In particular, the derivatives with respect to the current quark masses are equivalent to the ones with respect to the meson masses [40]:

$$\hat{m} \frac{\partial}{\partial \hat{m}} \Sigma_q = M_\pi^2 \left(\frac{\partial}{\partial M_\pi^2} + \frac{1}{2} \frac{\partial}{\partial M_K^2} + \frac{1}{3} \frac{\partial}{\partial M_\eta^2} \right) \Sigma_q, \quad (\text{D1})$$

$$\hat{m}_s \frac{\partial}{\partial \hat{m}} \Sigma_q = M_{K\eta}^2 \left(\frac{\partial}{\partial M_\pi^2} + \frac{1}{2} \frac{\partial}{\partial M_K^2} + \frac{1}{3} \frac{\partial}{\partial M_\eta^2} \right) \Sigma_q, \quad (\text{D2})$$

$$\hat{m} \frac{\partial}{\partial \hat{m}_s} \Sigma_q = M_\pi^2 \left(\frac{1}{2} \frac{\partial}{\partial M_K^2} + \frac{2}{3} \frac{\partial}{\partial M_\eta^2} \right) \Sigma_q, \quad (\text{D3})$$

$$\hat{m}_s \frac{\partial}{\partial \hat{m}_s} \Sigma_q = M_{K\eta}^2 \left(\frac{\partial}{\partial M_K^2} + \frac{4}{3} \frac{\partial}{\partial M_\eta^2} \right) \Sigma_q, \quad (\text{D4})$$

with $M_{K\eta}^2 = -M_K^2 + 3M_\eta^2/2$. Below we give the exact expressions for the typical two types of derivatives:

$$\begin{aligned} \hat{m} \frac{\partial}{\partial \hat{m}} \Sigma &= \hat{m} - \frac{9g^2 M_\pi^2}{64\pi} \left\{ \frac{M_\pi}{F_\pi^2} + \frac{M_K}{3F_K^2} + \frac{M_\eta}{27F_\eta^2} \right\} - \frac{3g^2 M_\pi^2}{32\pi^2 m} \left\{ \frac{M_\pi^2}{F_\pi^2} + \frac{M_K^2}{3F_K^2} + \frac{M_\eta^2}{27F_\eta^2} \right\} \\ &\quad - 4c_1 M_\pi^2 + \frac{3c_2 M_\pi^2}{128\pi^2} \left\{ \frac{M_\pi^2}{F_\pi^2} + \frac{4}{3} \frac{M_K^2}{F_K^2} + \frac{M_\eta^2}{3F_\eta^2} + \frac{M^2}{\mathcal{F}_1^2} \right\} \\ &\quad - \frac{c_5}{3} M_\pi^2 + 2\hat{e}_1 M_\pi^2 M^2 - \frac{\hat{e}_5}{36} M_\pi^2 (M_K^2 - M_\pi^2), \end{aligned} \quad (\text{D5})$$

$$\begin{aligned} \hat{m}_s \frac{\partial}{\partial \hat{m}_s} \Sigma_s &= \hat{m}_s - \frac{9g^2 M_{K\eta}^2}{64\pi} \left\{ \frac{4}{3} \frac{M_K}{F_K^2} + \frac{16}{27} \frac{M_\eta}{F_\eta^2} \right\} - \frac{3g^2 M_{K\eta}^2}{32\pi^2 m} \left\{ \frac{4}{3} \frac{M_K^2}{F_K^2} + \frac{16}{27} \frac{M_\eta^2}{F_\eta^2} \right\} \\ &\quad - 4c_1 M_{K\eta}^2 + \frac{3c_2 M_{K\eta}^2}{128\pi^2} \left\{ \frac{M_\pi^2}{F_\pi^2} + \frac{4}{3} \frac{M_K^2}{F_K^2} + \frac{M_\eta^2}{3F_\eta^2} + \frac{M^2}{\mathcal{F}_2^2} \right\} \\ &\quad - \frac{4c_5}{3} M_{K\eta}^2 + 2\hat{e}_1 M_{K\eta}^2 M^2 + \frac{2\hat{e}_5}{9} M_{K\eta}^2 (M_K^2 - M_\pi^2), \end{aligned} \quad (\text{D6})$$

where

$$\frac{1}{\mathcal{F}_1^2} = \frac{1}{F_\pi^2} + \frac{2}{3F_K^2} + \frac{1}{9F_\eta^2}, \quad \frac{1}{\mathcal{F}_2^2} = \frac{4}{3F_K^2} + \frac{4}{9F_\eta^2}. \quad (\text{D7})$$

One should note that there are additional useful relations between different sigma-terms [18]. In particular, with the definitions of y_N and $\sigma_{KN}^{I=1}$ we can relate KN and ηN sigma-terms to the πN sigma-term as

$$\sigma_{KN}^u = \sigma_{\pi N} (1 + y_N) \frac{\hat{m} + m_s}{4\hat{m}} + \sigma_{KN}^{I=1}, \quad \sigma_{KN}^d = \sigma_{KN}^u - 2\sigma_{KN}^{I=1}, \quad (\text{D8})$$

$$\sigma_{\eta N} = \sigma_{\pi N} \frac{\hat{m} + 2y_N m_s}{3\hat{m}}.$$

[1] S. Weinberg, *Physica A* **96** 327 (1979).

[2] J. Gasser and H. Leutwyler, *Phys. Rept.* **87** 77 (1982); J. Gasser and H. Leutwyler, *Annals Phys.* **158** 142 (1984).

[3] J. Gasser, M. E. Sainio and A. Svarc, *Nucl. Phys. B* **307** 779 (1988).

[4] E. Jenkins and A. V. Manohar, *Phys. Lett. B* **255** 558 (1991); V. Bernard, N. Kaiser, J. Kambor and U. G. Meissner, *Nucl. Phys. B* **388** 315 (1992).

[5] T. Becher and H. Leutwyler, *Eur. Phys. J. C* **9** 643 (1999) [arXiv:hep-ph/9901384]; *JHEP* **0106** 017 (2001) [arXiv:hep-ph/0103263].

[6] P. J. Ellis and H. B. Tang, *Phys. Rev. C* **57** 3356 (1998) [arXiv:hep-ph/9709354].

[7] J. Schweizer, Diploma thesis, University of Bern (2000).

[8] B. Kubis and U. G. Meissner, *Nucl. Phys. A* **679** 698 (2001) [arXiv:hep-ph/0007056].

[9] B. Kubis and U. G. Meissner, *Eur. Phys. J. C* **18** 747 (2001) [arXiv:hep-ph/0010283].

[10] J. L. Goity, D. Lehmann, G. Prezeau and J. Saez, *Phys. Lett. B* **504** 21 (2001) [arXiv:hep-ph/0101011]; D. Lehmann and G. Prezeau, *Phys. Rev. D* **65** 016001 (2002) [arXiv:hep-ph/0102161].

[11] T. Fuchs, J. Gegelia, G. Japaridze and S. Scherer, *Phys. Rev. D* **68**, 056005 (2003) [arXiv:hep-ph/0302117]; *Eur. Phys. J. A* **19**, 35 (2004) [arXiv:hep-ph/0309234].

[12] G. V. Efimov and M. A. Ivanov, *The Quark Confinement Model of Hadrons*, (IOP Publishing, Bristol & Philadelphia, 1993).

[13] M. A. Ivanov, M. P. Locher and V. E. Lyubovitskij, *Few Body Syst.* **21** 131 (1996) [arXiv:hep-ph/9602372].

[14] M. A. Ivanov, V. E. Lyubovitskij, J. G. Korner and P. Kroll, *Phys. Rev. D* **56** 348 (1997) [arXiv:hep-ph/9612463]; M. A. Ivanov, J. G. Korner, V. E. Lyubovitskij and A. G. Rusetsky, *Phys. Rev. D* **60** 094002 (1999) [arXiv:hep-ph/9904421]; A. Faessler, T. Gutsche, M. A. Ivanov, J. G. Korner and V. E. Lyubovitskij, *Phys. Lett. B* **518** 55 (2001) [arXiv:hep-ph/0107205].

[15] A. Faessler, T. Gutsche, V. E. Lyubovitskij, K. Pumsa-ard, *Prog. Part. Nucl. Phys.* **55**, 12 (2005).

[16] T. Gutsche and D. Robson, *Phys. Lett. B* **229** 333 (1989).

[17] V. E. Lyubovitskij, T. Gutsche and A. Faessler, *Phys. Rev. C* **64** 065203 (2001) [arXiv: hep-ph/0105043].

[18] V. E. Lyubovitskij, T. Gutsche, A. Faessler and E. G. Drukarev, *Phys. Rev. D* **63** 054026 (2001) [arXiv:hep-ph/0009341]; T. Inoue, V. E. Lyubovitskij, T. Gutsche and A. Faessler, *Phys. Rev. C* **69** 035207 (2004) [arXiv:hep-ph/0311275].

[19] V. E. Lyubovitskij, T. Gutsche, A. Faessler and R. Vinh Mau, *Phys. Lett. B* **520** 204 (2001) [arXiv:hep-ph/0108134]; *Phys. Rev. C* **65** 025202 (2002) [arXiv:hep-ph/0109213]; V. E. Lyubovitskij, P. Wang, T. Gutsche and A. Faessler, *Phys. Rev. C* **66** 055204 (2002) [arXiv:hep-ph/0207225]; F. Simkovic, V. E. Lyubovitskij, T. Gutsche, A. Faessler and S. Kovalenko, *Phys. Lett. B* **544** 121 (2002) [arXiv:hep-ph/0112277]; K. Pumsa-ard, V. E. Lyubovitskij, T. Gutsche, A. Faessler and S. Cheedket, *Phys. Rev. C* **68** 015205 (2003) [arXiv:hep-ph/0304033]; T. Inoue, V. E. Lyubovitskij, T. Gutsche and A. Faessler, *Phys. Rev. C* **69** 035207 (2004) [arXiv:hep-ph/0311275]; S. Cheedket, V. E. Lyubovitskij, T. Gutsche, A. Faessler, K. Pumsa-ard and Y. Yan, *Eur. Phys. J. A* **20** 317 (2004) [arXiv:hep-ph/0212347]; K. Khosonthongkee, V. E. Lyubovitskij, T. Gutsche, A. Faessler, K. Pumsa-ard, S. Cheedket and Y. Yan, *J. Phys. G* **30** 793 (2004) [arXiv:hep-ph/0403119].

[20] G. Altarelli, N. Cabibbo, L. Maiani and R. Petronzio, *Nucl. Phys. B* **69** 531 (1974); N. Cabibbo and R. Petronzio, *Nucl. Phys. B* **137** 395 (1978).

[21] A. Manohar and H. Georgi, *Nucl. Phys. B* **234** 189 (1984).

[22] M. Osipenko *et al.* [CLAS Collaboration], *Phys. Rev. D* **67** 092001 (2003) [arXiv:hep-ph/0301204]; C. Hadjidakis *et al.* [CLAS Collaboration], *Phys. Lett. B* **605** 256 (2005) [arXiv:hep-ex/0408005].

[23] D. L. Adams *et al.* [FNAL-E704 Collaboration], *Phys. Lett. B* **264** 462 (1991).

[24] C. E. Allgower *et al.*, *Phys. Rev. D* **65** 092008 (2002).

[25] V. V. Mochalov, S. M. Troshin and A. N. Vasiliev, *Phys. Rev. D* **69** 077503 (2004) [arXiv:hep-ph/0310224].

[26] R. Petronzio, S. Simula and G. Ricco, *Phys. Rev. D* **67** 094004 (2003) [Erratum-ibid. D **68** 099901 (2003)] [arXiv:hep-ph/0301206]; A. E. Dorokhov and I. O. Cherednikov, *Phys. Rev. D* **67** 114017 (2003) [arXiv:hep-ph/0212357]; N. I. Kochelev, *Phys. Lett. B* **565** 131 (2003) [arXiv:hep-ph/0304171]; D. Melikhov and S. Simula, *Eur. Phys. J. C* **37** 437 (2004) [arXiv:hep-ph/0402009]; J. M. Laget, *Phys. Rev. D* **70** 054023 (2004) [arXiv:hep-ph/0406153]; S. Noguera, S. Scopetta and V. Vento, *Phys. Rev. D* **70** 094018 (2004) [arXiv:hep-ph/0409059]; M. M. Kaskulov and P. Grabmayr, *Eur. Phys. J. A* **19**, 157 (2004) [arXiv:nucl-th/0308015]; M. M. Kaskulov and P. Grabmayr, *Phys. Rev. C* **69**, 028201 (2004) [arXiv:nucl-th/0306070].

[27] S. Théberge, A. W. Thomas and G. A. Miller, *Phys. Rev. D* **22** 2838 (1980) [Erratum-ibid. D **23** 2106 (1981)]; *Phys. Rev. D* **24** 216 (1981); S. Théberge and A. W. Thomas, *Nucl. Phys. A* **393** 252 (1983); A. W. Thomas, *Adv. Nucl. Phys.* **13** 1 (1984).

[28] E. Oset, R. Tegen and W. Weise, *Nucl. Phys. A* **426** 456 (1984) [Erratum-ibid. A **453** 751 (1986)]; R. Tegen, *Annals Phys.* **197** 439 (1990); S. A. Chin, *Nucl. Phys. A* **382** 355 (1982).

[29] D. Diakonov and V. Y. Petrov, *Nucl. Phys. B* **245** 259 (1984); *Nucl. Phys. B* **272** 457 (1986); D. Diakonov, V. Y. Petrov and M. Praszalowicz, *Nucl. Phys. B* **323** 53 (1989).

[30] A. Chodos, R. L. Jaffe, K. Johnson, C. B. Thorn and V. F. Weisskopf, *Phys. Rev. D* **9** 3471 (1974).

[31] N. Fettes, U. G. Meissner and S. Steininger, *Nucl. Phys. A* **640** 199 (1998) [arXiv:hep-ph/9803266].

[32] B. Kubis, T. R. Hemmert and U. G. Meissner, *Phys. Lett. B* **456**, 240 (1999) [arXiv:hep-ph/9903285].

[33] J. Gasser and H. Leutwyler, *Nucl. Phys. B* **250** 465 (1985).

[34] G. Ecker, J. Gasser, A. Pich and E. de Rafael, Nucl. Phys. B **321** 311 (1989); G. Ecker, J. Gasser, H. Leutwyler, A. Pich and E. de Rafael, Phys. Lett. B **223** 425 (1989).

[35] J.J. Sakurai, *Currents and Mesons*, Chicago Lectures in Physics, Chicago, London, New York, 1967.

[36] R. L. Jaffe and X. D. Ji, Phys. Rev. Lett. **67**, 552 (1991); H. X. He and X. D. Ji, Phys. Rev. D **52**, 2960 (1995) [arXiv:hep-ph/9412235]; H. C. Kim, M. V. Polyakov and K. Goeke, Phys. Lett. B **387**, 577 (1996) [arXiv:hep-ph/9604442]; X. M. Jin and J. Tang, Phys. Rev. D **56**, 5618 (1997) [arXiv:hep-ph/9705269].

[37] M. A. B. Bég and A. Zepeda, Phys. Rev. D **6** 2912 (1972). H. Genz and G. Hohler, Phys. Lett. B **61**, 389 (1976).

[38] H. Hellmann, *Einführung in die Quantenchemie* (Deuticke Verlag, Leipzig, 1937); R. P. Feynman, Phys. Rev. **56** 340 (1939).

[39] B. L. Ioffe, Nucl. Phys. B **188**, 317 (1981) [Erratum-ibid. B **191**, 591 (1981)]; B. L. Ioffe and A. V. Smilga, Phys. Lett. B **133**, 436 (1983); Nucl. Phys. B **232**, 109 (1984); V. A. Nesterenko and A. V. Radyushkin, Phys. Lett. B **128**, 439 (1983).

[40] J. Gasser, Annals Phys. **136**, 62 (1981).

[41] B. Borasoy and U. G. Meissner, Annals Phys. **254**, 192 (1997) [arXiv:hep-ph/9607432].

[42] T. Fuchs, J. Gegelia and S. Scherer, J. Phys. G **30**, 1407 (2004) [arXiv:nucl-th/0305070]; B. C. Lehnhart, J. Gegelia and S. Scherer, J. Phys. G **31**, 89 (2005) [arXiv:hep-ph/0412092].

[43] M. Frink, U. G. Meissner and I. Scheller, Eur. Phys. J. A **24**, 395 (2005) [arXiv:hep-lat/0501024].

[44] S. Gusken, K. Schilling, R. Sommer, K. H. Mutter and A. Patel, Phys. Lett. B **212**, 216 (1988); G. Martinelli and C. T. Sachrajda, Nucl. Phys. B **316**, 355 (1989); D. B. Leinweber, Phys. Rev. D **45**, 252 (1992); S. J. Dong, J. F. Lague and K. F. Liu, Phys. Rev. D **54**, 5496 (1996) [arXiv:hep-ph/9602259]; D. B. Leinweber, A. W. Thomas and R. D. Young, Phys. Rev. Lett. **92**, 242002 (2004) [arXiv:hep-lat/0302020]; D. Arndt and B. C. Tiburzi, Phys. Rev. D **68**, 094501 (2003) [arXiv:hep-lat/0307003]; M. Procura, T. R. Hemmert and W. Weise, Phys. Rev. D **69**, 034505 (2004) [arXiv:hep-lat/0309020]; M. Gockeler, T. R. Hemmert, R. Horsley, D. Pleiter, P. E. L. Rakow, A. Schafer and G. Schierholz [QCDSF Collaboration], Phys. Rev. D **71**, 034508 (2005) [arXiv:hep-lat/0303019]; D. B. Leinweber *et al.*, Phys. Rev. Lett. **94** 212001 (2005) [arXiv:hep-lat/0406002].

[45] M. Gari and W. Krumpelmann, Phys. Lett. B **141**, 295 (1984); R. A. Williams and S. R. Cotanch, Phys. Rev. Lett. **77**, 1008 (1996); K. Watanabe and H. Takahashi, Phys. Rev. D **51**, 1423 (1995); S. Dubnicka, A. Z. Dubnickova and P. Weisenpacher, J. Phys. G **29**, 405 (2003) [arXiv:hep-ph/0208051].

[46] G. Hellstern, R. Alkofer, M. Oettel and H. Reinhardt, Nucl. Phys. A **627**, 679 (1997) [arXiv:hep-ph/9705267]; D. Ebert and T. Jurke, Phys. Rev. D **58**, 034001 (1998) [arXiv:hep-ph/9710390]; R. Alkofer, A. Holl, M. Kloker, A. Krassnigg and C. D. Roberts, Few Body Syst. **37**, 1 (2005) [arXiv:nucl-th/0412046]; T. Van Cauteren, D. Merten, T. Corthals, S. Janssen, B. Metsch, H. R. Petry and J. Ryckebusch, Eur. Phys. J. A **20**, 283 (2004) [arXiv:nucl-th/0310058]; D. Merten, U. Loring, K. Kretzschmar, B. Metsch and H. R. Petry, Eur. Phys. J. A **14**, 477 (2002) [arXiv:hep-ph/0204024].

[47] P. Alberto, E. Ruiz Arriola, M. Fiolhais, F. Grummer, J. N. Urbano and K. Goeke, Phys. Lett. B **208**, 75 (1988); C. V. Christov, A. Z. Gorski, K. Goeke and P. V. Pobylitsa, Nucl. Phys. A **592**, 513 (1995) [arXiv:hep-ph/9507256]; R. F. Wagenbrunn, S. Boffi, W. Klink, W. Plessas and M. Radici, Phys. Lett. B **511**, 33 (2001) [arXiv:nucl-th/0010048]; R. F. Wagenbrunn, L. Y. Glozman, W. Plessas, S. Boffi, M. Radici and W. Klink, Eur. Phys. J. A **18**, 155 (2003).

[48] S. Weinberg, Phys. Rev. Lett. **67**, 3473 (1991); **65**, 1181 (1990); S. Peris, Phys. Rev. D **46**, 1202 (1992); D. A. Dicus, D. Minic, U. van Kolck and R. Vega, Phys. Lett. B **284**, 384 (1992); S. Peris and E. de Rafael, Phys. Lett. B **309**, 389 (1993) [arXiv:hep-ph/9304262]; W. Broniowski, A. Steiner and M. Lutz, Phys. Rev. Lett. **71** 1787 (1993) [arXiv:hep-ph/9304292].

[49] S. Eidelman *et al.* [Particle Data Group Collaboration], Phys. Lett. B **592** 1 (2004).

[50] J. J. Kelly, Phys. Rev. C **66** 065203 (2002) [arXiv:hep-ph/0204239].

[51] J. Friedrich and T. Walcher, Eur. Phys. J. A **17** 607 (2003) [arXiv:hep-ph/0303054].

[52] S. J. Brodsky, J. R. Hiller, D. S. Hwang and V. A. Karmanov, Phys. Rev. D **69**, 076001 (2004) [arXiv:hep-ph/0311218].

[53] A. V. Belitsky, X. d. Ji and F. Yuan, Phys. Rev. Lett. **91**, 092003 (2003) [arXiv:hep-ph/0212351].

[54] R. Madey *et al.* [E93-038 Collaboration], Phys. Rev. Lett. **91**, 122002 (2003) [arXiv:nucl-ex/0308007].

[55] R. Schiavilla and I. Sick, Phys. Rev. C **64**, 041002 (2001) [arXiv:nucl-ex/0107004].

[56] M. K. Jones *et al.* [Jefferson Lab Hall A Collaboration], Phys. Rev. Lett. **84** 1398 (2000) [arXiv:nucl-ex/9910005].

[57] O. Gayou *et al.* [Jefferson Lab Hall A Collaboration], Phys. Rev. Lett. **88** 092301 (2002) [arXiv:nucl-ex/0111010].

[58] R. C. Walker *et al.*, Phys. Rev. D **49** 5671 (1994).

[59] G. Kubon *et al.*, Phys. Lett. B **524**, 26 (2002) [arXiv:nucl-ex/0107016].

[60] I. Sick, Phys. Lett. B **576**, 62 (2003) [arXiv:nucl-ex/0310008].

[61] J. J. de Swart, Rev. Mod. Phys. **35**, 916 (1963).

Table 1. SU(6) couplings α_E^{Bi} and α_M^{Bi} .

	α_E^{Bu}	α_E^{Bd}	α_E^{Bd}	α_M^{Bu}	α_M^{Bd}	α_M^{Bs}
p	2	1	0	$\frac{4}{3}$	$-\frac{1}{3}$	0
n	1	2	0	$-\frac{1}{3}$	$\frac{4}{3}$	0
Λ^0	1	1	1	0	0	1
Σ^+	2	0	1	$\frac{4}{3}$	0	$-\frac{1}{3}$
Σ^-	0	2	1	0	$\frac{4}{3}$	$-\frac{1}{3}$
Ξ^-	0	1	2	0	$-\frac{1}{3}$	$\frac{4}{3}$
Ξ^0	1	0	2	$-\frac{1}{3}$	0	$\frac{4}{3}$
$\Sigma^0 \Lambda^0$	0	0	0	$\frac{1}{\sqrt{3}}$	$-\frac{1}{\sqrt{3}}$	0

Table 2. Magnetic moments of the baryon octet (in units of the nucleon magneton μ_N)

	Set I			Set II			Exp.
	3q	Meson Cloud	Total	3q	Meson Cloud	Total	
μ_p	2.357	0.436	2.793	2.357	0.436	2.793	2.793
μ_n	-1.571	-0.342	-1.913	-1.571	-0.342	-1.913	-1.913
μ_{Λ^0}	-0.786	0.173	-0.613	-0.518	-0.095	-0.613	-0.613 ± 0.004
μ_{Σ^+}	2.357	0.317	2.674	2.085	0.373	2.458	2.458 ± 0.010
μ_{Σ^0}	0.786	0.005	0.791	0.570	0.073	0.643	-
μ_{Σ^-}	-0.786	-0.306	-1.092	-0.935	-0.225	-1.160	-1.160 ± 0.025
μ_{Ξ^0}	-1.571	0.136	-1.435	-1.058	-0.192	-1.250	-1.250 ± 0.014
μ_{Ξ^-}	-0.7855	0.2921	-0.4934	-0.5580	-0.0927	-0.6507	-0.6507 ± 0.003
$ \mu_{\Sigma^0 \Lambda^0} $	1.36	0.27	1.63	1.34	0.27	1.61	1.61 ± 0.08

Table 3. Comparison of the parameters of the original phenomenological ansatz in Ref. [51] to an equivalent set, which is obtained by fitting to our results for the charge form factor of the proton.

	Ref. [51]	Present result
a_{10}	1.041	1.059
a_{11}	0.765	0.777
a_{20}	-0.041	-0.059
a_{21}	6.2	4.3
a_b	-0.23	-0.31
Q_b	0.07	0.12
σ_b	0.21	0.23

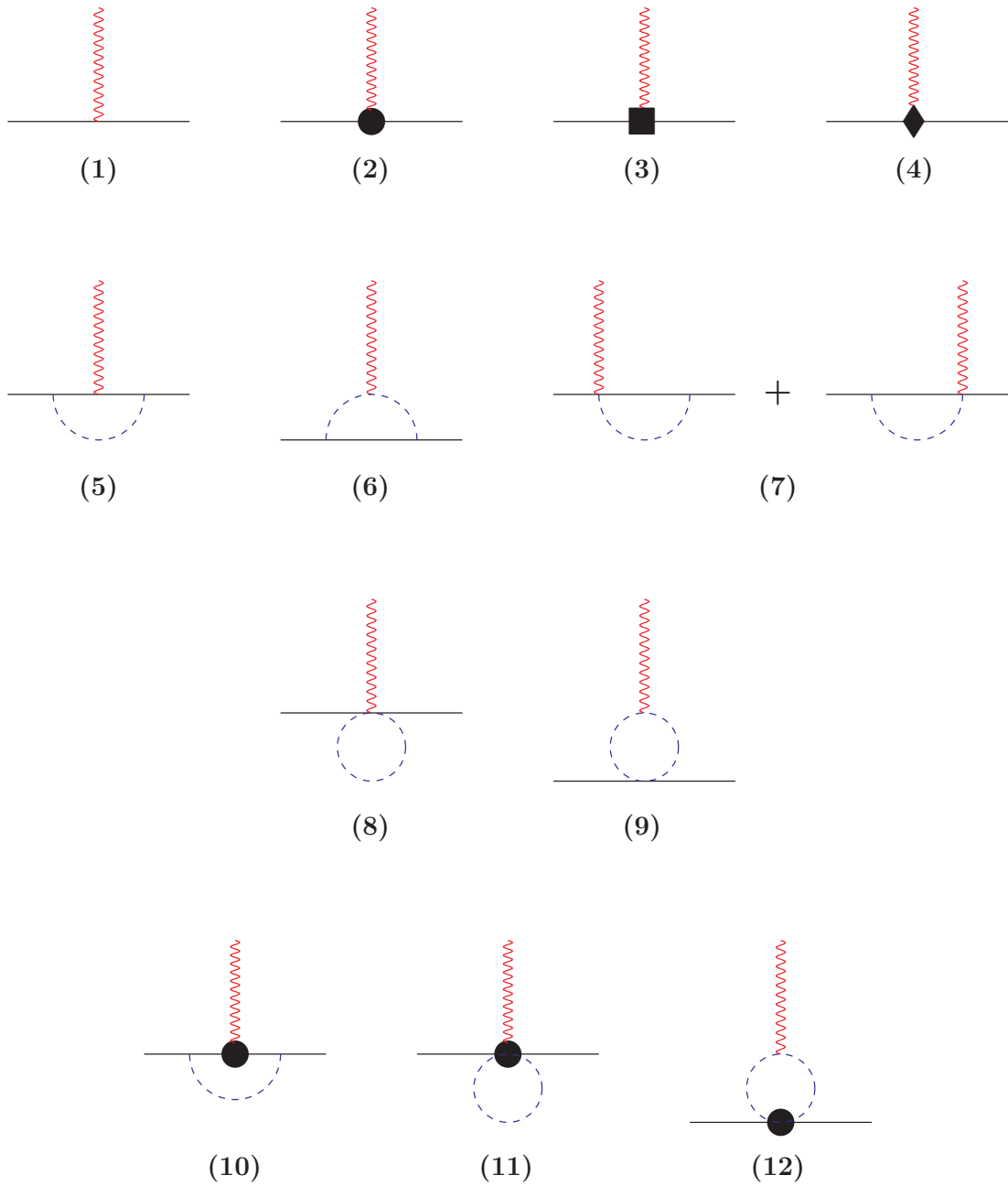


Fig. 1. Diagrams including pseudoscalar meson contributions to the EM quark transition operator up to fourth order. Solid, dashed and wiggly lines refer to quarks, pseudoscalar mesons and the electromagnetic field, respectively. Vertices denoted by a black filled circle, box and diamond correspond to insertions from the second, third and fourth order chiral Lagrangian.

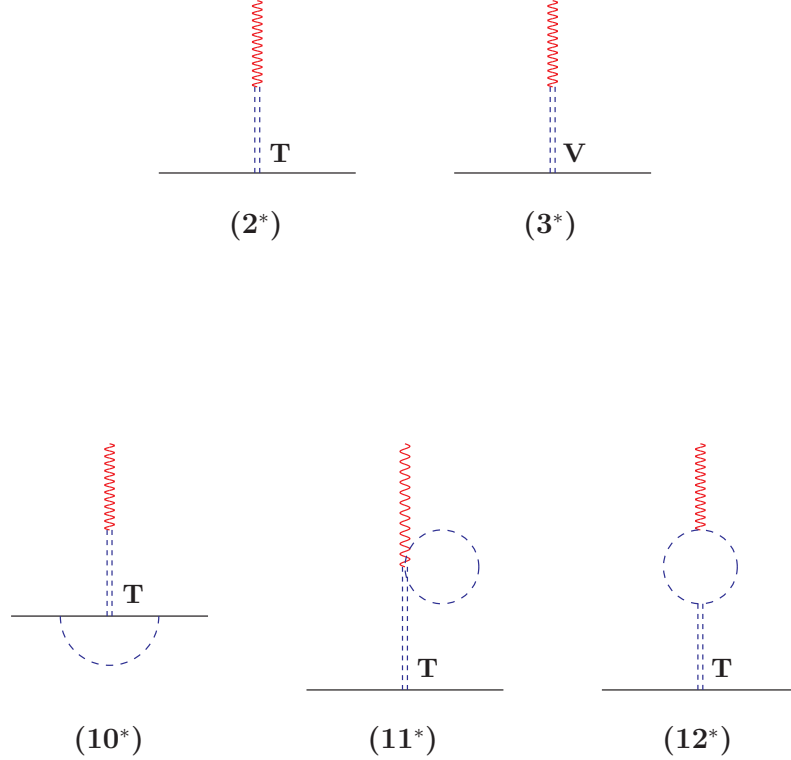


Fig. 2. Diagrams including vector-meson contributions to the EM quark transition operator. Double-dashed lines correspond to vector mesons. The symbols **V** and **T** refer to the vectorial and tensorial couplings of vector mesons to quarks.

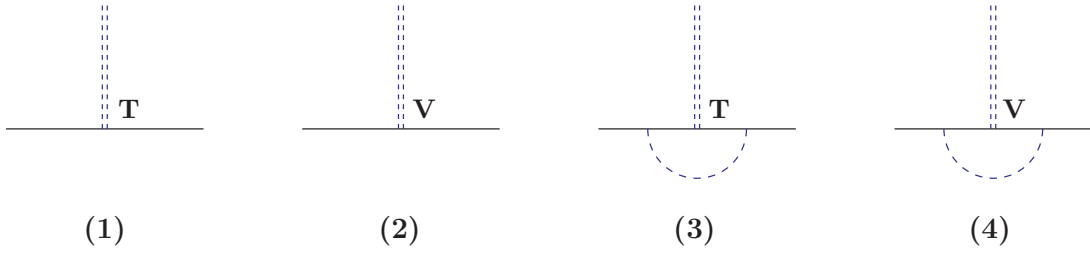


Fig. 3. Diagrams contributing to the quark operator describing strong interaction of vector mesons to quarks. The symbols **V** and **T** refer to the vectorial and tensorial couplings of vector mesons to quarks.

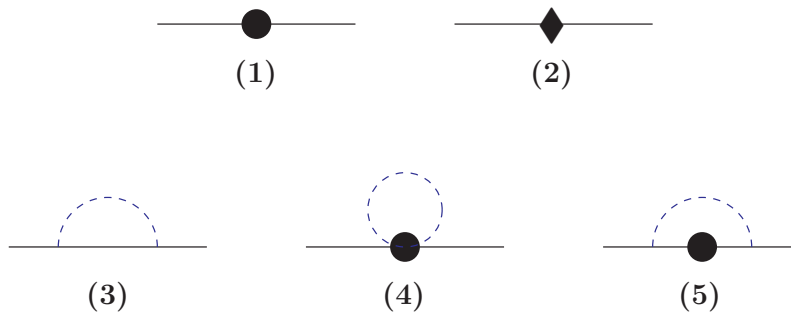
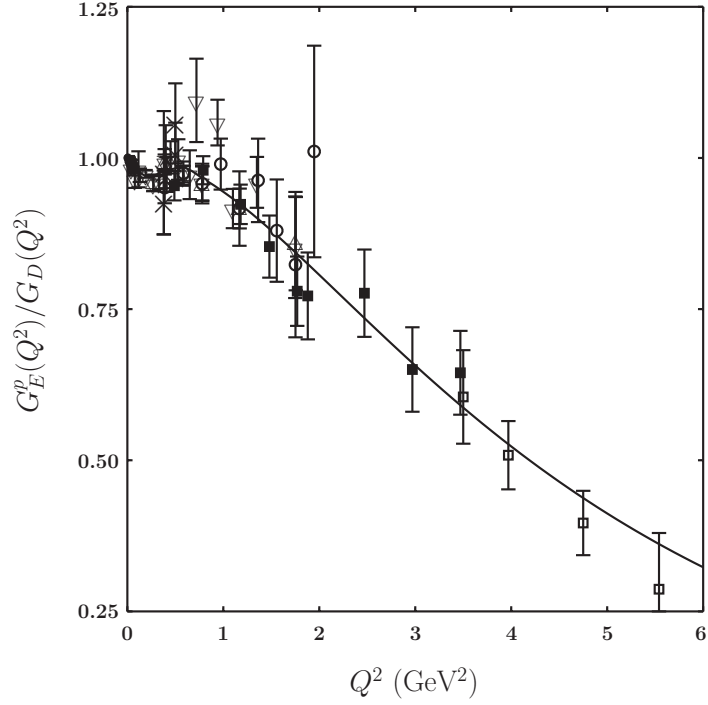
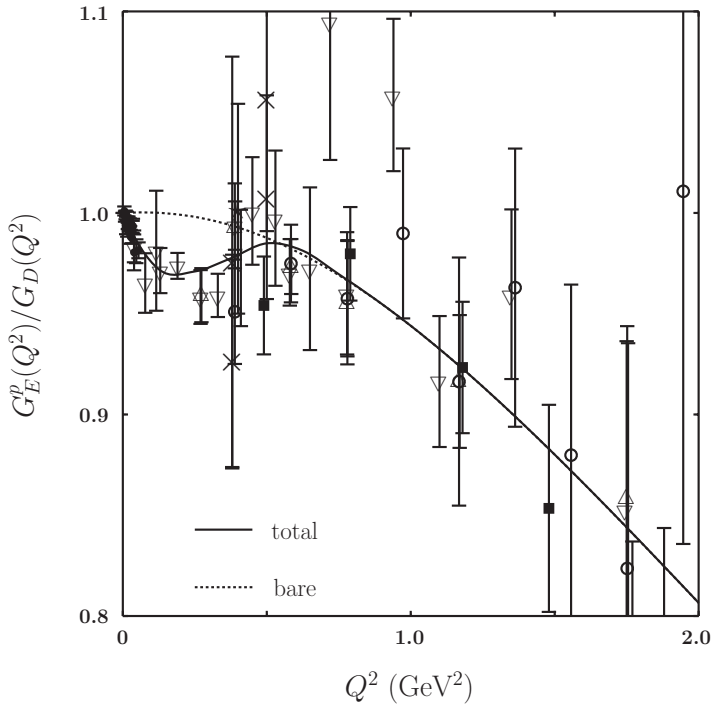


Fig. 4. Diagrams contributing to the mass operator of the quark at one loop. Vertices denoted by a black filled circle and diamond correspond to insertions from the second and fourth order chiral Lagrangian.

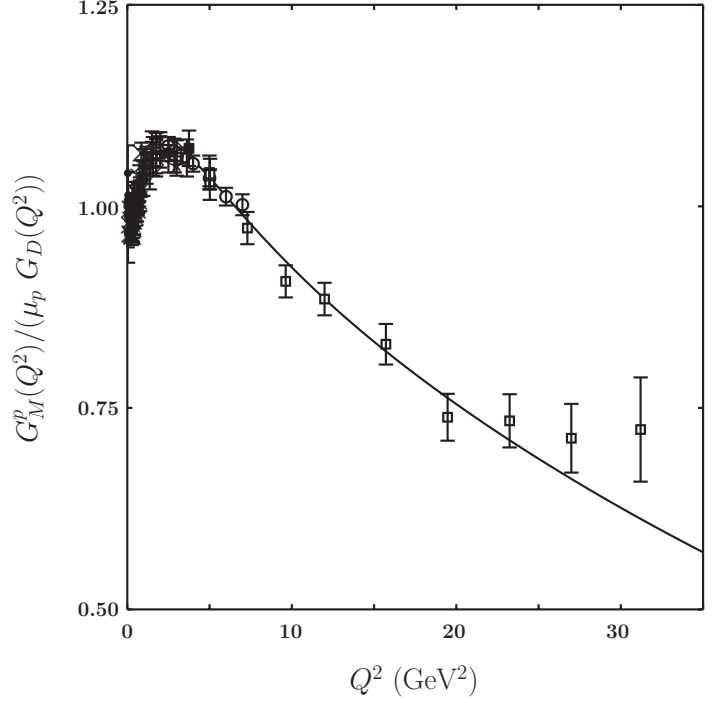


(a)

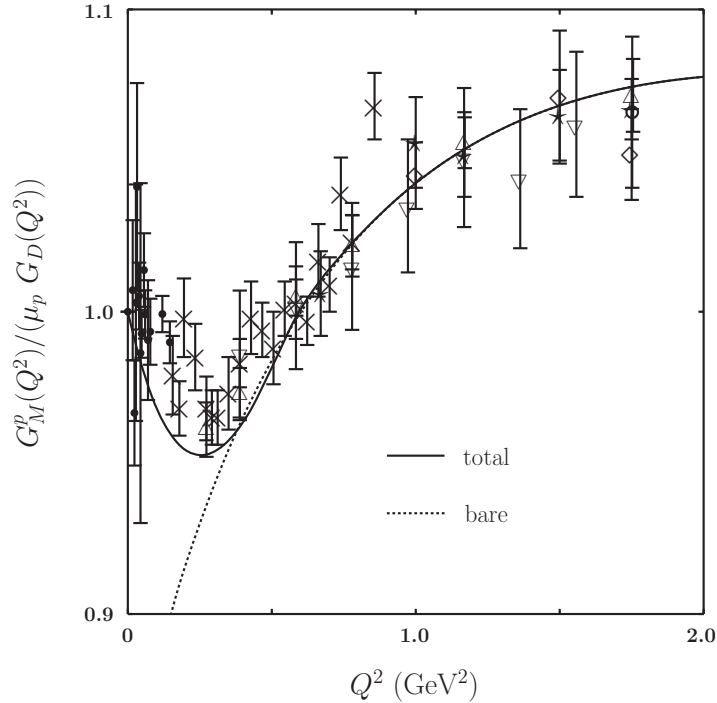


(b)

Fig. 5. Ratio $G_E^p(Q^2)/G_D(Q^2)$: (a) Overall range, (b) Up to $Q^2 = 2$ GeV 2 , the solid line is the total contribution and the dotted line is the bare contribution. Experimental data are taken from compilation of Ref. [51].

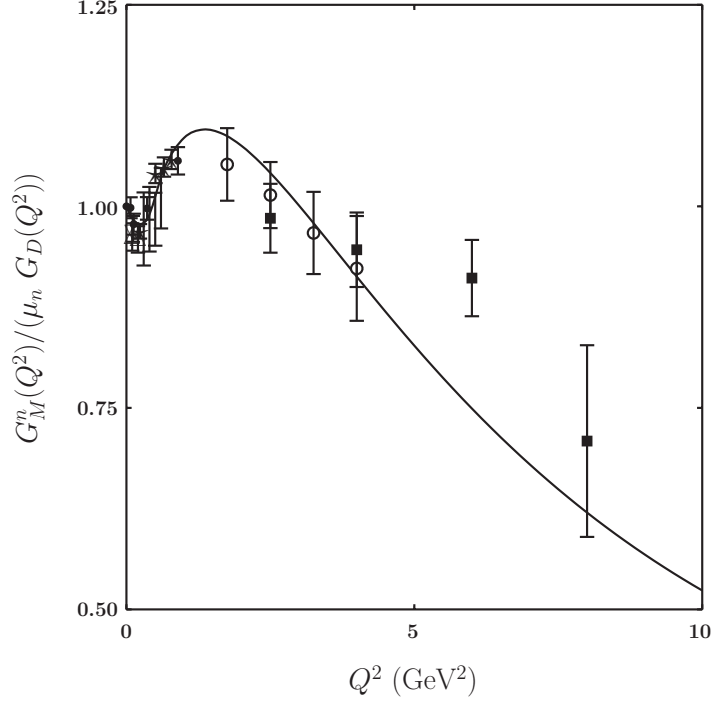


(a)



(b)

Fig. 6. Ratio $G_M^p(Q^2)/(\mu_p G_D(Q^2))$: (a) Overall range, (b) Up to $Q^2 = 2$ GeV 2 , the solid line is the total contribution and the dotted line is the bare contribution. Experimental data are taken from compilation of Ref. [51].



(a)

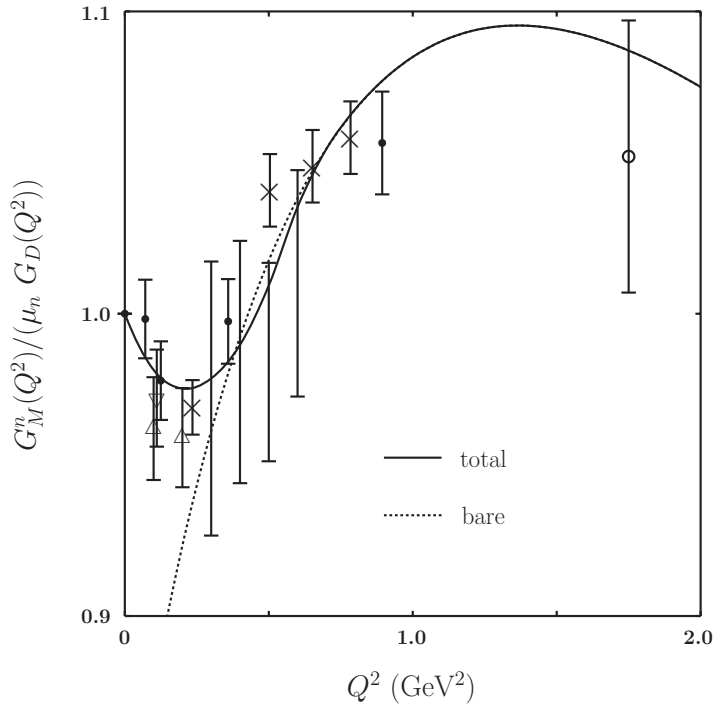


Fig. 7. Ratio $G_M^n(Q^2)/(\mu_n G_D(Q^2))$: (a) Overall range, (b) Up to $Q^2 = 2$ GeV 2 , the solid line is the total contribution and the dotted line is the bare contribution. Experimental data are taken from compilation of Ref. [51].

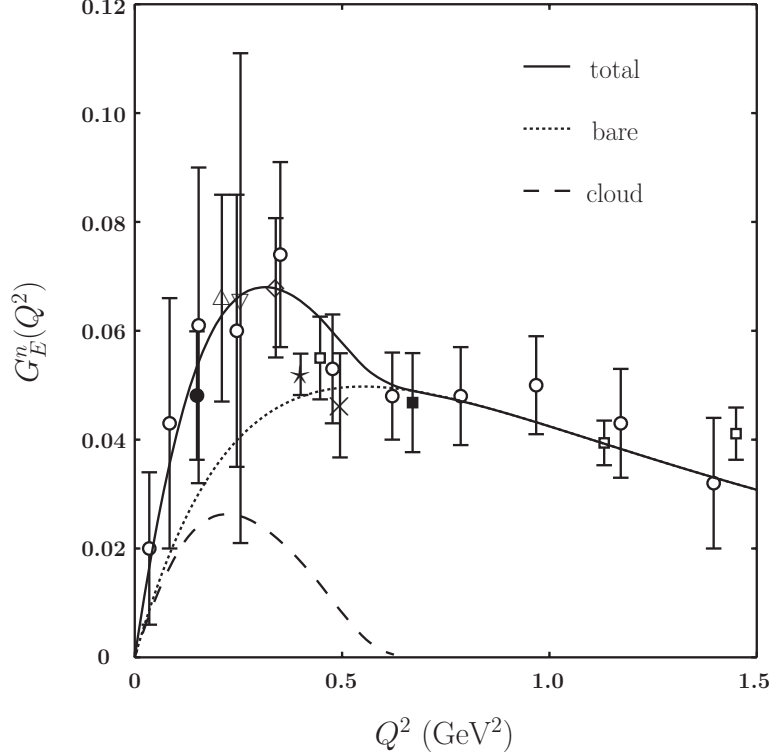


Fig. 8. Neutron charge form factor $G_E^n(Q^2)$ and the contribution due to the meson cloud in comparison to the experimental data. Experimental data are taken from compilation of Ref. [51] and Ref. [54, 55].

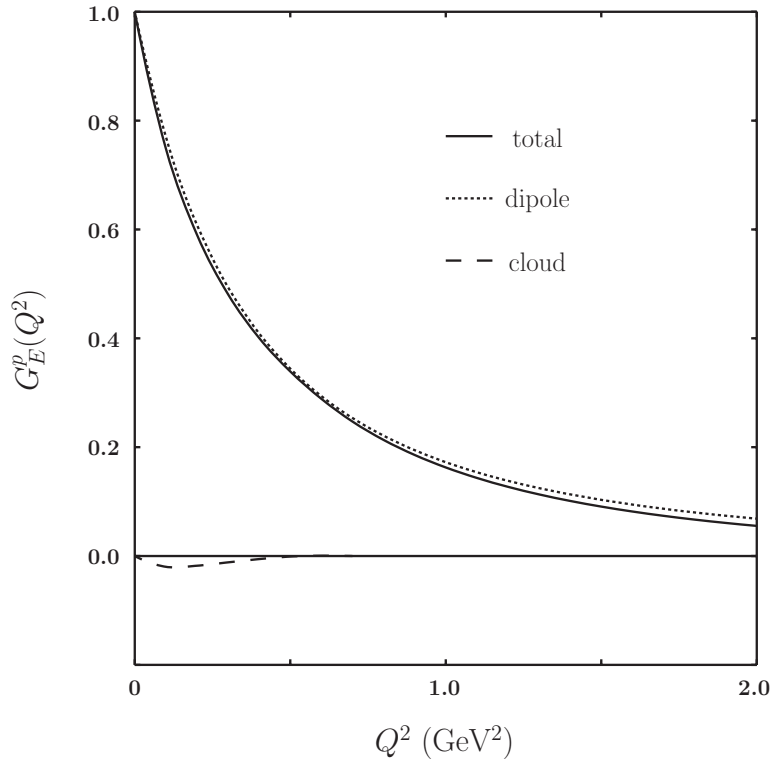


Fig. 9. Proton charge form factor $G_E^p(Q^2)$ and the contribution due to the meson cloud in comparison to the dipole fit.

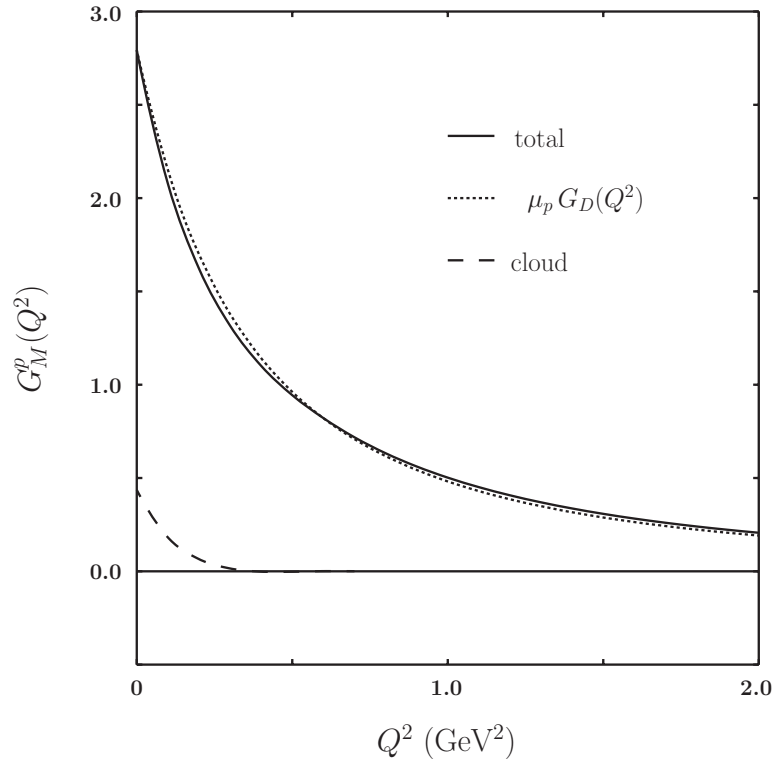


Fig. 10. Proton magnetic form factor $G_M^p(Q^2)$ and the contribution due to the meson cloud in comparison to the dipole fit.

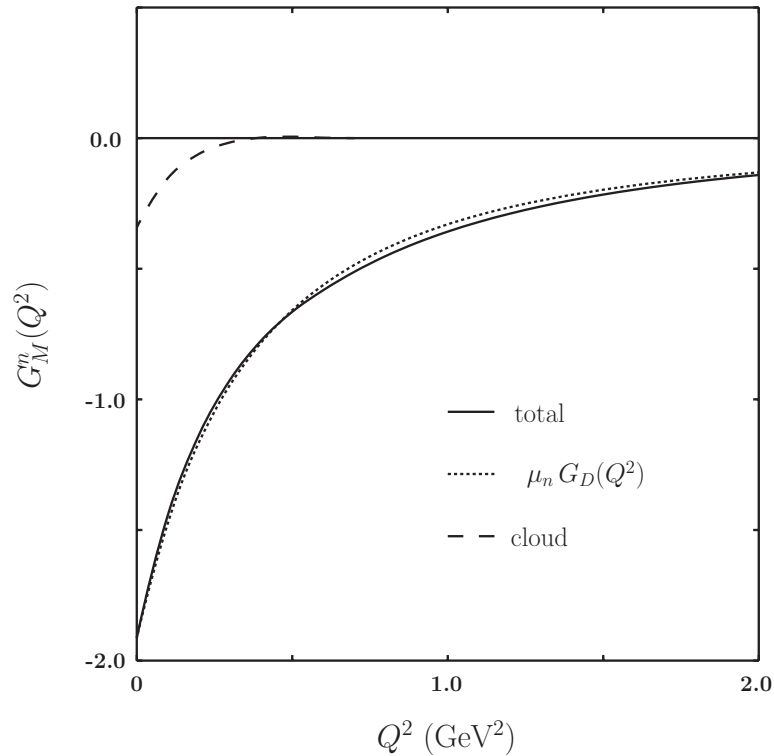


Fig. 11. Neutron magnetic form factor $G_M^n(Q^2)$ and the contribution due to the meson cloud in comparison to the dipole fit.

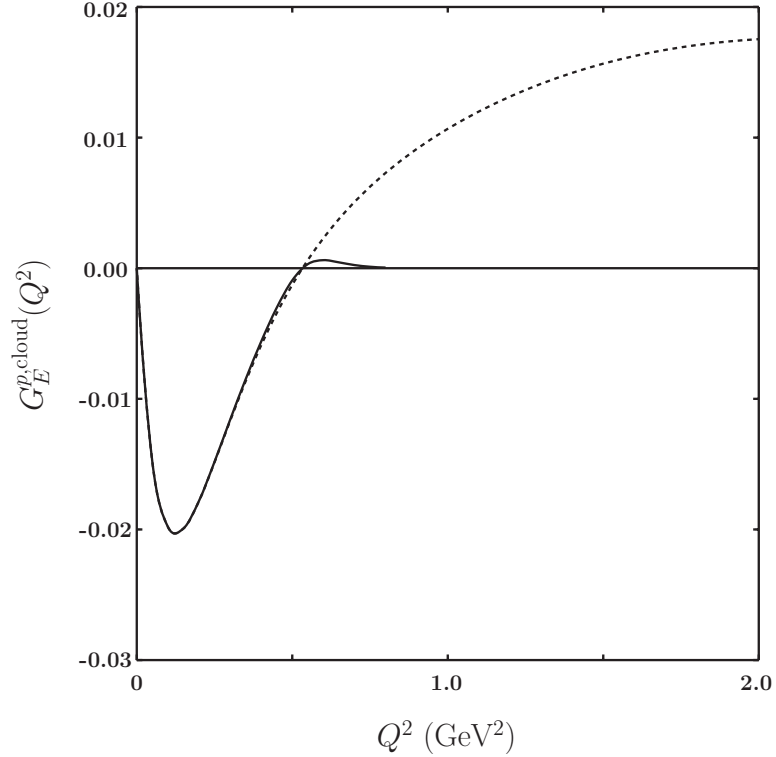


Fig. 12. The meson cloud contribution to the proton charge form factor $G_E^{p,cloud}(Q^2)$ with the cutoff function $f_{cut}(Q^2)$ (solid line) and without $f_{cut}(Q^2)$ (dotted line).

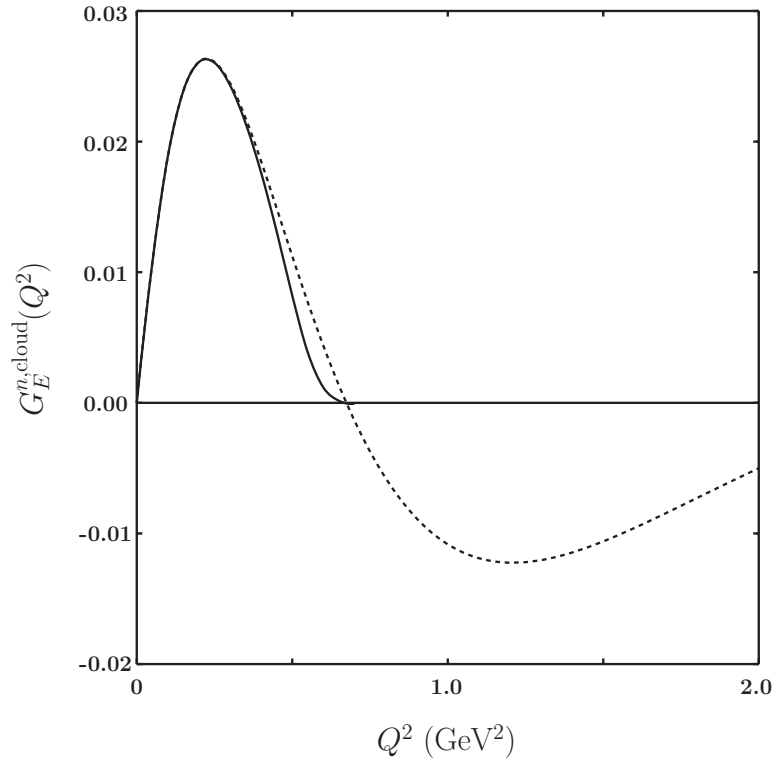


Fig. 13. The meson cloud contribution to the neutron charge form factor $G_E^{n,cloud}(Q^2)$ with the cutoff function $f_{cut}(Q^2)$ (solid line) and without $f_{cut}(Q^2)$ (dotted line).

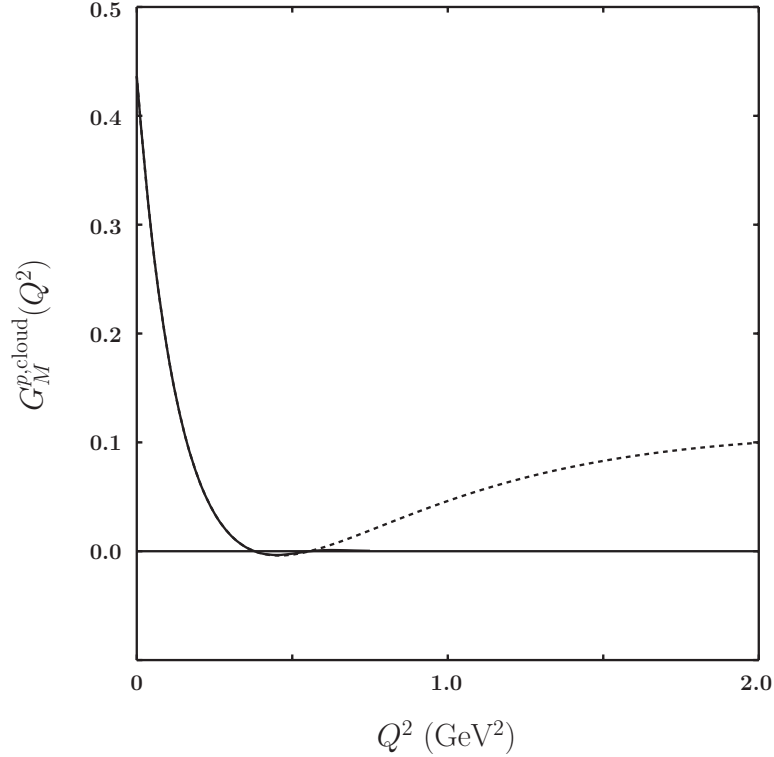


Fig. 14. The meson cloud contribution to the proton magnetic form factor $G_M^{p,cloud}(Q^2)$ with the cutoff function $f_{cut}(Q^2)$ (solid line) and without $f_{cut}(Q^2)$ (dotted line).

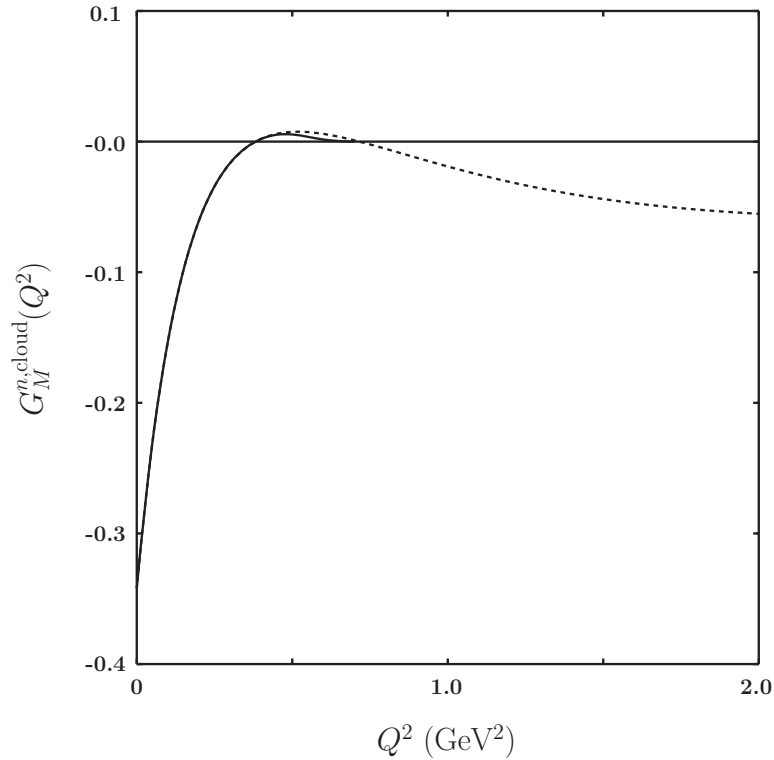


Fig. 15. The meson cloud contribution to the neutron magnetic form factor $G_M^{n,cloud}(Q^2)$ with the cutoff function $f_{cut}(Q^2)$ (solid line) and without $f_{cut}(Q^2)$ (dotted line).

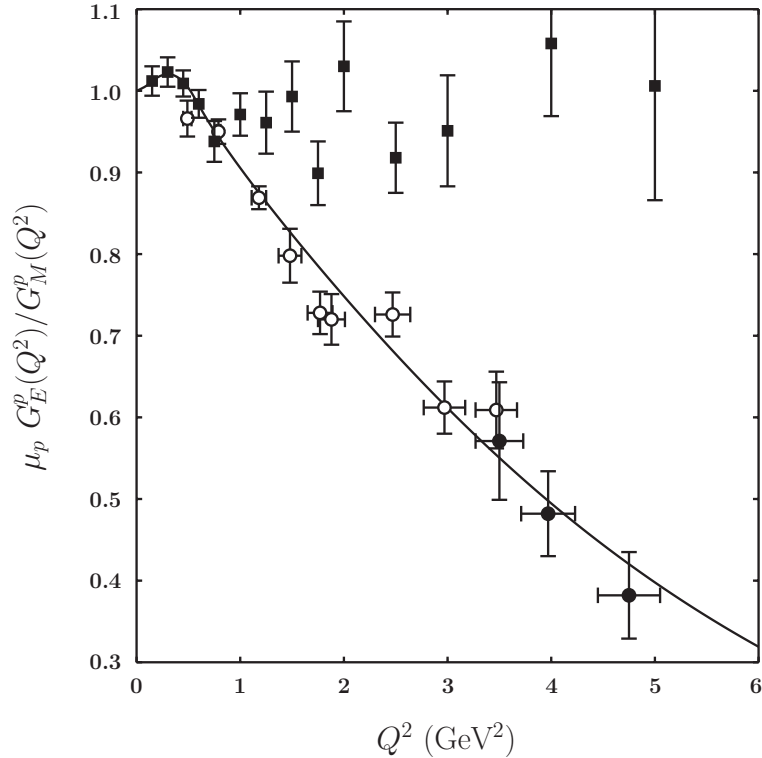
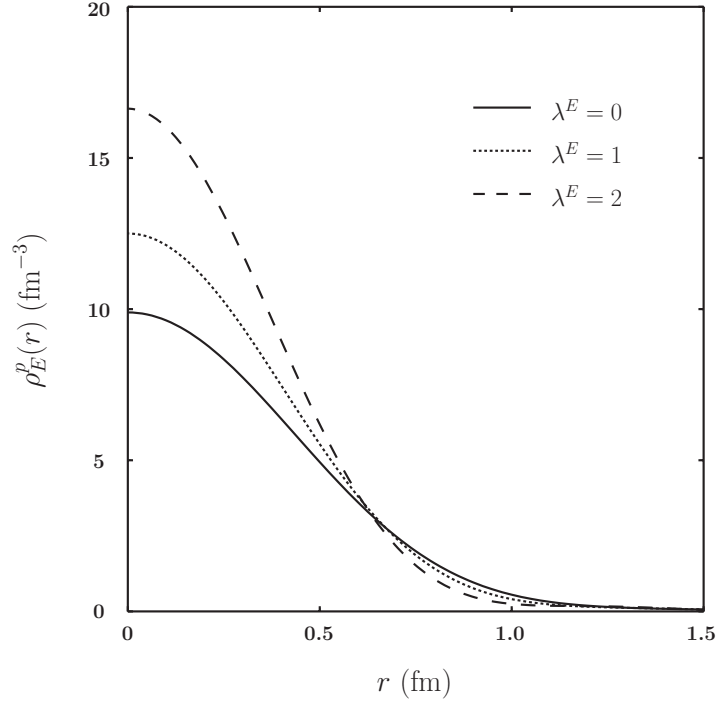
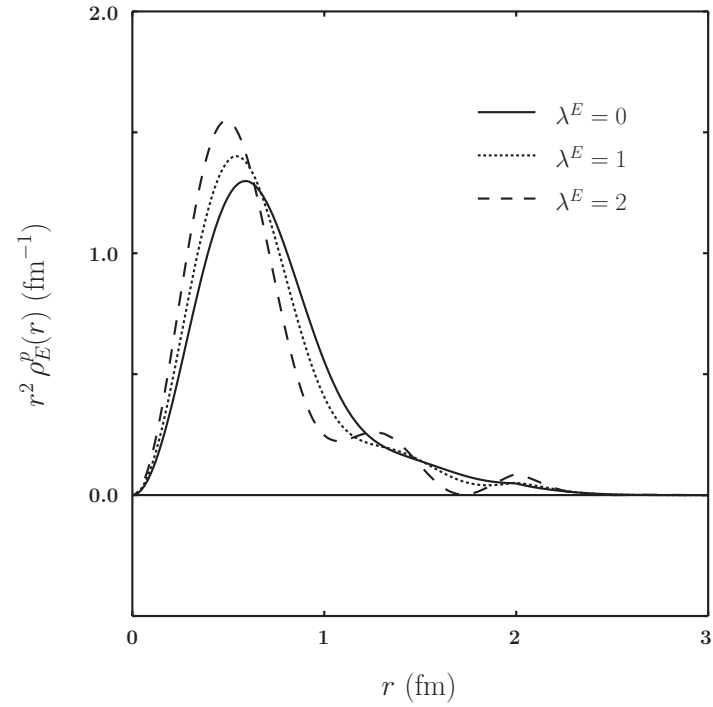


Fig. 16. Ratio $\mu_p G_E^p(Q^2)/G_M^p(Q^2)$ in comparison to the experimental data. Experimental data are taken from Refs. [56, 57, 58].

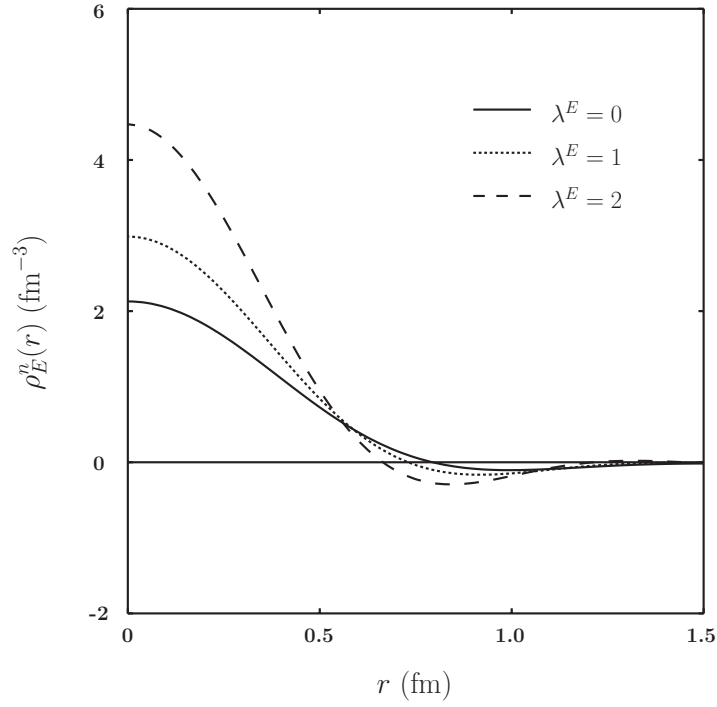


(a)

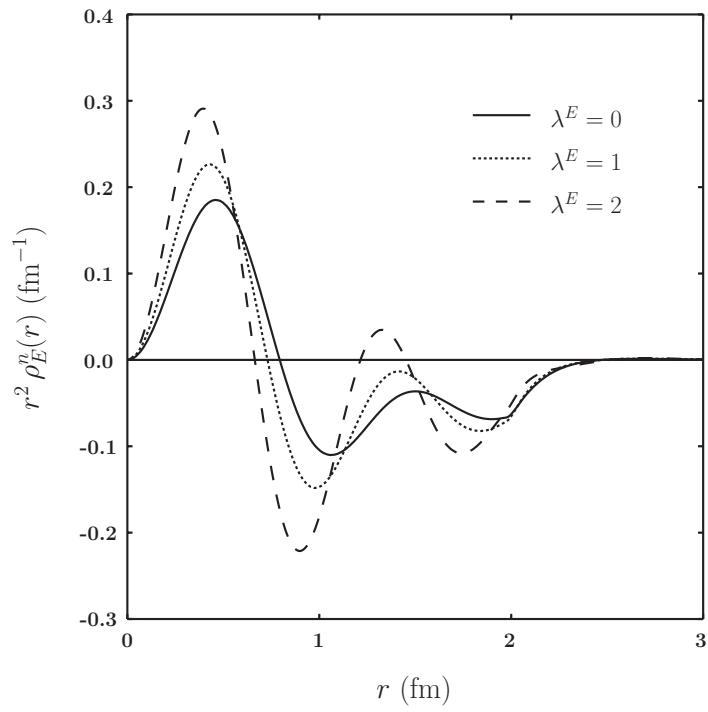


(b)

Fig. 17. Variation of the charge density of the proton $\rho_E^p(r)$ and $r^2 \rho_E^p(r)$ with λ^E : $\lambda^E = 0$ (solid line), $\lambda^E = 1$ (dotted line), and $\lambda^E = 2$ (dashed line).



(a)



(b)

Fig. 18. Variation of the charge density of the neutron $\rho_E^n(r)$ and $r^2 \rho_E^n(r)$ with λ^E : $\lambda^E = 0$ (solid line), $\lambda^E = 1$ (dotted line), and $\lambda^E = 2$ (dashed line).

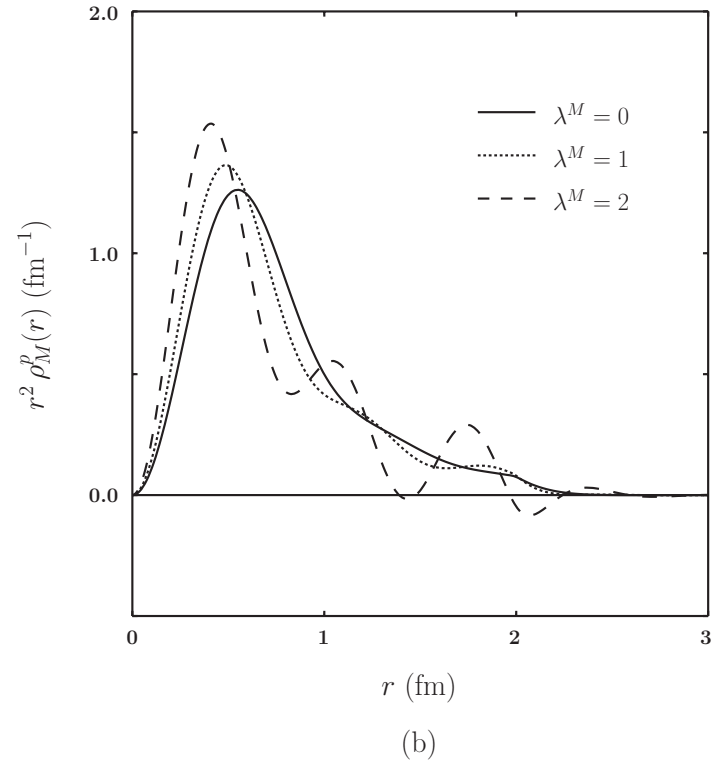
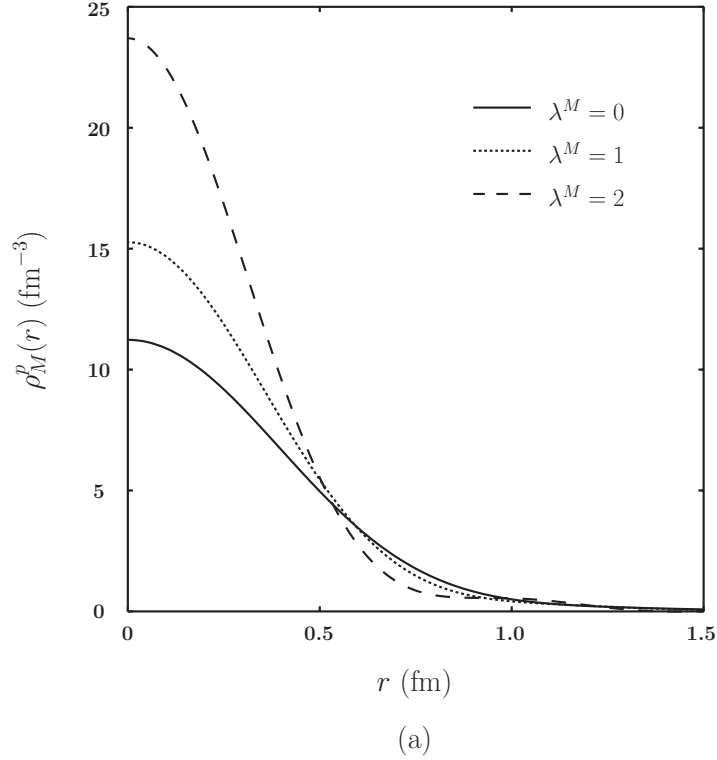
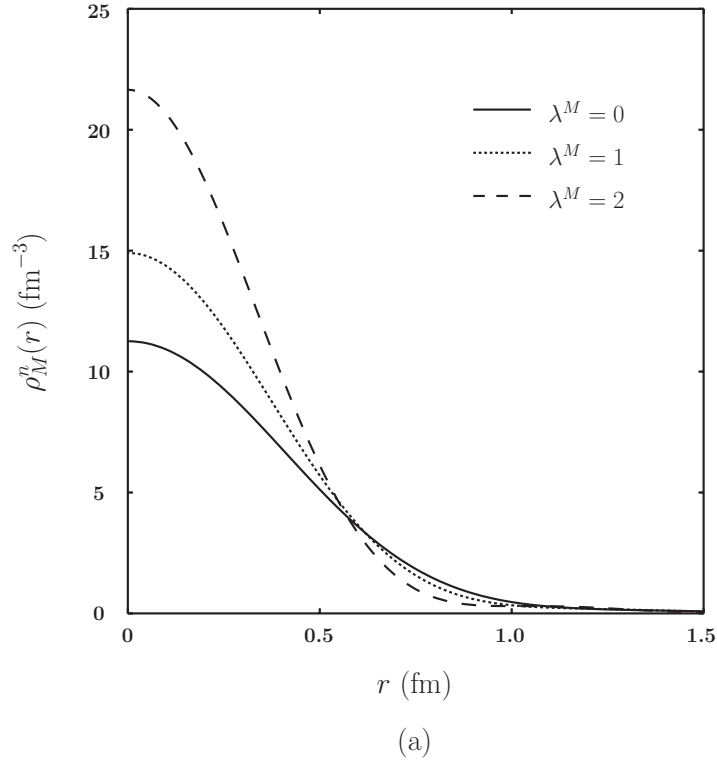
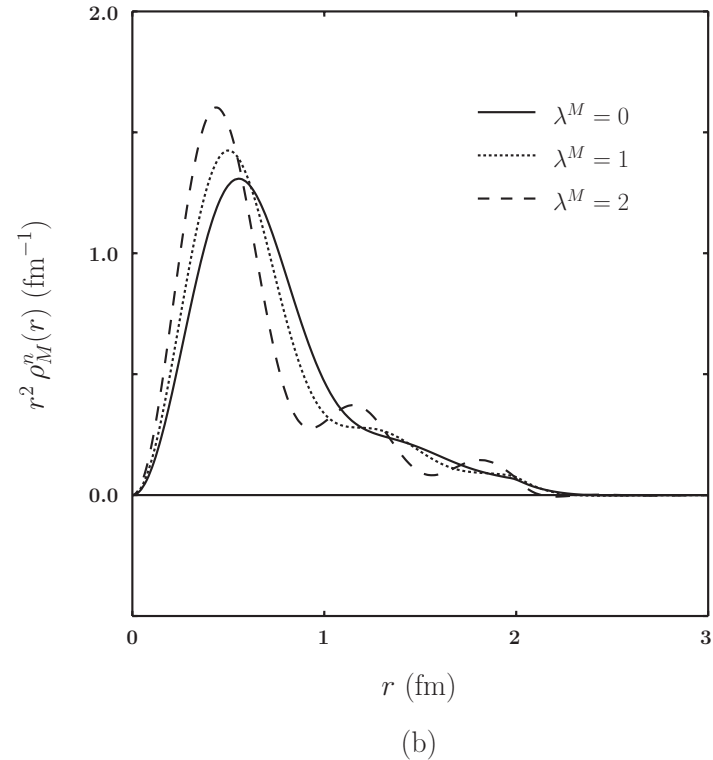


Fig. 19. Variation of the magnetization density of the proton $\rho_M^p(r)$ and $r^2 \rho_M^p(r)$ with λ^M : $\lambda^M = 0$ (solid line), $\lambda^M = 1$ (dotted line), and $\lambda^M = 2$ (dashed line).

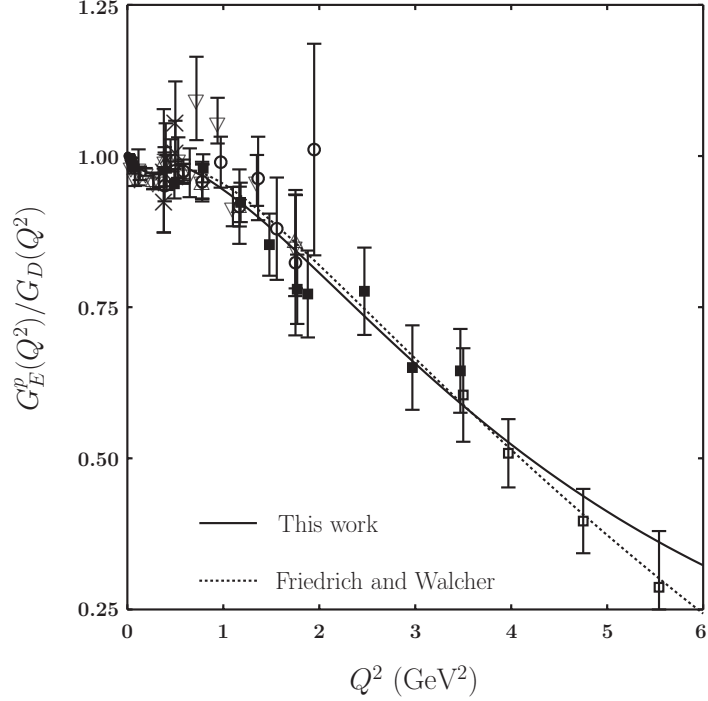


(a)

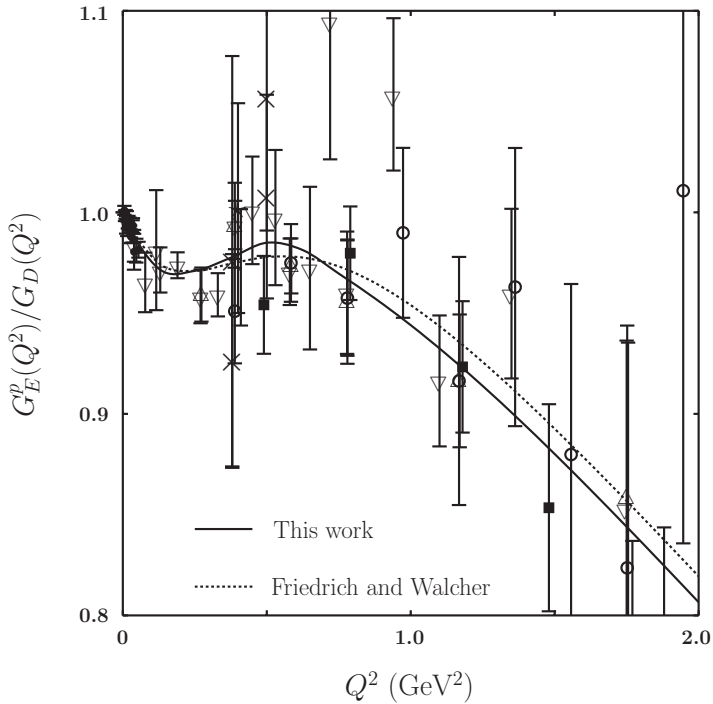


(b)

Fig. 20. Variation of the magnetization density of the neutron $\rho_M^n(r)$ and $r^2 \rho_M^n(r)$ with λ^M : $\lambda^M = 0$ (solid line), $\lambda^M = 1$ (dotted line), and $\lambda^M = 2$ (dashed line).



(a)



(b)

Fig. 21. The ratio of the charge proton form factor to the dipole form factor, the comparison of our result (solid line) to the result reported in Ref. [51] (dotted line) : (a) overall range, (b) Up to $Q^2 = 2$ GeV^2 . Experimental data are taken from compilation of Ref. [51].